

A NOVEL, ALGAL-BASED CHEMICAL ABSORPTION SYSTEM
FOR POST-COMBUSTION CARBON DIOXIDE CAPTURE

By

Adam John Smerigan

A THESIS

Submitted to
Michigan State University
in partial fulfillment of the requirements
for the degree of

Biosystems Engineering - Master of Science

2021

ABSTRACT

A NOVEL, ALGAL-BASED CHEMICAL ABSORPTION SYSTEM FOR POST-COMBUSTION CARBON DIOXIDE CAPTURE

By

Adam John Smerigan

Post-combustion carbon dioxide capture using amine solutions is an integral technology for reducing carbon dioxide emissions from the energy sector. However, environmental impacts and economic costs are restricting the implementation of amine absorbents. This study investigated the development of a sustainable algal based chemical absorption process to capture post-combustion carbon dioxide efficiently. Microalgal biomass was hydrolyzed to amino acids under basic conditions at 134°C. The supernatant of the hydrolysate was purged with carbon dioxide following centrifugation, and then underwent a desorption process to regenerate a chemical absorption algae-based solvent. A mass balance of the process showed that 31% of the mass into the process was recovered as an algal amino acid product. Another 30% exited the process as wet potassium carbonate which could be recovered as potassium hydroxide. The algal amino acid absorbent product contained 0.592 mol amino acid/L composed primarily of alanine, glutamic acid, glycine, aspartic acid, leucine, lysine, proline, etc. A trickling filter absorption column was built to determine the absorption capacity of the algal amino acid solution. The algal absorbent (1.27 ± 0.061 mol CO₂/mol amine) had a higher absorption capacity than a synthetic amino acid absorbent (0.747 ± 0.021 mol CO₂/mol amine) composed of glycine, alanine, proline, and lysine. Both solutions were regenerable showing no signs ($p < 0.05$) of deterioration after multiple absorption and desorption cycles regarding the pH of the solution, absorption capacity, and ATR-FTIR spectra. Using algal biomass as sustainable source of amino acids is a viable alternative to synthetic amino acid absorbents to effectively capture carbon dioxide in flue gas.

ACKNOWLEDGEMENTS

I would like to thank all the individuals who helped me create this thesis. Your guidance and support are greatly appreciated.

Thank you to my major advisor Dr. Wei Liao. Your guidance, compassion, and wisdom were invaluable. Your work ethic is inspiring, and I am glad I was able to share your enthusiasm for this project.

Thank you to Dr. Yan (Susie) Liu for serving on my committee. I want to thank you for giving me my start on research in our lab group and sparking my interest for graduate school.

Thank you to Dr. Milton Smith for serving on my committee. I appreciate the insight you gave into the chemistry and the time you devoted to help me succeed.

Thank you to Po-Jen Hsiao for the NMR and ATR-FTIR spectra. Your assistance was greatly appreciated. Thank you to Dr. Anthony Schillmiller and the RTSF Mass Spectrometry Center for the LCMS data. The amino acid concentration data were invaluable for this study.

I would also like to thank the entire research group. Without your support, friendship, and knowledge this would not have been possible. Thank you, Ashley Cutshaw, Annaliese Marks, Douglas Clements, Henry Frost, Blake Smerigan, Yurui Zheng, and Meicai Xu. Special thanks to Dr. Sibel Uludag-Demirer who went to great lengths to support me personally and academically. I greatly appreciate you and enjoyed the time we spent together.

Finally, I would like to thank my family and Sophie Morin for their love and encouragement. You helped me move along and work through any issues I had along the way.

TABLE OF CONTENTS

| | |
|---|-----|
| LIST OF TABLES | v |
| LIST OF FIGURES | vi |
| CHAPTER 1: Literature Review | 1 |
| INTRODUCTION | 1 |
| LITERATURE REVIEW | 4 |
| <i>Post-combustion carbon dioxide capture</i> | 4 |
| <i>Chemical absorption</i> | 5 |
| <i>Alkanolamine solutions</i> | 6 |
| <i>Amino acid solutions</i> | 7 |
| <i>Microalgae as a source of amino acids</i> | 10 |
| PILOT AND COMMERCIAL CHEMICAL ABSORPTION PROCESSES | 11 |
| SUMMARY OF KNOWLEDGE GAPS | 12 |
| OBJECTIVE AND HYPOTHESIS | 12 |
| CHAPTER 2: MATERIAL AND METHODS | 14 |
| CHEMICALS AND OTHER MATERIALS..... | 14 |
| NUCLEAR MAGNETIC RESONANCE (NMR)..... | 14 |
| LIQUID CHROMATOGRAPH/MASS SPECTROMETER (LCMS)..... | 15 |
| ABSORPTION | 17 |
| DESORPTION..... | 21 |
| MICROALGAL PROTEIN CONVERSION TO AMINO ACIDS AND PROCESSING..... | 23 |
| CHAPTER 3: ALGAE BIOMASS CONVERSION AND PROCESSING | 27 |
| CHAPTER 4: USING A SYNTHETIC AMINO ACID (GAPL) ABSORBENT FOR CO₂ ABSORPTION FROM A SYNTHETIC FLUE GAS CONTAINING 10% CO₂ | 32 |
| CHAPTER 5: ALGAL AMINO ACID SOLUTION ABSORPTION | 39 |
| CHAPTER 6: CONCLUSIONS AND FUTURE WORK | 47 |
| APPENDICES | 48 |
| APPENDIX A: CHAPTER 3 SUPPLEMENTAL INFORMATION..... | 49 |
| APPENDIX B: CHAPTER 4 SUPPLEMENTAL INFORMATION | 61 |
| APPENDIX C: CHAPTER 5 SUPPLEMENTAL INFORMATION | 71 |
| APPENDIX D: R-MARKDOWN FILE AND STATISTICS | 85 |
| APPENDIX E: ALGAL BIOMASS INFORMATION | 111 |
| APPENDIX F: DAIRY ONE FORAGE LABORATORY PROCEDURES..... | 113 |
| APPENDIX G: LAB IMAGES..... | 120 |
| REFERENCES | 124 |

LIST OF TABLES

| | |
|---|-----|
| Table 1: MS/MS Parameters for Function 1 (0-4.5min) | 16 |
| Table 2: MS/MS Parameters for Function 2 (4.5-6.55 min) | 16 |
| Table 3: MS/MS Parameters for Function 3 (6.55-13 min) | 17 |
| Table 4: Amino Acid Concentrations under Various Parr Reactor Conditions | 27 |
| Table 5: Energy Consumption of Process Equipment | 30 |
| Table 6: Absorption Totals for Different G/L Flow Ratios | 33 |
| Table 7: Synthetic Absorbent CO ₂ Absorption and Desorption Capacities | 34 |
| Table 8: Synthetic Absorbent pH over Four Absorption Cycles | 36 |
| Table 9: ATR-FTIR Peak Identification Table | 37 |
| Table 10: Algal Amino Acid Absorbent CO ₂ Absorption and Desorption Capacities | 40 |
| Table 11: Literature Absorption Capacities for Amino Acid and MEA Absorbents | 45 |
| Table 12: Energy Consumption for Algal Absorption and Desorption | 46 |
| Table 13: Pairwise Comparisons of Mean Amino Acid Concentrations for Parr Reactor Conditions | 49 |
| Table 14: Pairwise Comparisons between Gas to Liquid Flow Ratios | 61 |
| Table 15: Synthetic Absorbent CO ₂ Absorption and Desorption Capacities | 62 |
| Table 16: Algal Amino Acid Absorbent CO ₂ Absorption and Desorption Capacities | 71 |
| Table 17: Algal Amino Acid Absorbent pH over Absorption Cycles | 72 |
| Table 18: Absorption Capacities for the Synthetic and Algal Amino Acid Absorbents | 72 |
| Table 19: <i>C. sorokiniana</i> Biomass Composition | 111 |
| Table 20: <i>C. sorokiniana</i> Fatty Acid Composition | 112 |

LIST OF FIGURES

| | |
|---|----|
| Figure 1: Carbon Capture Technologies Flow Diagram ¹⁰ | 3 |
| Figure 2: Technology tree for Carbon Dioxide Separation ¹² | 4 |
| Figure 3: Zwitterion Reaction Mechanism | 7 |
| Figure 4: Base-catalyzed Reaction Mechanism | 7 |
| Figure 5: Generic Amino Acid Ionization in Acidic, Neutral, and Alkaline Conditions | 8 |
| Figure 6: Products of the Reaction of Amino Acids with Carbon Dioxide | 9 |
| Figure 7: Amino Acid Carbon Capture Reaction Scheme ²⁵ | 9 |
| Figure 8: Absorption Experimental Setup | 20 |
| Figure 9: Desorption Experimental Setup | 22 |
| Figure 10: Microalgal Biomass Conversion and Processing Flow Diagram | 24 |
| Figure 11: Amino Acid Concentrations after each Processing Step | 29 |
| Figure 12: Mass Balance of the Biomass Conversion Process | 30 |
| Figure 13: Potassium Mass Balance of the Biomass Conversion Process | 30 |
| Figure 14: ATR-FTIR Spectra for the Algal Amino Acid Solution after a) Parr Reactor b) Centrifuge c) Acidification d) Desorption | 31 |
| Figure 15: Synthetic Amino Acid Absorbent Absorption Curve for a Gas to Liquid Flow Rate of 2.5 | 32 |
| Figure 16: Carbon Dioxide Absorbed for Varied Gas to Liquid Flow Ratios | 33 |
| Figure 17: Synthetic Absorbent CO ₂ Absorption and Desorption over Four Cycles | 35 |
| Figure 18: Synthetic Absorbent pH over Four Absorption and Desorption Cycles | 36 |
| Figure 19: Synthetic Amino Acid Absorbent ATR-FTIR Spectra a) Original, b) After Absorption, c) After Desorption | 38 |
| Figure 20: Algal Amino Acid Absorbent Absorption Curves | 39 |
| Figure 21: Algal Amino Acid Absorbent Absorption and Desorption Capacities | 41 |
| Figure 22: Algal Amino Acid Absorbent pH over Absorption and Desorption Cycles | 42 |

| | |
|--|----|
| Figure 23: Algal Amino Acid Absorbent ATR-FTIR Spectra a) original b) after absorption c) after desorption _____ | 43 |
| Figure 24: Cyclic Absorption Capacities for Absorbents in the Literature _____ | 46 |
| Figure 25: Amino Acid Concentrations after Parr Reactor for each Experiment _____ | 49 |
| Figure 26: Amino Acid Concentrations after Centrifuge for each Experiment _____ | 50 |
| Figure 27: Amino Acid Concentrations after Acidification for each Experiment _____ | 50 |
| Figure 28: Amino Acid Concentrations after Desorption for each Experiment _____ | 51 |
| Figure 29: Pairwise Comparisons of Amino Acid Concentrations for the Algal Amino Acid Solution for each Processing Step _____ | 51 |
| Figure 30: Algal Amino Acid Solution Percent Mass Liquid Yield after Centrifuge _____ | 52 |
| Figure 31: Algal Amino Acid Solution Percent Mass Liquid Yield Pairwise Comparisons _____ | 52 |
| Figure 32: Algal Amino Acid Solution Liquid Mass after Acidification _____ | 53 |
| Figure 33: Parr Slurry 1 ATR-FTIR Spectrum _____ | 53 |
| Figure 34: Parr Slurry 2 ATR-FTIR Spectrum _____ | 54 |
| Figure 35: Parr Slurry 3 ATR-FTIR Spectrum _____ | 54 |
| Figure 36: Parr Slurry 4 ATR-FTIR Spectrum _____ | 55 |
| Figure 37: Parr Centrifugate 1 ATR-FTIR Spectrum _____ | 55 |
| Figure 38: Parr Centrifugate 2 ATR-FTIR Spectrum _____ | 55 |
| Figure 39: Parr Centrifugate 3 ATR-FTIR Spectrum _____ | 56 |
| Figure 40: Parr Centrifugate 4 ATR-FTIR Spectrum _____ | 56 |
| Figure 41: Acidified Centrifugate 1 ATR-FTIR Spectrum _____ | 57 |
| Figure 42: Acidified Centrifugate 3 ATR-FTIR Spectrum _____ | 57 |
| Figure 43: Acidified Centrifugate 4 ATR-FTIR Spectrum _____ | 58 |
| Figure 44: Algal Amino Acid Product 1 ATR-FTIR Spectrum _____ | 58 |
| Figure 45: Algal Amino Acid Product 2 ATR-FTIR Spectrum _____ | 59 |
| Figure 46: Algal Amino Acid Product 3 ATR-FTIR Spectrum _____ | 59 |
| Figure 47: Algal Amino Acid Product 4 ATR-FTIR Spectrum _____ | 60 |

| | |
|--|----|
| Figure 48: Mean comparisons for various Gas to Liquid Flow Ratios _____ | 61 |
| Figure 49: Synthetic Absorbent CO ₂ Absorption and Desorption over Four Cycles in mol CO ₂ /L ____ | 62 |
| Figure 50: Pairwise Comparisons for Synthetic Amino Acid Absorbent Absorption Capacities for each Cycle _____ | 63 |
| Figure 51: Pairwise Comparisons for Synthetic Amino Acid Absorbent Desorption Capacities for each Cycle _____ | 63 |
| Figure 52: Pairwise Comparisons for Synthetic Amino Acid Absorbent Absorbed pH for each Cycle _ | 64 |
| Figure 53: Pairwise Comparisons for Synthetic Amino Acid Absorbent Desorbed pH for each Cycle _ | 64 |
| Figure 54: Synthetic Amino Acid Absorbent ATR-FTIR Spectrum a) prior to Absorption b) after Absorption 1 c) after Absorption 2 d) after Absorption 3 e) after Absorption 4 _____ | 65 |
| Figure 55: Synthetic Amino Acid Absorbent ATR-FTIR Spectrum a) after Desorption 1 b) after Desorption 2 c) after Absorption 3 d) after Desorption 4 _____ | 67 |
| Figure 56: Synthetic Amino Acid Absorbent NMR Spectrum a) prior to Absorption b) after Absorption 4 c) after Desorption 4 _____ | 69 |
| Figure 57: Amino Acid Concentration within the Algal Amino Acid Absorbent after Each Absorption | 71 |
| Figure 58: Algal Amino Acid Absorbent CO ₂ Absorbed and Desorbed over 8 Cycles in mol/L _____ | 72 |
| Figure 59: Absorption Capacities for the Synthetic and Algal Amino Acid Absorbents in mol/L _____ | 73 |
| Figure 60: Algal Amino Acid Absorbent ATR-FTIR Spectrum prior to Absorption _____ | 73 |
| Figure 61: Algal Amino Acid Absorbent ATR-FTIR Spectrum after Absorption 1 _____ | 74 |
| Figure 62: Algal Amino Acid Absorbent ATR-FTIR Spectrum after Absorption 2 _____ | 74 |
| Figure 63: Algal Amino Acid Absorbent ATR-FTIR Spectrum after Absorption 3 _____ | 75 |
| Figure 64: Algal Amino Acid Absorbent ATR-FTIR Spectrum after Absorption 4 _____ | 75 |
| Figure 65: Algal Amino Acid Absorbent ATR-FTIR Spectrum after Absorption 5 _____ | 76 |
| Figure 66: Algal Amino Acid Absorbent ATR-FTIR Spectrum after Absorption 6 _____ | 76 |
| Figure 67: Algal Amino Acid Absorbent ATR-FTIR Spectrum after Absorption 7 _____ | 77 |
| Figure 68: Algal Amino Acid Absorbent ATR-FTIR Spectrum after Absorption 8 _____ | 77 |
| Figure 69: Algal Amino Acid Absorbent ATR-FTIR Spectrum after Desorption 1 _____ | 78 |
| Figure 70: Algal Amino Acid Absorbent ATR-FTIR Spectrum after Desorption 2 _____ | 78 |

| | | |
|--|-------|-----|
| Figure 71: Algal Amino Acid Absorbent ATR-FTIR Spectrum after Desorption 4 | _____ | 79 |
| Figure 72: Algal Amino Acid Absorbent ATR-FTIR Spectrum after Desorption 5 | _____ | 79 |
| Figure 73: Algal Amino Acid Absorbent ATR-FTIR Spectrum after Desorption 6 | _____ | 80 |
| Figure 74: Algal Amino Acid Absorbent ATR-FTIR Spectrum after Desorption 7 | _____ | 80 |
| Figure 75: Algal Amino Acid Absorbent ATR-FTIR Spectrum after Desorption 8 | _____ | 80 |
| Figure 76: Algal Amino Acid Absorbent ATR-FTIR Spectrum after Desorption 1 after Dilution | _____ | 81 |
| Figure 77: Algal Amino Acid Absorbent ATR-FTIR Spectrum after Desorption 2 after Dilution | _____ | 81 |
| Figure 78: Algal Amino Acid Absorbent ATR-FTIR Spectrum after Desorption 3 after Dilution | _____ | 82 |
| Figure 79: Algal Amino Acid Absorbent ATR-FTIR Spectrum after Desorption 4 after Dilution | _____ | 82 |
| Figure 80: Algal Amino Acid Absorbent ATR-FTIR Spectrum after Desorption 5 after Dilution | _____ | 83 |
| Figure 81: Algal Amino Acid Absorbent ATR-FTIR Spectrum after Desorption 6 after Dilution | _____ | 83 |
| Figure 82: Algal Amino Acid Absorbent ATR-FTIR Spectrum after Desorption 7 after Dilution | _____ | 84 |
| Figure 83: Desorption Experimental Setup Photo a) not in use b) in use | _____ | 120 |
| Figure 84: Absorption Experimental Setup Photo a) not in use b) gas flow control setup c) column in use d) setup in use | _____ | 121 |
| Figure 85: Algal Amino Acid Absorbent Photo a) before absorption b) after absorption | _____ | 122 |
| Figure 86: Precipitated Solids after Acidification Photos a) solids and liquids b) dried solids | _____ | 123 |

CHAPTER 1: Literature Review

INTRODUCTION

Global climate change is a major issue facing the next generation. The effects of global climate change will be expensive and compromise health and safety in many regions of the United States¹. One of the main drivers to global climate change is the greenhouse effect from greenhouse gases emitted by human activities. Carbon dioxide originating from land use and industrial processes, as the primary greenhouse gas, accounts for 76% of all greenhouse gases emitted globally² and 55% of the observed global warming³. The United States, one of the top three greenhouse gas emitters in the world (after China and European Union), produces 15% of the total global carbon dioxide emissions². Within the United States, the electricity sector is the second largest contributor of greenhouse gas emissions after the transportation sector, at 25% of all emissions. These emissions are primarily in the form of carbon dioxide from non-renewable fuel sources. Electricity generation from fossil fuel sources accounts for 2,588 billion kWh in the United States compared to 1,529 billion kWh from nuclear and renewable sources⁴. Fossil fuels will continue to fill a large proportion of the energy needs in the United States. Though the emissions from this sector are trending slightly downward, down 11.8% from 1,819.95 million metric tons (MMmt) in 1990 to 1,606.02 MMmt of carbon dioxide equivalent⁵ in 2019, the electricity sector will continue to represent a significant portion of emissions and must be addressed to secure a sustainable climate future⁶.

A variety of opportunities are available to reduce the emissions from the electricity sector. These include improved efficiency of existing power plants, further implementation of renewable energy, increased end-use energy efficiency, and carbon capture and sequestration⁶. Currently, renewables and nuclear energy account for 37.2% of electricity generation in the

United States and the remaining generation comes from fossil fuels⁷. Increasing the efficiency of equipment in the power plants and at end use sites can improve energy efficiency by 30% or more⁸. However, carbon capture technologies are still required to achieve zero emission from these power plants. Accordingly, numerous technologies have been researched and developed to capture and store carbon dioxide emitted from the power industry. There are three primary methods of carbon dioxide capture including oxy-combustion, pre-combustion, and post-combustion. Some fuels, such as coal and natural gas, are pretreated by gasification and the water gas shift reaction prior to combustion. Pre-combustion capture removes the carbon dioxide evolved from these reactions. Oxyfuel combustion uses a pure oxygen feed to the combustion process allowing for a relatively pure, 80-98% carbon dioxide, product stream that can be compressed and stored. Finally, post-combustion techniques capture carbon dioxide from the flue gas of existing power plants⁹. Figure 1¹⁰ below shows the process flow for each of these treatments. Post-combustion carbon dioxide capture is the most easily implemented and is the focus of this study. Specifically, chemical absorption separations are investigated with observations of future research areas.

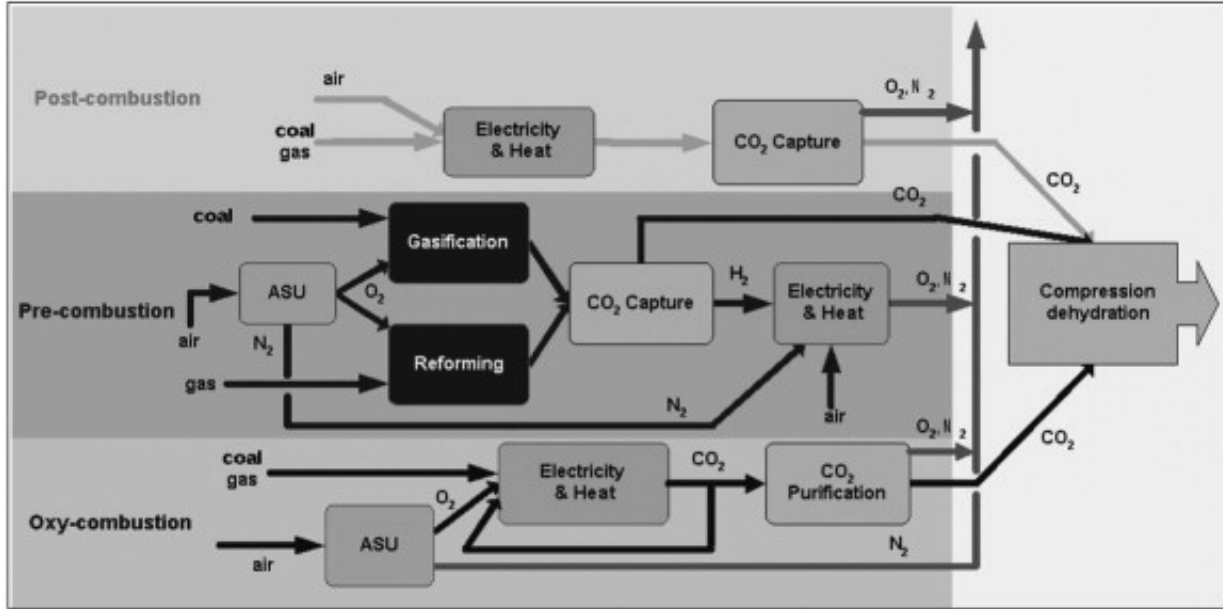


Figure 1: Carbon Capture Technologies Flow Diagram¹⁰

LITERATURE REVIEW

Post-combustion carbon dioxide capture

Post-combustion carbon capture technologies are of specific interest due to the ability to retrofit existing power plants with the technology. This will allow for very little disruption to the existing infrastructure and allow for continued use of fossil fuels for energy production. This is important because, economically, fossil fuels are still favored and will be for the foreseeable future¹¹. The ability to be easily implemented is counteracted by the main drawback of post-combustion processes, the separation¹². Carbon dioxide from the flue gas of power industry is more difficult to be separated than the other processes due to the low concentration of carbon dioxide in flue gas, 4-14% depending on fuel source⁹. There are numerous technologies attempting to address this challenge. Figure 2¹² below shows a tree of carbon dioxide separation technologies with the focus of this review circled in red.

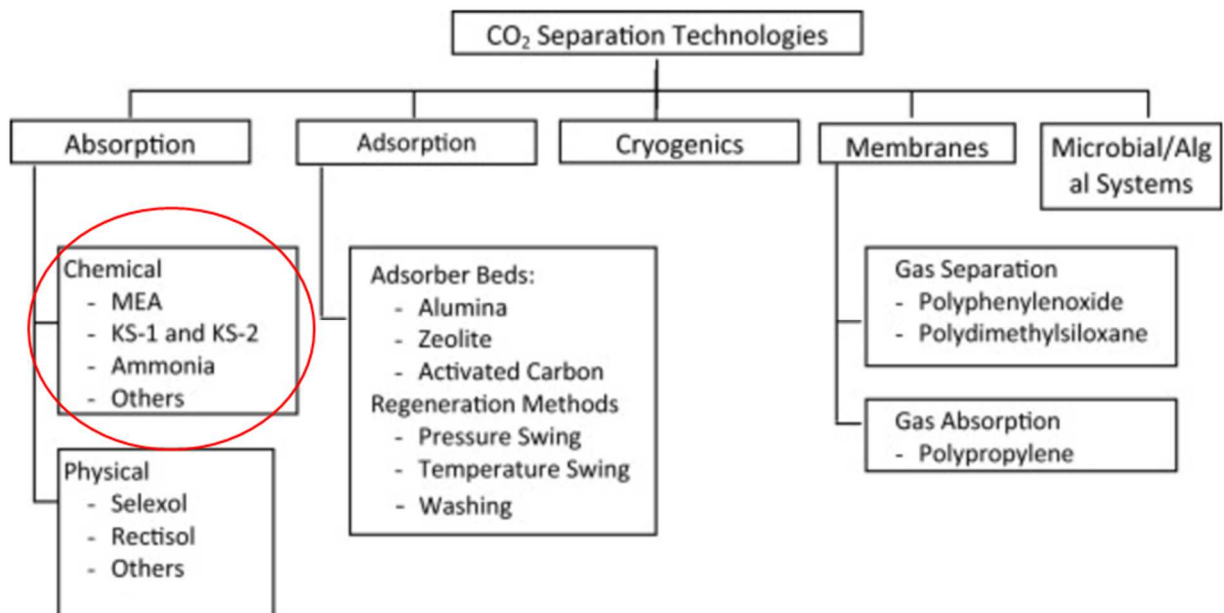


Figure 2: Technology tree for Carbon Dioxide Separation¹²

Chemical absorption

Of these technologies, chemical absorption, using monoethanolamine (MEA), amino acid, and other amine based solutions, has been intensively studied, and is most likely to be the first implemented in the near future¹². Chemical absorption has a high absorption capacity, has regenerable absorbents, and is the most mature carbon dioxide separation technology^{9,13}. Disadvantages of this technology include the environmental impact of absorbent degradation, a high heat requirement for regeneration of absorption absorbents, and variable efficiency of absorption at different carbon dioxide concentrations in the flue gas^{9,13}. The most used absorbent today is (MEA) due to the low cost of the chemical and high absorption efficiency. However, MEA has disadvantages which include low carbon dioxide loading capacity, degradation of absorbent by sulfur dioxide and oxygen, high corrosivity, and high energy consumption^{12,14}. Most research on the chemical absorption is being done on new types of absorbents that have a higher absorption capacity than MEA while also requiring less energy for absorbent regeneration¹². In addition, solutions with less toxicity and fewer environmental impacts are highly sought after. These solutions include alkanolamine solutions (the class of compound that MEA belongs) and amino acid solutions. Mixtures of these chemicals with themselves and other compounds are also being tested to attempt to combine the strengths of each individual component of the mixture^{15,16}.

Life cycle assessments have been performed to understand the impacts of the chemical absorption process in the power industry. However, environmental impacts of chemical absorption are significantly varied between different fossil fuel power plants, such as coal and natural gas plants. Since burning coal is inherently less environmentally friendly, chemical absorption can have more benefits than with a less environmentally impactful fuel, like natural

gas. To fully understand the impacts of chemical absorption technology both types of plants must be considered. The introduction of chemical absorption to a coal power plant shows a reduction of about 50% in the global warming potential¹⁷. Other benefits include a reduction of 50% or greater in the impact categories of human toxicity potential, acidification potential, and marine aquatic ecotoxicity potential, since the absorbent captures many toxic compounds from the flue gas¹⁷. For a natural gas power plant, a greater reduction in global warming potential of 58-68% is observed¹⁸. However, almost all other impact categories (i.e., human toxicity potential, acidification potential, marine ecotoxicity potential, and terrestrial ecotoxicity potential) were increased due to the toxicity of the degraded MEA, chemical wastes from production, and the effects of waste disposal, among other issues¹⁸. If the energy requirement and absorbent degradation is reduced, many of these negative impacts attributed to the chemical absorption technology can be avoided¹⁸.

Alkanolamine solutions

Alkanolamines are alkanes that contain a hydroxyl group and an amine group at the end of their carbon chains. The amines of these compounds can come in several forms: primary, secondary, or tertiary. Monoethanolamine (MEA), diethanolamine (DEA), triethanolamine (TEA), methyl diethanolamine (MDEA), and adenosine monophosphate (AMP) are all commonly used alkanolamines for carbon dioxide capture¹⁹. There are three primary reaction mechanisms for absorption: the zwitterion mechanism, termolecular mechanism, and base-catalyzed mechanism. Most alkanolamines (primary, secondary, and sterically hindered) follow the zwitterion mechanism shown in Figure 3.



Figure 3: Zwitterion Reaction Mechanism

Figure 4 below shows how tertiary amines follow the base-catalyzed hydration mechanism¹⁹.

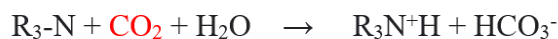


Figure 4: Base-catalyzed Reaction Mechanism

Alkanolamines typically have issues with high vapor pressures and oxidative degradation^{20,21}. The high vapor pressure indicates a high heat of desorption reducing the economic viability of the process. Further, the use of alkanolamines causes corrosion in equipment and creates higher capital expenses²¹. Additionally, the oxidative degradation of the compounds leads to environmental concerns by production of toxic compounds, such as formaldehyde and other heat soluble salts, and waste disposal after the absorbent experiences reductions in absorption capacity, enhanced corrosion, foaming, and other undesirable properties^{20,22}.

Amino acid solutions

Amino acid salt solutions are a viable alternative to the alkanolamine solutions^{23,24} and have multiple advantages over their alkanolamine counterparts. They are resistant to oxidative degradation which allows for further reuse due to the ionic nature of the absorbent²⁵. This, coupled with the fact that amino acid compounds are eco-friendly and found in nature, suggests the solution could be economically feasible and sustainable²¹. Amino acid solutions have also been shown to have similar absorption capacities as compared to alkanolamine solutions^{21,24} as

well as a higher surface tension^{21,23}. Additionally, sterically hindered amine groups commonly found in amino acids require less heat for desorption^{26,27}. This shows the ability of amino acid solutions for comparable carbon dioxide and acid gas reduction at a potentially lower environmental expense.

Amino acids have an amine group and a carboxylic group at each end of their structure forming an amphoteric compound that has a charge change based on the pH of the solution, as shown in Figure 5.

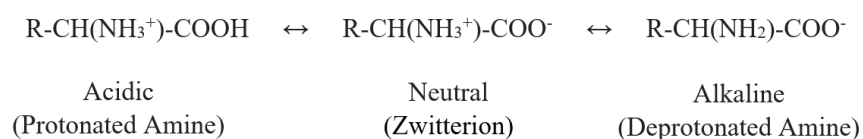


Figure 5: Generic Amino Acid Ionization in Acidic, Neutral, and Alkaline Conditions

At high pH, amino acids act as a base which allows for the lone pairs on the nitrogen from the deprotonated amine group to attack carbon dioxide to form carbamate, as shown in Figure 6. This carbamate can then react with water to form bicarbonate and recover the deprotonated amine group required for further reaction with carbon dioxide. At low pH, when a deprotonated amine reacts with carbon dioxide and water, bicarbonate can be formed in addition to a zwitterion which is unable to react further with carbon dioxide.

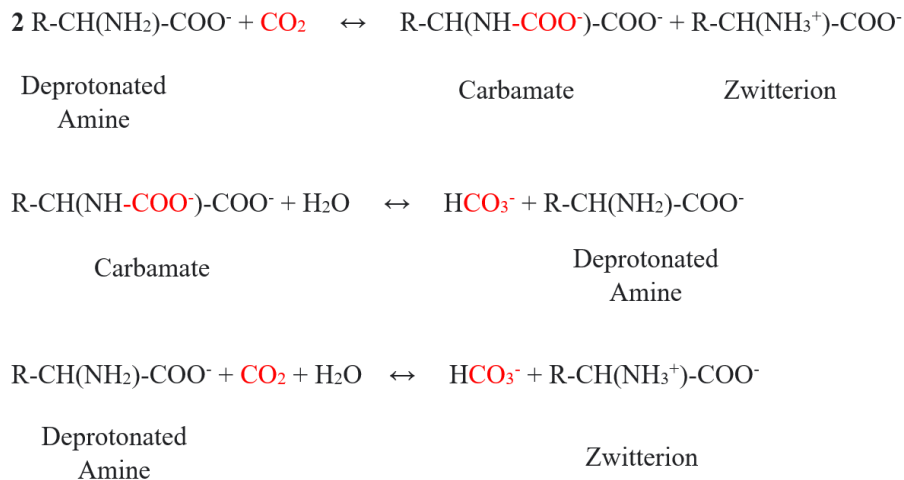


Figure 6: Products of the Reaction of Amino Acids with Carbon Dioxide

Therefore, pH is an important characteristic to observe when determining the performance of an amino acid solution. In addition, amino acids with a lower pKa have better kinetics and a large operational pH range²⁶ due to this pH dependence. A condensed reaction scheme for amino acid absorption is shown below in Figure 7²⁵.

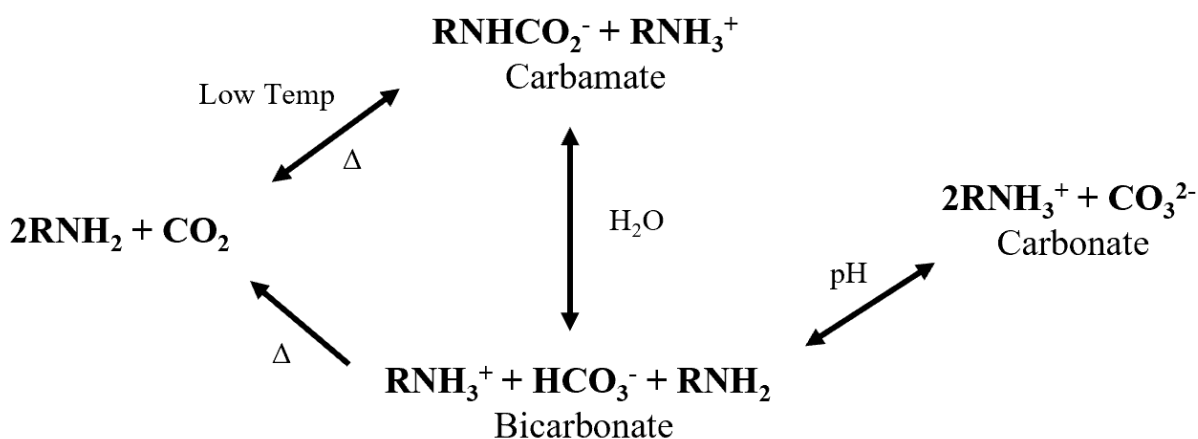


Figure 7: Amino Acid Carbon Capture Reaction Scheme²⁵

From Figure 7, when the solution with high pH is first introduced to carbon dioxide, the deprotonated amine group will react with carbon dioxide to produce carbamate. The carbamate exists in equilibrium with bicarbonate and carbonate with the equilibrium favoring bicarbonate. This carbamate then reacts with water to form bicarbonate and a regenerated amine group which can again react with carbon dioxide when in its deprotonated form. This reaction can continue as long as hydrolysis occurs, and the pH of the solution favors the deprotonated amine group²⁵. Further absorption will continue to reduce the pH of the solution as bicarbonate and carbonate acidify the solution and equilibrium is reached with bicarbonate being the primary product.

Microalgae as a source of amino acids

One possible source of amino acids is microalgae. Microalgae contains large amounts of proteins²⁸ that can be hydrolyzed into amino acids²⁹ through thermal, chemical, and biological reactions. After the hydrolysis, the algae slurry containing a significant amount of free amino acids imitates an amino acid absorption absorbent and could potentially be used as an economically viable and sustainable alternative to replace synthetic amino acid solutions. Conveniently, microalgae achieve their maximum growth rate with higher than atmospheric carbon dioxide concentrations³⁰ with the most biomass being produced at concentrations as high as 10%³¹. Introducing the flue gas from power plants to microalgae cultivation has been shown to increase the growth rate and therefore carbon removal of the microalgae^{32,33}. Additionally, microalgae have the ability to remove acid gases from the flue gas³².

The microalgae used for carbon dioxide capture from the flue gas could be harvested and hydrolyzed as mentioned above to produce an amino acid absorption absorbent. The absorbent would capture additional carbon dioxide from the flue gas which could then be fed back into the algae reactor to produce more microalgae and capture more carbon³⁰. Adding carbon capture

absorbents back into the algal culture provides another carbon source in the form of bicarbonate which could increase the carbon fixation efficiency of the microalgae by up to eight times³⁴. Using an algae based absorption solution can also avoid toxicity to the culture compared to other absorbents such as ammonia³⁵. This approach could greatly increase the cost effectiveness of the post-combustion absorption process and reduce negative environmental externalities. The algae grown can also be used to create other value-added products (i.e., protein-rich animal feed and polymer precursor) to increase the economic viability of the process³⁴. No research has yet been completed using an algal based amino acid solution for carbon dioxide absorption so important parameters such as absorption capacity and heat of regeneration for this solution need to be investigated.

PILOT AND COMMERCIAL CHEMICAL ABSORPTION PROCESSES

Several pilot and commercial plants have been developed by organizations including the University of Texas, CSIRO, University of Stuttgart (CASTOR), BASF, Hitachi, and DOW³⁶. Post-combustion carbon dioxide capture processes would increase the cost of electricity by 80-85%^{37,38} and incur an energy penalty of 35% or more but, with the introduction of new amine absorbents and process intensification, this energy penalty can be reduced to around 15%³⁸. For plants, one major cost comes from absorbent regeneration which accounts for 50-80% of energy costs³⁶. Several test plants have attempted to tackle this issue by selecting new absorbents with a low heat of absorption^{36,37,39,40}. Absorbents with low heat of absorptions allow for reduced heating during absorbent regeneration and energy savings. Additionally, absorbents are selected for their absorption capacity, kinetics, and cyclic capacity⁴¹. Absorbents with higher capacities and kinetics require less solution and residence time in the column leading to smaller columns and reduced capital costs. Absorbents with high cyclic capacities will reduce costs related to

absorbent degradation including absorbent disposal, maintenance costs, and operational costs. Another route of increasing the economic viability of the plants include utilizing the captured carbon dioxide to create a value-added product through processes such as biogas upgrading⁴² or algae cultivation.

SUMMARY OF KNOWLEDGE GAPS

This review establishes that chemical absorption using amino acid absorbents is a viable process for post-combustion carbon dioxide capture. However, the lack of incentives for capturing carbon dioxide inhibits the widespread use of the process. Combined use of algae cultivation and biomass conversion to amino acid absorbents, among other products (i.e., polymer and biofuels), could provide an economical, sustainable, and environmentally friendly alternative to other types of post-combustion chemical absorbents. The complex composition of the algal based absorbent may even provide additional advantages due to synergistic chemistries between compounds⁴³. Despite this, no research has been conducted on the use of algal based amino acid absorbents for post-combustion capture of carbon dioxide. There is limited literature on the optimal conditions for the conversion of algae biomass to amino acids. Additionally, there is no process for isolating these amino acids from the rest of the solution after conversion. The absorption capacity, absorption rate, and regenerability of an algal-based amino acid absorbent are also unknown. This information is of great importance to the design of equipment and determination of process costs.

OBJECTIVE AND HYPOTHESIS

The goal of this study is to develop an algal based chemical absorption process to capture post-combustion carbon dioxide efficiently and sustainably. The hypothesis is that algal-based amino acids should synergistically enhance absorption capacity and improve technical feasibility

of the amino acid absorbent for post-combustion carbon dioxide capture. Correspondingly, five objectives are investigated in this study:

1. Develop a process for converting algal biomass into a mixed amino acid salt absorbent
2. Create an absorption unit that can accommodate the algal amino acid absorbent for carbon dioxide absorption
3. Determine the absorption and cyclic capacity of the algal amino acid absorbent
4. Use analytical spectroscopy to observe changes in the composition of absorbents
5. Conduct a mass and energy balance of the process.

CHAPTER 2: MATERIAL AND METHODS

CHEMICALS AND OTHER MATERIALS

The amino acids Glycine, Alanine, Proline and Lysine HCl powder were purchased from the Bulk Supplements Company. Potassium Hydroxide (KOH) was purchased from Fisher Scientific with a purity of greater than or equal to 85%. The synthetic amino acid solution (GAPL Solution) was mixed with water to create concentrations of 0.25M of glycine, 0.25M alanine, 0.25M proline, and 0.15M lysine for a total of 0.9M amino acid. The additional water generated from amino acid hydrolysis was poured off prior to adding the potassium hydroxide. Some amino acids were lost in this process. Using the *Liquid Chromatograph/Mass Spectrometer (LCMS)* method described below, the concentrations of the amino acids were determined to be 0.232M glycine, 0.216M alanine, 0.213M proline, and 0.174M lysine for a total of 0.835M amino acid. Potassium hydroxide was added to a 1M concentration accounting for 85% purity. The solution had a starting pH around 13. Bone dry carbon dioxide and air were obtained in gas cylinders from Airgas. Polyethylene tubing and brass fittings were used to connect to the regulators on the compressed air cylinders. Algal amino acid processing samples were tested for potassium concentration using the Tetraphenylborate method (HACH, Method 8049, Loveland, CO).

NUCLEAR MAGNETIC RESONANCE (NMR)

The NMR spectra were collected either on a Bruker Avance III HD 500 MHz NMR spectrometer equipped with 5mm iProbe (X-nucleus optimized double resonance broad band probe) or on a Varian Inova 500 MHz NMR spectrometer equipped with 5mm PFG broad band switchable probe. Both spectrometers operate at a frequency of 125 MHz for ^{13}C and 500 MHz for ^1H . All the NMR experiments were run at 25 °C. The NMR samples were prepared by

diluting 0.5 mL of the aqueous amino acid solutions after absorption or desorption with 0.1 mL of deuterium oxide (D_2O) for the signal lock. 1,4-dioxane was added as chemical shift reference.

Quantitative ^{13}C NMR spectra were collected on either of the spectrometers (Bruker HDIII 500 MHz NMR and Varian Inova 500 MHz NMR). The samples ran with Bruker used the following parameters: pulse duration $p_1 = 5 \mu s$ for 45° pulse; number of scans, NS = 800-1600 (more number of scans were used for the three and four amino acid mixtures to get better signal-to-noise ratio); acquisition time, AQ = 1.10 s; and relaxation delay, $D_1 = 60$ s (relaxation time of nuclei $D_1 \geq 5T_1$, T_1 : the longest carbon nuclei relaxation time constant). The samples ran on the Varian were with the following parameters: pulse duration $p_1 = 5.25 \mu s$ for 45° pulse, number of scans, NS = 800-1600; acquisition time, AQ = 1.04 s; and relaxation delay, $D_1 = 60$ s (relaxation time of nuclei $D_1 \geq 5T_1$, T_1 : the longest carbon nuclei relaxation time constant). The ^{13}C NMR spectra were phase corrected automatically, baseline corrected (Whittaker Smoother), and integrated using MestReNova software v.14.2.0.

LIQUID CHROMATOGRAPH/MASS SPECTROMETER (LCMS)

Samples were analyzed by LC/MS/MS using a Waters Xevo TQS Micro interfaced with a Waters Acquity H-class UPLC. 10 μl of sample was injected onto a Waters Acquity HSS-T3 column (2.1x100 mm; 1.7 μm particle size). The 13-minute gradient for separation of amino acids was as follows: initial conditions were 100% mobile phase A (10 mM PFHA in water) and 0% mobile phase B (acetonitrile), hold for 1 min at 100% A, linear ramp to 65% B at 8 min, ramp to 90% B at 8.01 min, hold at 90%B until 9 min, return to initial condition of 100%A at 9.01 min, hold at 100% A until 13 min. The flow rate was 0.3 ml/min and the column temperature was $40^\circ C$. Compounds were ionized by electrospray ionization in positive ion mode with a capillary voltage of 1.0 kV. Source temperature was $150^\circ C$, desolvation temp was $350^\circ C$

and desolvation and cone gas flows were 800 L/hr and 40 L/hr respectively. MS/MS data were obtained using a multiple reaction monitoring method with parameters shown in Table 1, Table 2, and Table 3 below. ¹³C and ¹⁵N-labeled amino acid internal standards were from Sigma (767964-1EA). Data processing was done using the Targetlynx tool in Masslynx.

Table 1: MS/MS Parameters for Function 1 (0-4.5min)

| Parent Ion | Daughter Ion | Dwell Time (s) | Cone Voltage | Collision Energy | Amino Acid |
|-------------------|---------------------|-----------------------|---------------------|-------------------------|--|
| 76 | 30 | 0.1 | 17 | 8 | Glycine |
| 79 | 32 | 0.1 | 17 | 8 | ¹³ C ₂ , ¹⁵ N-Glycine |
| 90.1 | 44 | 0.03 | 17 | 8 | Alanine |
| 94.1 | 47.1 | 0.03 | 17 | 8 | ¹³ C ₃ , ¹⁵ N-Alanine |
| 106.1 | 60 | 0.03 | 19 | 10 | Serine |
| 110.1 | 63 | 0.03 | 19 | 10 | ¹³ C ₃ , ¹⁵ N-Serine |
| 120.1 | 74 | 0.03 | 19 | 8 | Threonine |
| 122 | 76 | 0.03 | 18 | 15 | Cysteine |
| 125.1 | 78.1 | 0.03 | 19 | 8 | ¹³ C ₄ , ¹⁵ N-Threonine |
| 126 | 79 | 0.03 | 18 | 15 | ¹³ C ₃ , ¹⁵ N-Cysteine |
| 133.1 | 74 | 0.03 | 19 | 14 | Asparagine |
| 134.1 | 74 | 0.03 | 19 | 10 | Aspartic acid |
| 139.1 | 77 | 0.03 | 19 | 11 | ¹³ C ₄ , ¹⁵ N-Aspartic acid |
| 147.1 | 84 | 0.03 | 16 | 14 | Glutamine |
| 148.1 | 84 | 0.03 | 19 | 14 | Glutamic acid |
| 154.1 | 89.1 | 0.03 | 17 | 14 | ¹³ C ₅ , ¹⁵ N-Glutamine |

Table 2: MS/MS Parameters for Function 2 (4.5-6.55 min)

| Parent Ion | Daughter Ion | Dwell Time (s) | Cone Voltage | Collision Energy | Amino Acid |
|-------------------|---------------------|-----------------------|---------------------|-------------------------|---|
| 116 | 70 | 0.03 | 21 | 10 | Proline |
| 118.1 | 72 | 0.03 | 17 | 9 | Valine |
| 122.1 | 75.1 | 0.03 | 21 | 10 | ¹³ C ₅ , ¹⁵ N-Proline |
| 124.1 | 77.1 | 0.03 | 17 | 9 | ¹³ C ₅ , ¹⁵ N-Valine |
| 150.1 | 104 | 0.03 | 19 | 9 | Methionine |
| 156.1 | 109.1 | 0.03 | 19 | 9 | ¹³ C ₅ , ¹⁵ N-Methionine |
| 182.1 | 136.1 | 0.03 | 20 | 12 | Tyrosine |
| 192.1 | 145.1 | 0.03 | 20 | 12 | ¹³ C ₉ , ¹⁵ N-Tyrosine |

Table 3: MS/MS Parameters for Function 3 (6.55-13 min)

| Parent Ion | Daughter Ion | Dwell Time (s) | Cone Voltage | Collision Energy | Amino Acid |
|-------------------|---------------------|-----------------------|---------------------|-------------------------|------------------------|
| 132.1 | 86 | 0.03 | 19 | 9 | Leucine |
| 139.1 | 92 | 0.03 | 19 | 9 | 13C5,15N-Leucine |
| 147.1 | 84 | 0.03 | 19 | 14 | Lysine |
| 155.1 | 90.1 | 0.03 | 19 | 14 | 13C6,15N2-Lysine |
| 156.1 | 110 | 0.03 | 20 | 12 | Histidine |
| 165.1 | 118.1 | 0.03 | 20 | 12 | 13C6,15N3-Histidine |
| 166.1 | 120 | 0.03 | 20 | 10 | Phenylalanine |
| 175.1 | 70 | 0.03 | 24 | 18 | Arginine |
| 176.1 | 129.1 | 0.03 | 20 | 10 | 13C9,15N-Phenylalanine |
| 185.1 | 75 | 0.03 | 24 | 18 | 13C6,15N4-Arginine |
| 205.1 | 146 | 0.03 | 19 | 14 | Tryptophan |
| 218.1 | 156 | 0.03 | 19 | 14 | 13C11,15N2-Tryptophan |

ABSORPTION

Trickling Filter Absorption Column

A trickling filter absorption column was made to address foaming issues when the gas contacted the algal amino acid solution. The column was made with 5.08cm diameter furniture grade clear PVC pipe. It was capped with a PVC plug connected by a PVC union. A primer and adhesive were used to bond the PVC pieces together. A drill press was used to bore holes for stainless steel fittings. Two male, 0.635cm NPT fittings were added to the top and bottom of the column for a total of four fittings. One female, 0.635cm NPT fitting was connected to a male fitting on the top and bottom of the column. Epoxy was used to ensure a seal between the fittings and the PVC. A Topfin small air stone was attached to the bottom stainless-steel fitting and was used to purge the gas into the reactor. This purge stone was covered by a PVC pipe cap to prevent direct liquid contact to avoid foaming. The reactor is about 45.72cm long and 5.08cm in diameter for a total volume of 926.7 cm³. P-series 16 Pall rings were added into the column for

increased surface area for the gas-liquid interface. The entire system including the column is shown in Figure 8 below.

Experimental Setup

The gas stream into the reactor was created by mixing the compressed high purity grade carbon dioxide and air (Airgas). First, the gas from each cylinder was fed to a rotameter (VWR, Radnore, PA), maximum flow rates of 0.5LPM and 2.5LPM for CO₂ and air respectively, and then the outlets from each rotameter were connected to a tee connection and mixed to achieve 10% (v/v) carbon dioxide in the inlet stream. The gas then passed through the gas flow meter (OMEGA, FMA, LP1620A-V2, Digital, Stamford, CT). Before connecting the gas stream to the absorption column, the two rotameters were adjusted to achieve the correct gas flow rate and composition by reading the output from the gas flow meter and IR gas analyzer (Quantek, Model 908 IR Gas Analyzer, Grafton, MA). Synthetic amino acid absorbents and algal amino acid absorbents were run at gas flow rates of 0.6LPM and 1.0LPM, respectively. After connecting the gas stream, the outlet of the column was monitored until the concentration of carbon dioxide reached the desired level, 10% carbon dioxide (v/v), indicating that the absorbent is fully saturated.

To setup the column, 300 mL of the absorbent was added to a beaker and the inlet to the metering pump (Iwaki America Inc., EWN-B16PCUR, Holliston, MA) was placed inside the beaker. The outlet of the pump was connected to one of the stainless-steel fitting at the top of the reactor. The other fitting connected the gas outlet to the IR gas analyzer. Once the pump was turned on, the liquid would fall through the column (200 mL/min), being dispersed by the pall rings, before reaching the bottom. At the bottom of the column, one of the two fittings was connected to the air purge stone using 3 inches of plastic tubing. The other fitting was the outlet

for the liquid. A shut-off valve (Grainger, 3ZLG9, Lake Forest, IL) was used to create a 100 mL hold-up in the bottom of the reactor to prevent bubbling out of the column. The liquid outlet returns the liquid back into the beaker for recirculation through the reactor. The pump was run until the carbon dioxide concentration increased to the original concentration (10% v/v CO₂) before the introduction of the absorbent. Absorptions were run at 23°C and atmospheric pressure. At the end of the experiment, the pH of the absorbent was measured with a pH probe (Fisher Scientific, Accumet Basic A15, Waltham, MA), and a sample was taken for NMR and ATR-FTIR (Jasco, FT/IR-660 ATR PRO ONE, Oklahoma City, OK). For absorption cycles, the mass and pH of the solution was measured, and a sample was taken after each absorption and desorption. For the synthetic amino acid absorbent cycles, the experiment was terminated after the carbon dioxide concentration in the gas outlet stream increased to 2% to reduce experiment time. For the algal amino acid absorbent absorption cycles, the mass of solution lost after each cycle was remade using same pH, DI water and sampled to track the amino acid concentrations after dilution. The absorption system is shown below in Figure 8.

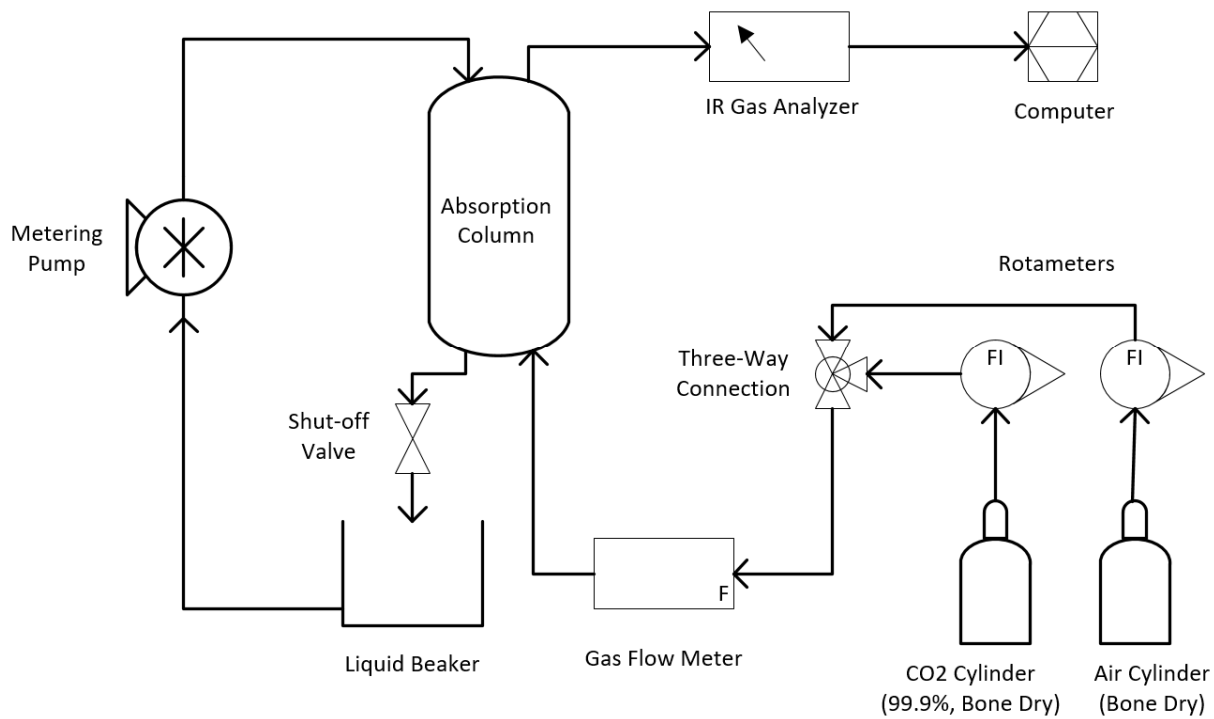


Figure 8: Absorption Experimental Setup

Calculation

During the absorption experiment, the outlet carbon dioxide concentration was measured to calculate the total carbon dioxide absorbed by the absorbent. Knowing the gas flow and inlet concentration, the total amount of carbon dioxide absorbed can be calculated by area of integration method using the CO₂ concentration profiles with operation time. The first integral sums the total mass of carbon dioxide entering the column based on the gas flow, inlet concentration, and time. The second integral sums the total mass of carbon dioxide that leaves the column. This first integral is then subtracted by the second integral to determine the mass of carbon dioxide captured by the absorbent. This is represented as a single integral below.

$$m_{\text{CO}_2, \text{abs}} = \frac{Q_G}{V_L \cdot MW} \int_0^t (c_{\text{in}} - c_{\text{out}}) dt \text{ ----- Equation 1}$$

Where $m_{\text{CO}_2,\text{abs}}$ is the amount of carbon dioxide absorbed (mol/L), Q_G is the gas flow rate through the column (LPM), V_L is the volume of absorbent used (L), MW is the molecular weight of carbon dioxide (g/mol), c_{in} and c_{out} are the concentrations of carbon dioxide going into and leaving the column respectively (g/L), and t is the total absorption time (min). Carbon dioxide concentration was converted from percent by volume to g/L by dividing the percentage by 100 and multiplying by 1.964 (the molecular weight of CO_2 divided by the molar volume from the ideal gas law at standard temperature and pressure (STP)). The mass of carbon dioxide absorbed was converted to mol/mol amine using a conversion factor of the number of amines per mol of amino acid and the amino acid concentrations in solution determined by LCMS. This calculation was performed using the trapezoidal rule in Excel (2019) and the trapz function in MATLAB (R2019b). RStudio (Version 1.3.1056) was used to run ANOVA using the lm function and pairwise comparisons were completed using the package emmeans and Tukey's method.

DESORPTION

Experimental Setup

For the synthetic amino acid absorbent, a 24/40, two-necked, 1L round bottom flask was used to hold 300mL of the absorbent for desorption. A 24/40, two-necked, 2L round bottom flask was used for the algal amino acid absorbent for increased head space to accommodate for the bubbling of the solution during desorption. In one neck of the flask, a Dimroth column was used to condense water vapor using cool tap water to prevent loss from the absorbent solution. The other neck of the flask was used as an inlet for an air sweep gas to force carbon dioxide out of the head space of the flask and maintain a constant gas flow through the system. The flow rate of this gas stream was adjusted to around 0.6LPM using a rotameter and recorded using a gas flow meter. This sweep gas allowed for more accurate measurement of carbon dioxide leaving the

system and prevented carbon dioxide accumulation in the headspace. From the top of the condenser, tubing was used to connect to the IR gas analyzer. The round bottom flask was placed on a heating mantle (Glas-Col, 0412, Terre Haute, IN). A stirring bar was placed in the flask and the heating mantle was placed on top of a stir plate which was set to low for homogenous boiling. The absorbent was heated until there was no significant change in the concentration of carbon dioxide in the outlet over time. The algal amino acid absorbent was heated using a ramped heating method by using a voltage controller (Glas-Col, PL-312 Minitrol, Terre Haute, IN) to reduce bubbling within the flask. The heat initially is set at medium (50%) heat for 30mins then is increased to 75% heat for 15min, 90% heat for 15min, and finally 100% heat until the endpoint is reached. The absorbent was allowed to cool before the pH was taken and a sample was gathered for NMR or FTIR. The desorption system is shown below in Figure 9.

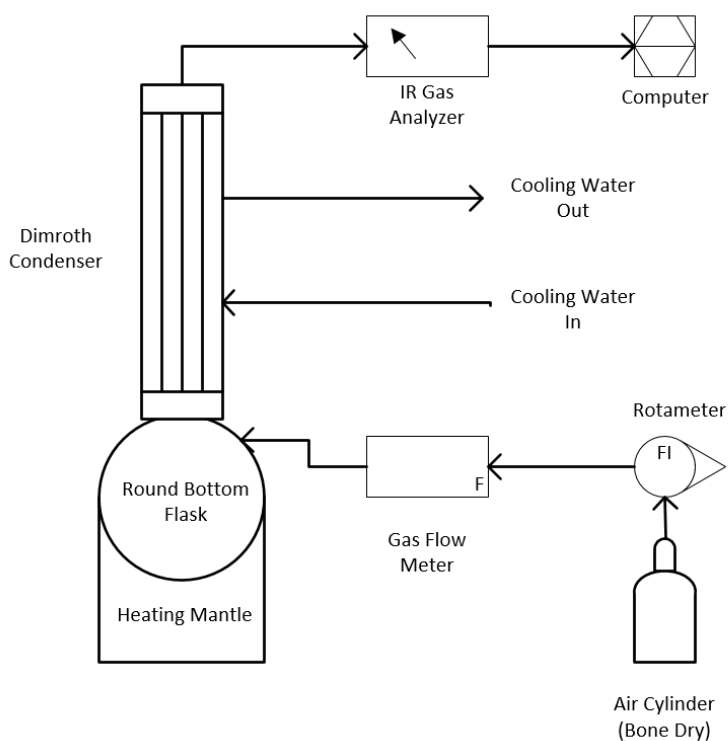


Figure 9: Desorption Experimental Setup

Calculation

The amount of carbon dioxide released from the desorption was calculated using the carbon dioxide concentration in the outlet, the gas flow rate, and time. The integral shown below was used to calculate the total CO₂ desorbed.

$$m_{\text{CO}_2,\text{des}} = \frac{Q_G}{V_L \cdot \text{MW}} \int_0^t (c_{\text{out}}) dt \text{ ----- Equation 2}$$

Where $m_{\text{CO}_2,\text{des}}$ is the amount of carbon dioxide released from the absorbent (mol/L), Q_G is the gas flow rate through the column (LPM), V_L is the volume of absorbent used (L), MW is the molecular weight of carbon dioxide (g/mol), c_{out} is the concentrations of carbon dioxide leaving the column (g/L), and t is the total absorption time (min). This integral was evaluated using the trapezoidal rule in Excel (2019) and the trapz function in MATLAB (R2019b), as well. The mass of carbon dioxide desorbed was converted to mol/mol amine using a conversion factor of the number of amines per mol of amino acid and the amino acid concentrations in solution determined by LCMS. RStudio (Version 1.3.1056) was used to run ANOVA using the `lm` function and pairwise comparisons were completed using the package `emmeans` and Tukey's method.

MICROALGAL PROTEIN CONVERSION TO AMINO ACIDS AND PROCESSING

Experimental Setup

Algal biomass was converted to an algal amino acid product through four processing steps. To get 1L of product, four separate experiments were completed following the process explained in this section. The mass and pH of the solution was recorded after each step and a sample was taken for ATR-FTIR and LCMS analysis. Figure 10 below shows the processing steps for the algal biomass prior to the absorption experiments.

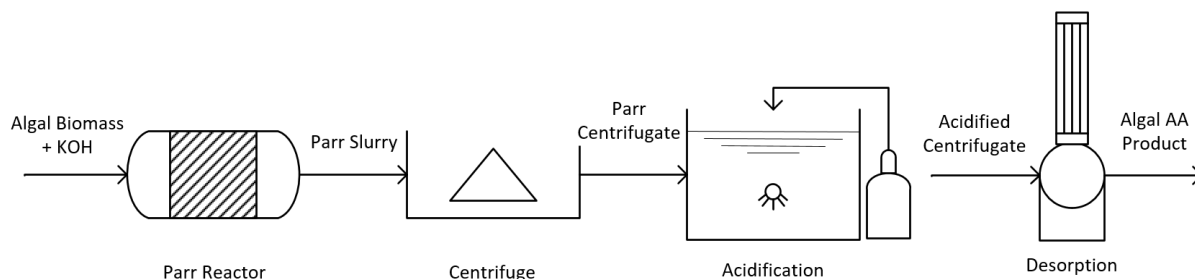


Figure 10: Microalgal Biomass Conversion and Processing Flow Diagram

Algae biomass was collected from a recirculating algae culture⁴⁴ and stored in the freezer. The characteristics of *Chlorella sorokiniana* are shown in Appendix E. Before use, about 250g of the frozen algal biomass thawed for a day. Two samples were taken for total solids analysis and were placed in an oven at 105°C for 12h. Then the mass of the biomass was recorded using a balance (OHAUS, Scout Pro, Parsippany, NJ) giving 0.21g dry algal biomass per gram of wet biomass. Using the Jones factor (6.25g Protein/g N)⁴⁵ and the protein content of the algae⁴⁶, the amount of potassium hydroxide required for the specified ratios are calculated as follows:

$$\frac{0.586\text{g protein}}{\text{g dry algal biomass}} \cdot \frac{1\text{g N}}{6.25\text{g protein}} \cdot \frac{1\text{ mol N}}{14\text{g}} = \frac{0.00670\text{mol N}}{\text{g dry algal biomass}}$$

$$\frac{0.00670\text{mol N}}{\text{g dry algal biomass}} \cdot \frac{0.21\text{g dry algal biomass}}{\text{g wet algal biomass}} \cdot \frac{56.106\text{g}}{1\text{ mol KOH}} = \frac{0.0790\text{g KOH}}{\text{g wet algal biomass}}$$

Based on the calculation above, 19.75g KOH per 250g algal biomass were added for a 1:1 molar ratio of protein to potassium hydroxide. For a 1:5 ratio, the mass of potassium hydroxide was multiplied by five to get 98.75g KOH per 250g algal biomass. The potassium hydroxide was added slowly and mixed until completely dissolved. The Parr reactor, consisting of the motor (Pacific Scientific, SR3642-4982-7-56BC-CU, Moline, IL), reaction vessel (Parr Instrument Company, MAWP 1900psi at 350°C, Moline, IL), and controller (Parr Instrument

Company, 4848, Moline, IL), was filled with the algal biomass and potassium hydroxide solution and set to the conditions specified in Table 5. After the reaction time was complete, the reactor was turned off and the solution was cooled for 24h. The reactor was then emptied, and a sample of the solution was taken for ATR-FTIR, LCMS, and potassium analysis. The rest of the Parr algae slurry was stored in the refrigerator at 4°C. RStudio (Version 1.3.1056) was used to run an ANOVA using the lm function and pairwise comparisons were completed using the package emmeans and Tukey's method to test for the most ideal reactor conditions.

Parr Slurries from runs G, H, I, and J were then put through several processing steps. First, the Parr algal slurry contains solids that must be removed. A centrifuge (Beckman Coulter, Allegra X-12R Centrifuge, Brea, CA) was used to separate these solids at 5°C and 10,000rpm for 10min. The liquid was collected from the tubes and the solids remaining were placed on a scale and their mass was recorded. Two samples were kept in the refrigerator at 4°C for ATR-FTIR, LCMS, and potassium analysis. The pH of each Parr centrifugate was recorded as well. The centrifugate was stored in the refrigerator between processing steps.

The Parr centrifugate still has a high concentration of potassium hydroxide that must be removed to prevent solid precipitation during absorption and to recycle for conversion. An air purge stone was connected to rubber tubing and placed in a 2L beaker. Pure carbon dioxide was released using a rotameter and gas flow meter into the centrifugate from the pressurized gas cylinder. The carbon dioxide reacted with the free hydroxide in the solution to form potassium carbonate and bicarbonate acidifying the solution. A stir bar was placed in the centrifugate and the beaker was placed on a stir plate set on medium. The gas flow rate started at 2.5LPM before being gradually reduced over 45min to a minimum of 0.5LPM to alleviate excessive bubbling of the solution. The pH of the solution was measured in situ and the experiment was ended when

there was no significant pH change over time. The acidified centrifugate was then immediately poured into a beaker and allowed to sit for 24h. The liquid layer at the top of the beaker was poured off and sampled for ATR-FTIR, LCMS, and potassium analysis. The mass of the wet solid layer was measured on a scale and either stored in the refrigerator or placed in the oven at 105°C for 24h and measured for dry mass.

The acidified centrifugate now has too low of a pH (typically around 8.5) to be effective in absorption and must be regenerated. This method is the same as the desorption process for algal amino acid solutions detailed above in the Desorption Experimental Setup Section. Once there is no significant change in carbon dioxide concentration over time, the solution was cooled. The pH was recorded, and a sample was taken for ATR-FTIR, LCMS, and potassium analysis. At this point, the four solutions after desorption were combined into a 2L beaker, mixed, the pH was measured, and a sample was taken for ATR-FTIR and LCMS.

CHAPTER 3: ALGAE BIOMASS CONVERSION AND PROCESSING

Varying the conditions of protein to KOH ratio, reaction temperature, and reaction time, the most effective conditions were chosen to create the algal amino acid absorbent. The conditions with the highest amino acid concentration were considered the best conditions for this study. From Table 4 below, samples G, H, I, and J were used to create the absorbent and are included for more statistical power. The ratio of protein to KOH has the most significant effect on amino acid concentration (AA Conc.) when averaged across the other conditions with a mean of 68.7g/L. The 1:5 ratio of protein to KOH performed significantly better than the 1:1 ratio ($p < 0.05$). The levels of reaction temperature and reaction time tested in this study did not have a significant effect on the amino acid concentration when averaged across the other factors ($p > 0.05$). Therefore, the conditions of a 1:5 ratio, 3h reaction time, and 134°C temperature were selected for the Parr reactor to prepare algal based amino acid salt solution. Appendix A has a table including the significance of each pairwise comparison.

Table 4: Amino Acid Concentrations under Various Parr Reactor Conditions

| Sample ID | KOH mol Ratio | Reaction Temp (°C) | Reaction Time (h) | AA Conc. (g/L) |
|-----------|---------------|--------------------|-------------------|----------------|
| A | 1:5 | 134 | 3 | 59.37 |
| B | 1:5 | 134 | 7 | 69.62 |
| C | 1:1 | 121 | 5 | 14.43 |
| D | 1:1 | 121 | 7 | 16.76 |
| E | 1:1 | 134 | 5 | 14.66 |
| F | 1:1 | 134 | 7 | 13.86 |
| G | 1:5 | 134 | 3 | 75.95 |
| H | 1:5 | 134 | 3 | 69.23 |
| I | 1:5 | 134 | 3 | 63.35 |
| J | 1:5 | 134 | 3 | 60.21 |

After reacting the algal biomass in the Parr reactor, excess solids and KOH were removed from the solution in the next three processing steps: centrifuge, acidification, and desorption. These were described previously in the *Microalgal Protein Conversion to Amino Acids and Solution Processing* Section in Chapter 2. Figure 11 below shows the concentration of individual amino acids after each processing step. There is no significant ($p > 0.05$) difference between the mean amino acid concentrations of the four processing steps confirming that amino acids are not lost throughout the process. Some of the major amino acids in the biomass are alanine, glutamic acid, glycine, aspartic acid, leucine, lysine, and proline. Many of these amino acids are observed in similar quantities among microalgae species⁴⁷⁻⁴⁹. However, the quantity of arginine, threonine, and serine are relatively low compared to reported values, while alanine and glycine have higher values than some of those reported in the literature⁴⁷⁻⁴⁹. Glycine, alanine, proline, and lysine compose 45.8% of the amino acid concentration of the solution. Since this is such a large proportion, a synthetic solution of these four amino acids is studied in the next Chapter as a control absorption solution to the algal absorbent.

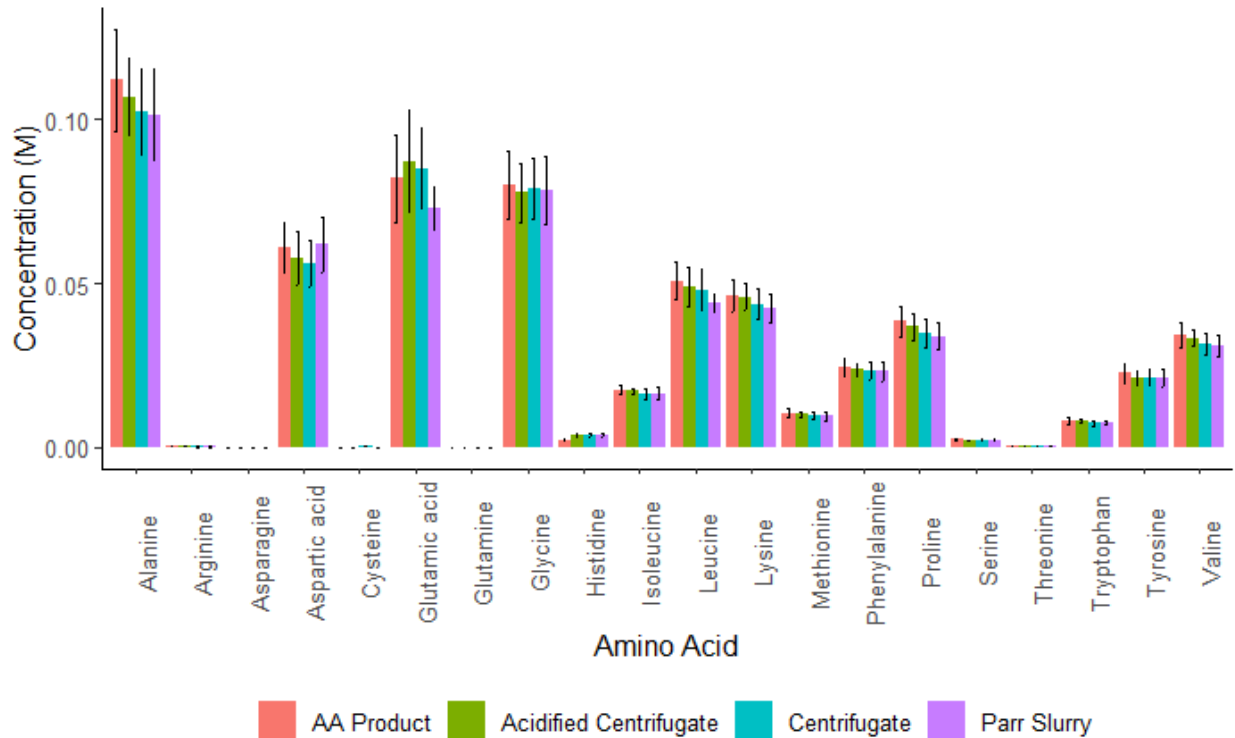


Figure 11: Amino Acid Concentrations after each Processing Step

A mass balance was conducted to observe the flow of different materials throughout the process. This information could then be used to recycle compounds such as KOH as they leave the system. As can be observed from Figure 12, 31% of the mass that enters the system leaves as the algal amino acid absorbent. Another 30% leaves as wet solids after the acidification step. The solids from this are formed from the reaction between carbon dioxide and hydroxide to create carbonate in the solution. Due to the large amount of KOH added to the biomass, the carbonate is formed to an extent that exceeds the solubility within the solution and precipitates as a solid. Since the liquid was separated by simply pouring off the top layer, there is residual liquid within the solids (55% dry mass). This leaves 211.5g of dry solids, most of which (79.4%) are potassium carbonate, as shown by Figure 13, that can be recycled to KOH using a kilning process⁵⁰. This would greatly reduce the costs of the biomass conversion process. The centrifuge

solids compose the final 34% of the mass leaving the process. The remainder of mass not accounted for is lost during the transfer between glassware. The energy consumed by each piece of equipment is shown in Table 5 and are overestimates calculated using the current and voltage listed on the devices. The conversion of algal biomass to amino acids in the Parr reactor accounts for most of the energy consumed during the process at 76% of the total energy consumed.

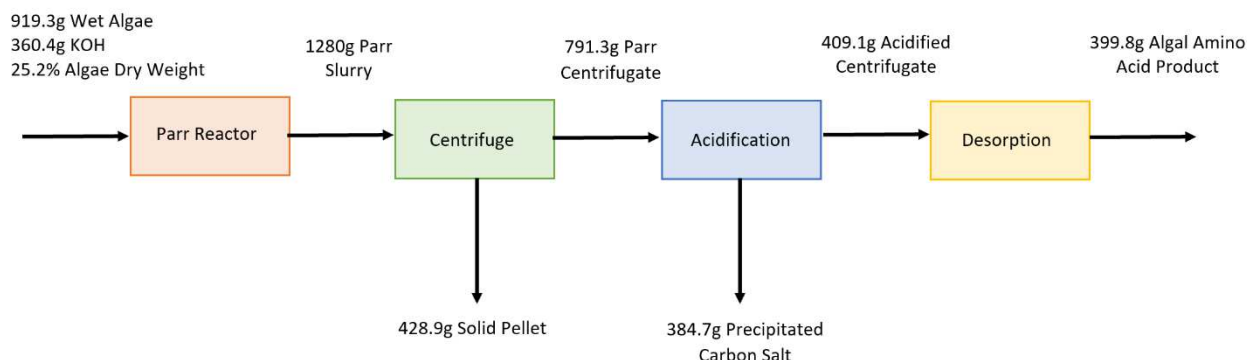


Figure 12: Mass Balance of the Biomass Conversion Process

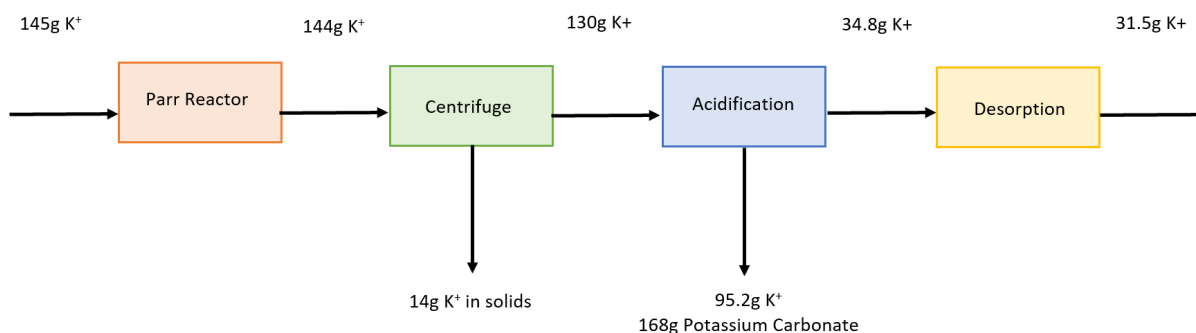


Figure 13: Potassium Mass Balance of the Biomass Conversion Process

Table 5: Energy Consumption of Process Equipment

| | Energy Consumption (kWh/kg Solution) |
|---------------------|--------------------------------------|
| Parr Reactor | 9.99 |
| Centrifuge | 1.19 |
| Desorption | 2.04 |

The ATR-FTIR spectra shown in Figure 14 below show the change in the algal amino acid solution after each process step. The biggest change occurs after the acidification step where

new peaks are recorded at around 1300 and 1350 cm^{-1} . These two peaks disappear after desorption showing that the absorbent is ready to be reused for absorption. The peaks at 1560 and 1630 cm^{-1} are relatively unchanged throughout the process. The pH change likely accounts for the changes in rank order between the two peaks since the acidification step is around 3 pH units lower than the other steps.

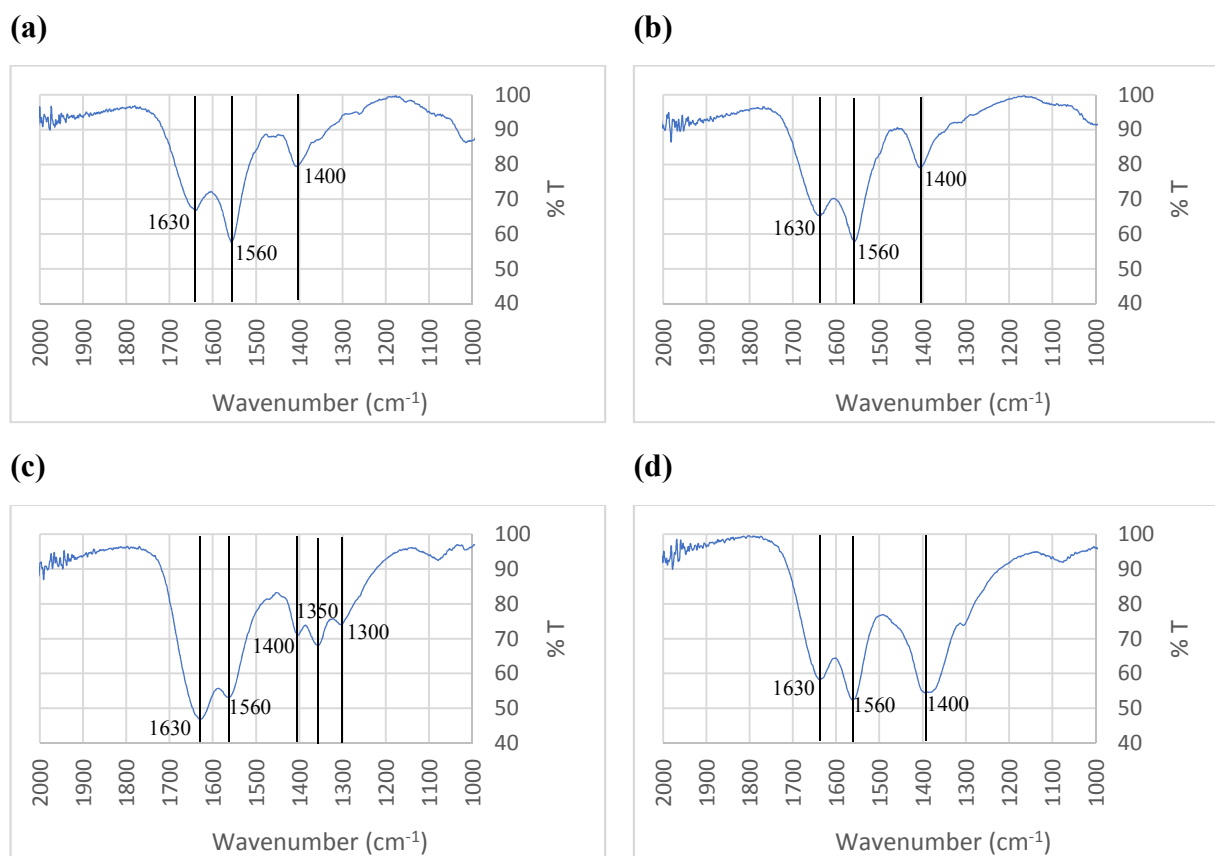


Figure 14: ATR-FTIR Spectra for the Algal Amino Acid Solution after a) Parr Reactor b) Centrifuge c) Acidification d) Desorption

CHAPTER 4: USING A SYNTHETIC AMINO ACID (GAPL) ABSORBENT FOR CO₂ ABSORPTION FROM A SYNTHETIC FLUE GAS CONTAINING 10% CO₂

The first objective of this research was to develop an absorption column that was able to utilize the algal amino acid absorbent. The trickling filter absorption column was first tested with a synthetic amino acid absorbent to ensure it was operating properly and to determine the effective gas to liquid (G/L) flow ratios. Several G/L flow ratios were tested to determine an effective range for carbon dioxide absorption experiments. Figure 15 shows the synthetic amino acid absorption curve for a G/L flow ratio of 0.5 LPM. All curves have a similar shape but differ in the length of the complete absorption region (CO₂ at 0%) at different G/L flow ratios.

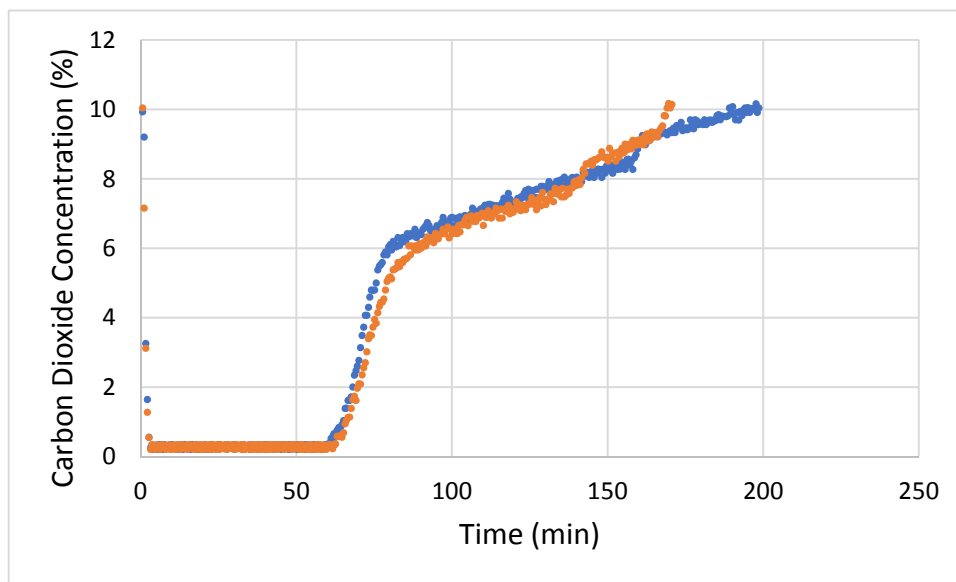


Figure 15: Synthetic Amino Acid Absorbent Absorption Curve for a Gas to Liquid Flow Rate of 2.5

As Table 6 and Figure 16 show below, a G/L flow ratio of 3 absorbs the most carbon dioxide and was used in the following synthetic amino acid absorption cycle experiments. The statistical analysis shows that the means of two G/L ratios, 0.5 and 4, were determined to be significantly ($p < 0.05$) different from all other means. The means of G/L ratios 1.875, 2.5, and 3

are significantly ($p < 0.05$) higher than the means of G/L ratios 0.5 and 4 but are not significantly ($p > 0.05$) different from each other. The significance of each pairwise comparison can be found in Appendix B.

Table 6: Absorption Totals for Different G/L Flow Ratios

| G/L ratio | Gas Flow (LPM) | Liquid Flow (LPM) | Amount Absorbed (mol CO₂/mol Amine) |
|------------------|-----------------------|--------------------------|---|
| 0.5 | 0.1 | 0.2 | 0.223 ± 0.011^a |
| 1.875 | 0.375 | 0.2 | 0.662 ± 0.051^c |
| 2.5 | 0.5 | 0.2 | 0.687 ± 0.007^c |
| 3 | 0.6 | 0.2 | 0.746 ± 0.021^c |
| 4 | 0.8 | 0.2 | 0.535 ± 0.025^b |

*Means sharing the same letter within the same column are not significantly different based on a Type I error rate of 5%

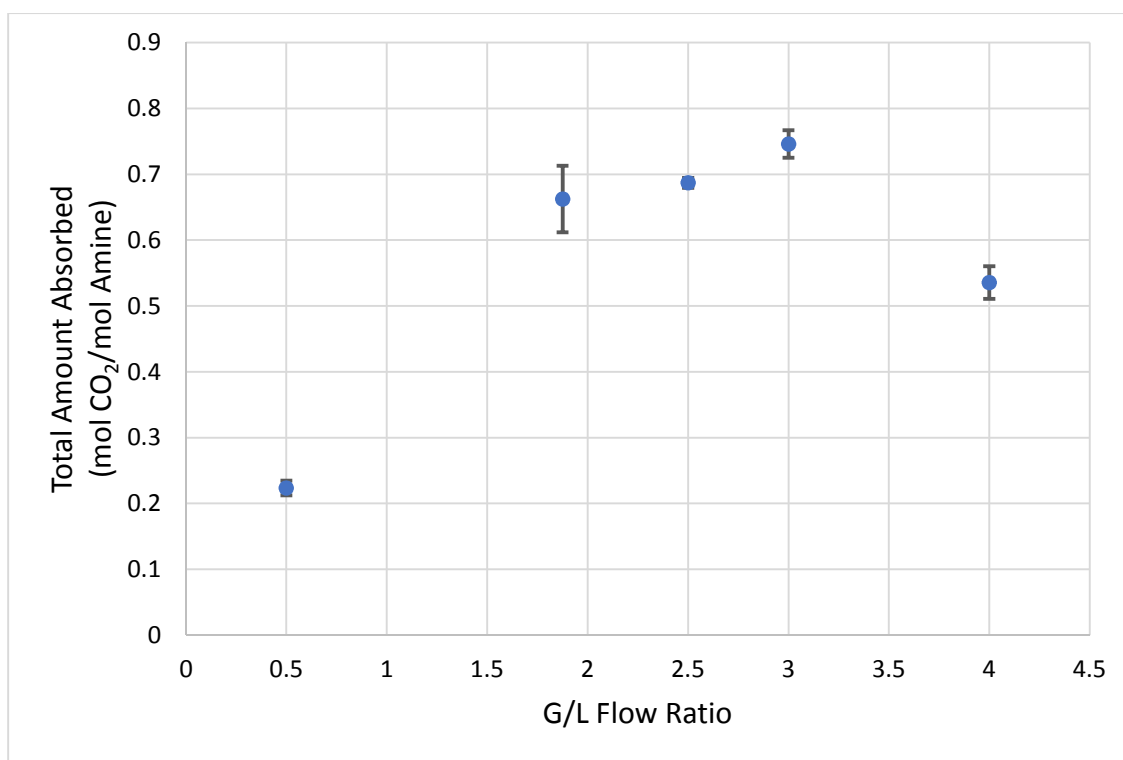


Figure 16: Carbon Dioxide Absorbed for Varied Gas to Liquid Flow Ratios

A baseline for the regenerability of the algal amino acid absorbent is necessary.

Therefore, the synthetic amino acid absorbent was tested across 4 absorption and desorption

cycles. After the first cycle, the amount absorbed by the solution seemed to stabilize and there were no significant ($p>0.05$) differences between the means of the last three cycles. The significant difference between the amount of carbon dioxide absorbed in the first absorption and the following absorptions is likely due to excess hydroxide ions in the absorbent which are converted to carbonate after the first absorption. This carbonate is unable to be converted back into hydroxide during desorption as shown by the amount of carbon dioxide released in Table 7 and Figure 17 below. This results in an absorbent with a maximum absorption capacity that is directly related to the amount of carbon dioxide that can be released from the solution. Since there is no evidence of a significant ($p>0.05$) change in the amount desorbed across the 4 cycles, it was assumed that the absorbent was completely regenerable after the initial absorption.

Table 7: Synthetic Absorbent CO₂ Absorption and Desorption Capacities

| | Cycle Number | | | |
|---|----------------------|---------------------|---------------------|------------------------|
| | 1 | 2 | 3 | 4 |
| Amount Absorbed (mol/mol Amine) | 0.466 ± 0.023^a | 0.348 ± 0.022^b | 0.338 ± 0.022^b | 0.354 ± 0.040^{ab} |
| Amount Desorbed (mol/mol Amine) | 0.287 ± 0.0002^a | 0.296 ± 0.024^a | 0.301 ± 0.015^a | 0.310 ± 0.026^a |

*Means sharing the same letter within the same row are not significantly different based on a Type I error rate of 5%

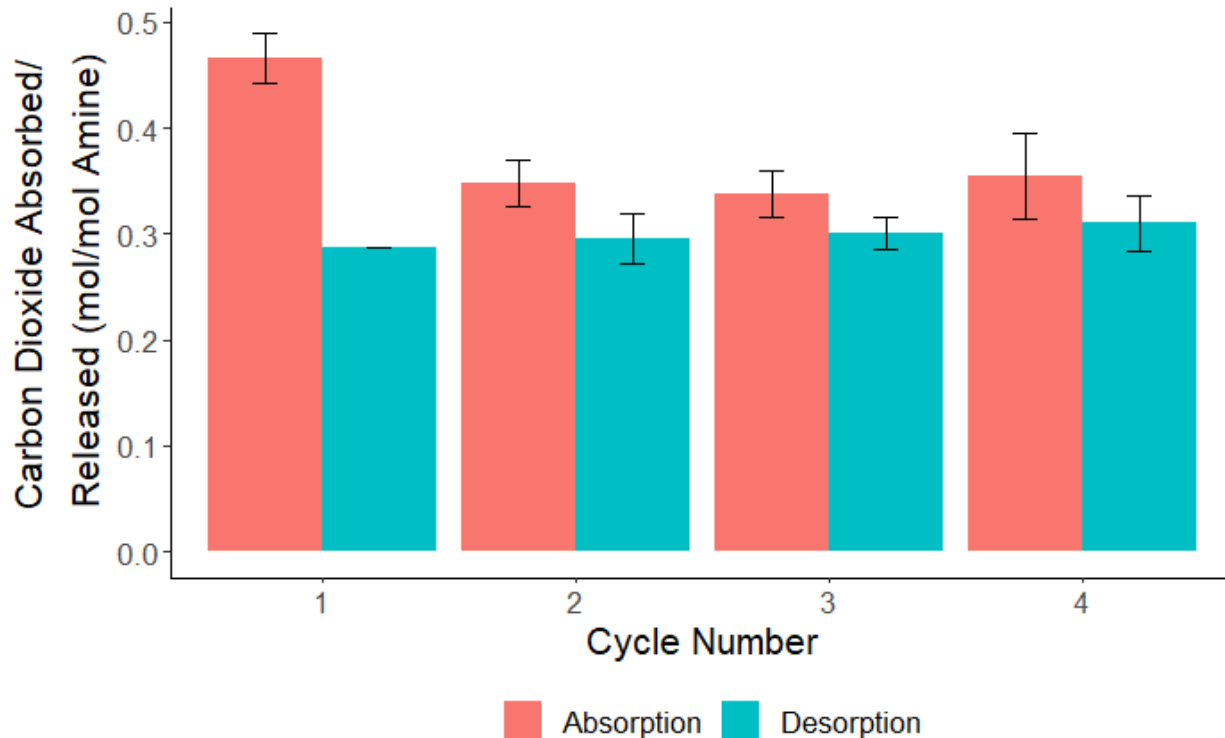


Figure 17: Synthetic Absorbent CO₂ Absorption and Desorption over Four Cycles

The regenerability of the absorbent is further confirmed by the pH data, as shown in Table 8 and Figure 18. The capacity of an absorbent is directly correlated to its pH. At high pH, the amine groups in the absorbent are deprotonated and are free to continue to bond carbon dioxide. An increase in the pH of the absorbent indicates that the absorbent regained its ability to react with carbon dioxide. There is an initial unrecoverable drop in pH after the first absorption. This is likely due to excess hydroxyl groups in the absorbent bonding to carbon dioxide to form carbonate in the solution. These carbonate molecules are not removed during desorption because they are more stable than bicarbonate and carbamate and create a permanent decrease in the pH of the absorbent.

Table 8: Synthetic Absorbent pH over Four Absorption Cycles

| | Initial | Abs 1 | Des 1 | Abs 2 | Des 2 | Abs 3 | Des 3 | Abs 4 | Des 4 |
|---------------------------|--------------------|-------------------|--------------------|--------------------|--------------------|-------------------|--------------------|--------------------|--------------------|
| pH | 12.97 ^a | 9.82 ^b | 11.50 ^d | 9.73 ^{bc} | 11.36 ^d | 9.47 ^c | 11.45 ^d | 9.67 ^{bc} | 11.42 ^d |
| Standard Deviation | 0.0566 | 0.0707 | 0.0283 | 0.0141 | 0.1626 | 0.1414 | 0.0919 | 0.0495 | 0.0636 |

*Means sharing the same letter within the same row are not significantly different based on a Type I error rate of 5%

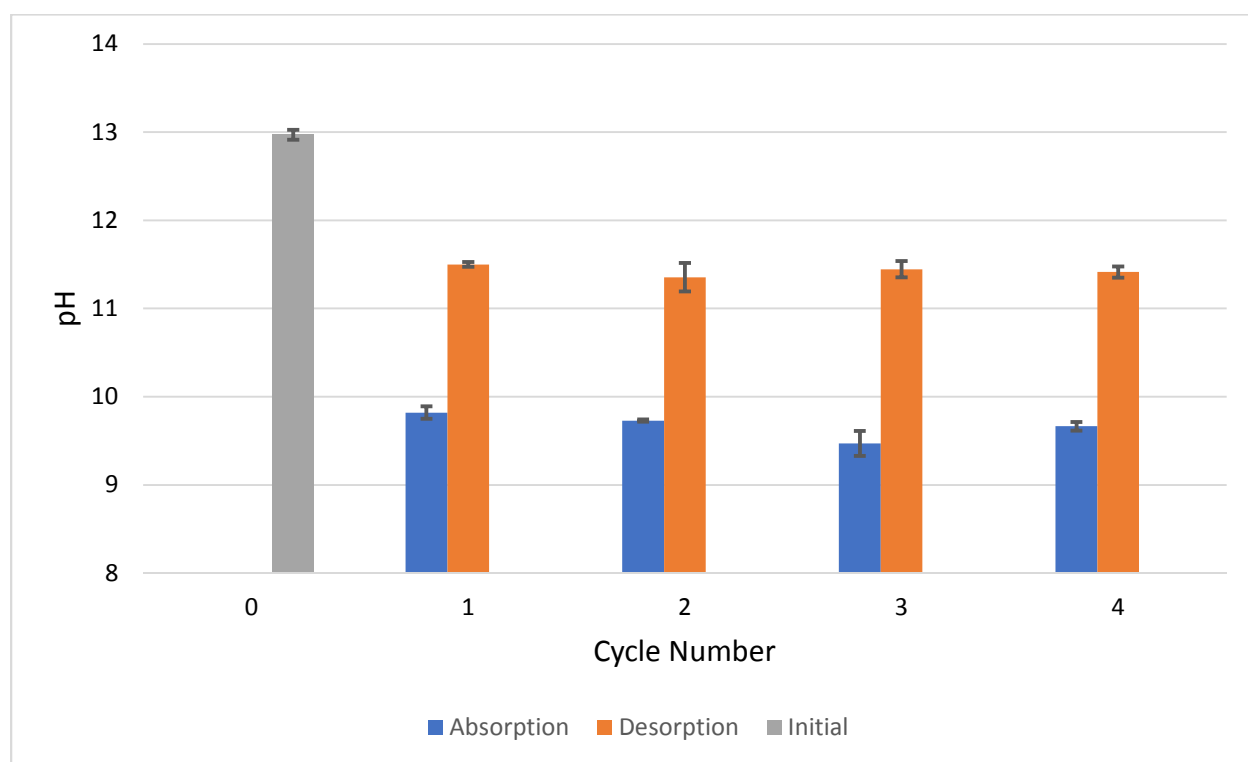


Figure 18: Synthetic Absorbent pH over Four Absorption and Desorption Cycles

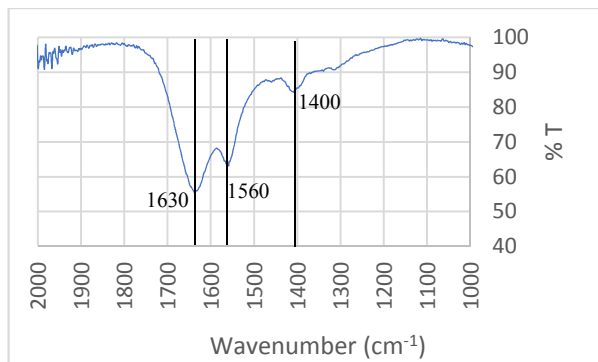
ATR-FTIR was used to analyze the change in the absorbent after absorption and desorption. Figure 19 shows the composition of the original absorbent, absorbent after absorption, and absorbent after desorption. After absorption, two additional peaks are generated at around 1350cm^{-1} and 1300cm^{-1} . After desorption, those peaks disappear, and the spectra very closely resembles the spectra of the original solution. The peaks at 1350cm^{-1} and 1300cm^{-1} correspond to the generation of bicarbonate⁵¹⁻⁵³ and carbamate^{51,52} during absorption, respectively. Since these peaks disappear, it shows that the absorbent is regenerable and that the

absorbent regains the chemistry of the original solution. The peaks at around 1400cm^{-1} and 1563cm^{-1} are estimated to be carboxylates from carbonate since they do not disappear after desorption. The peaks at 1633cm^{-1} and 3000cm^{-1} are assigned to water⁵¹⁻⁵³. Table 9 below shows the peak assignments

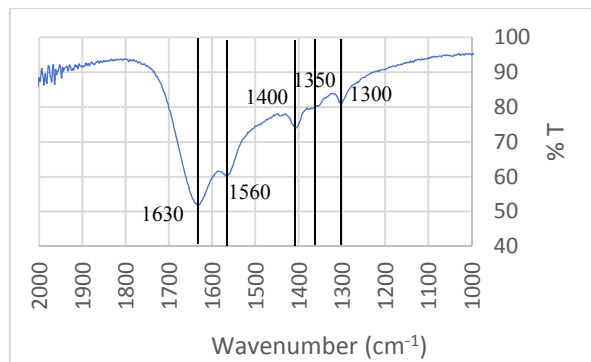
Table 9: ATR-FTIR Peak Identification Table

| Species | Frequency (cm^{-1}) | Type | Literature Frequency (cm^{-1}) |
|------------------------------|--|---|---|
| Carbamate | 1300 | ν N-COO ⁻ | 1283 ⁵² , 1322 ⁵¹ |
| Bicarbonate | 1350 | ν_{sy} CO | 1360 ⁵³ |
| Carboxylate/Carbonate | 1400 and 1560 | ν_{as} and ν_{s} COO- | 1595 and 1405 ⁵² |
| H₂O | 1630 | δ_{d} H-O-H | 1625 ⁵³ |

(a)



(b)



(c)

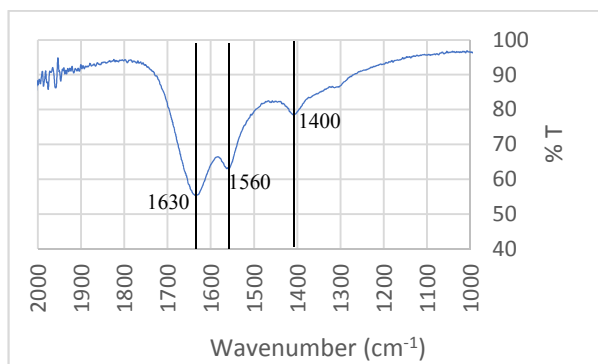


Figure 19: Synthetic Amino Acid Absorbent ATR-FTIR Spectra **a)** Original, **b)** After Absorption, **c)** After Desorption

CHAPTER 5: ALGAL AMINO ACID SOLUTION ABSORPTION

Another objective of the research was to determine the absorption and cyclic capacity of the algal amino acid absorbent. This information is important for determining the environmental and economic advantages of using algal amino acid absorbents for post combustion carbon dioxide capture. Figure 20 below shows the algal absorption curve for all 8 of the absorption cycles. The leftward trend of the plot is due to the dilution of the absorbent solution. Overall, the curve has the same shape across cycles and shows the repeatability of the experiment.

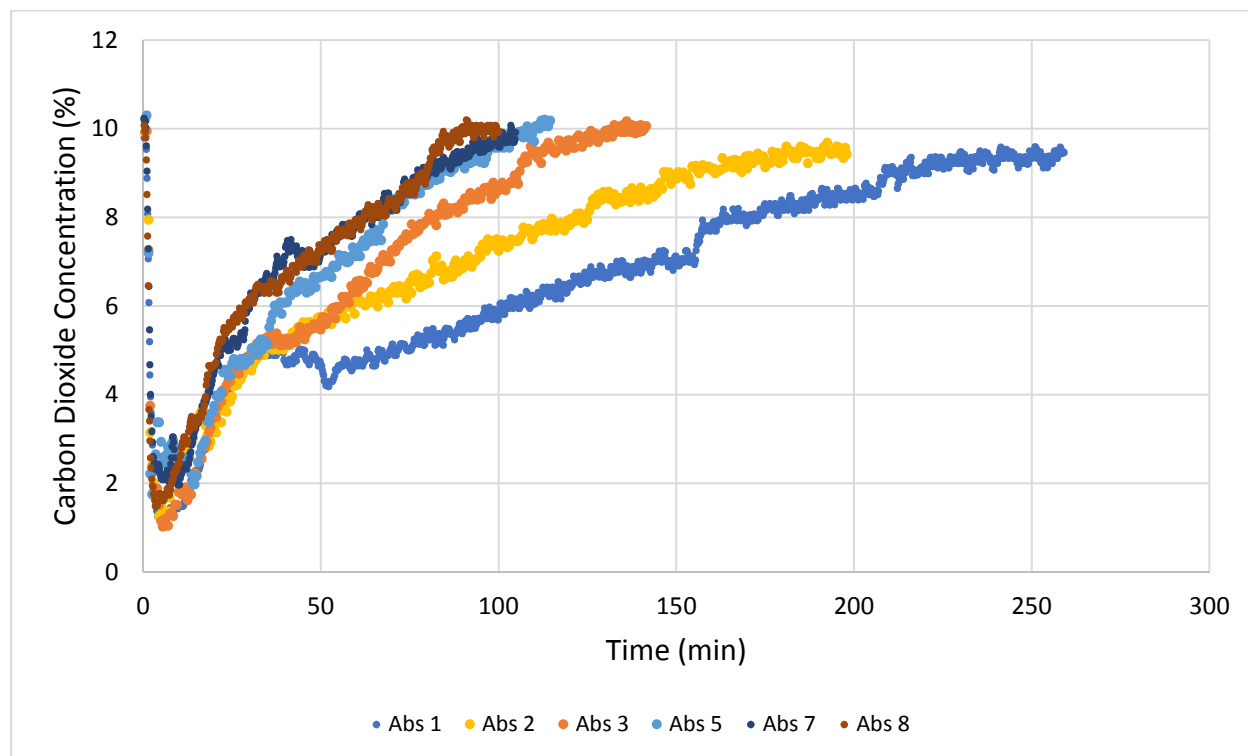


Figure 20: Algal Amino Acid Absorbent Absorption Curves

The absorption capacity and regenerability of the algal amino acid absorbent was determined by completing 8 absorption and desorption cycles. There were atypical experimental conditions during cycles 4 and 6 and the data were removed for greater clarity of results. Table 10 and Figure 21 below show the amount of carbon dioxide absorbed and desorbed for the

cycles. Appendix C has more information on the amount of CO₂ absorbed and desorbed for each cycle. Like the synthetic absorbent results (GAPL solution), there was a drop in absorption capacity of the solution after the first absorption. The absorption stabilizes after the first absorption and there does not appear to be a significant difference between the absorptions from cycles 2 through 8. This is likely due to excess hydroxyl groups in the solution that are used up during the first absorption. The following absorptions are representative of the regenerability of the absorbent. It appears that the absorbent is highly regenerable after the first absorption. The desorption values match the absorption values showing little accumulation of carbon dioxide in the absorbent. Also, there does not appear to be any downward trend of the absorption capacity.

Table 10: Algal Amino Acid Absorbent CO₂ Absorption and Desorption Capacities

| | Cycle Number | |
|---|--------------------|--------------|
| | 1 | 2-8 |
| Average CO₂ Absorbed (mol/mol Amine) | 2.02 ¹ | 1.27 ± 0.061 |
| Average CO₂ desorbed (mol/mol Amine) | 0.967 ¹ | 1.18 ± 0.093 |

*: ¹ indicates that the standard deviation cannot be computed for cycle 1 due to no replicates

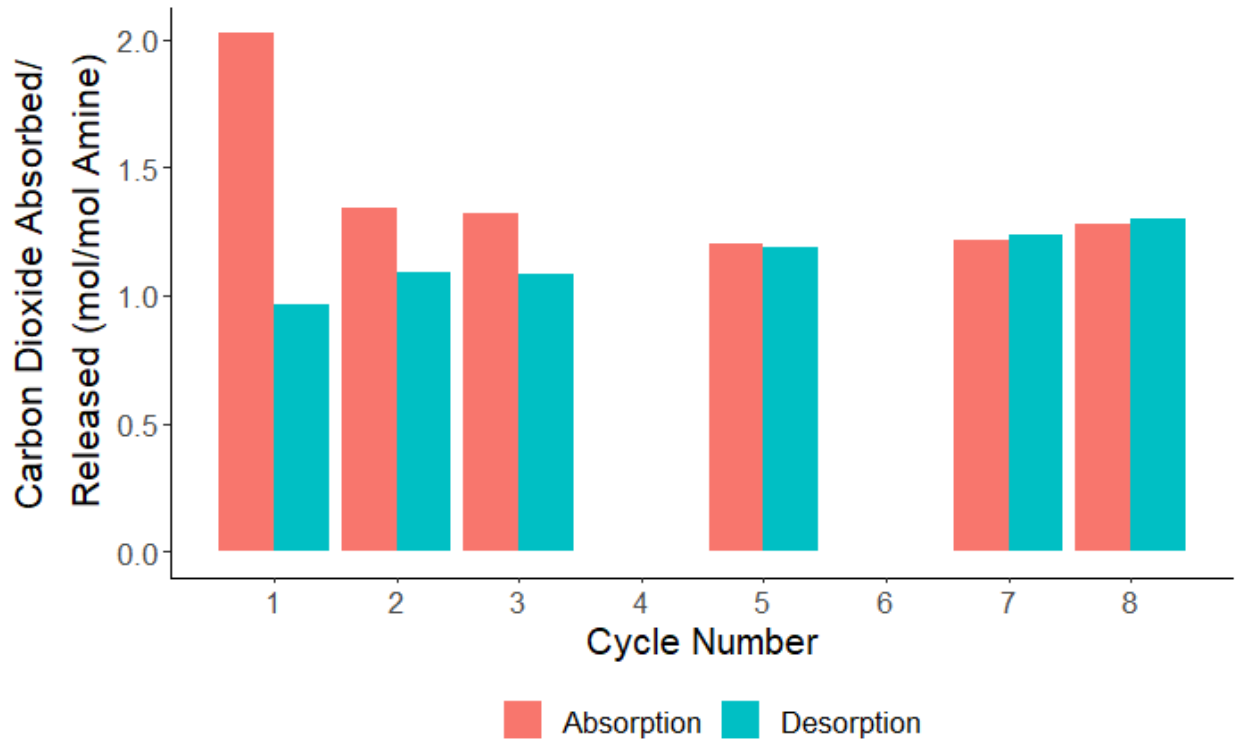


Figure 21: Algal Amino Acid Absorbent Absorption and Desorption Capacities

The pH of the algal amino acid absorbent is quite steady with a change of about 0.4 pH units after 8 cycles. However, Figure 22 shows a slight downward trend due to the dilutions. Appendix C shows the pH values of the solution after each cycle. Interestingly, there is not a large drop in pH after the first absorption like was observed in the synthetic absorbent. This is likely due to the precipitation of the formed carbonate and bicarbonate in the algal absorbent. During the acidification step, the algal absorbent was oversaturated with carbonate causing it to precipitate from solution as a solid. The synthetic absorbent lacks this step and retains the carbonates in solution causing a reduction in pH not seen in the algal absorbent results. This theory is validated by the observation of solids at the bottom of the absorption beaker after the

first algal absorption. Therefore, acidification of the algal absorbent should be completed twice or for a longer period to ensure all free potassium hydroxide is reacted prior to absorption.

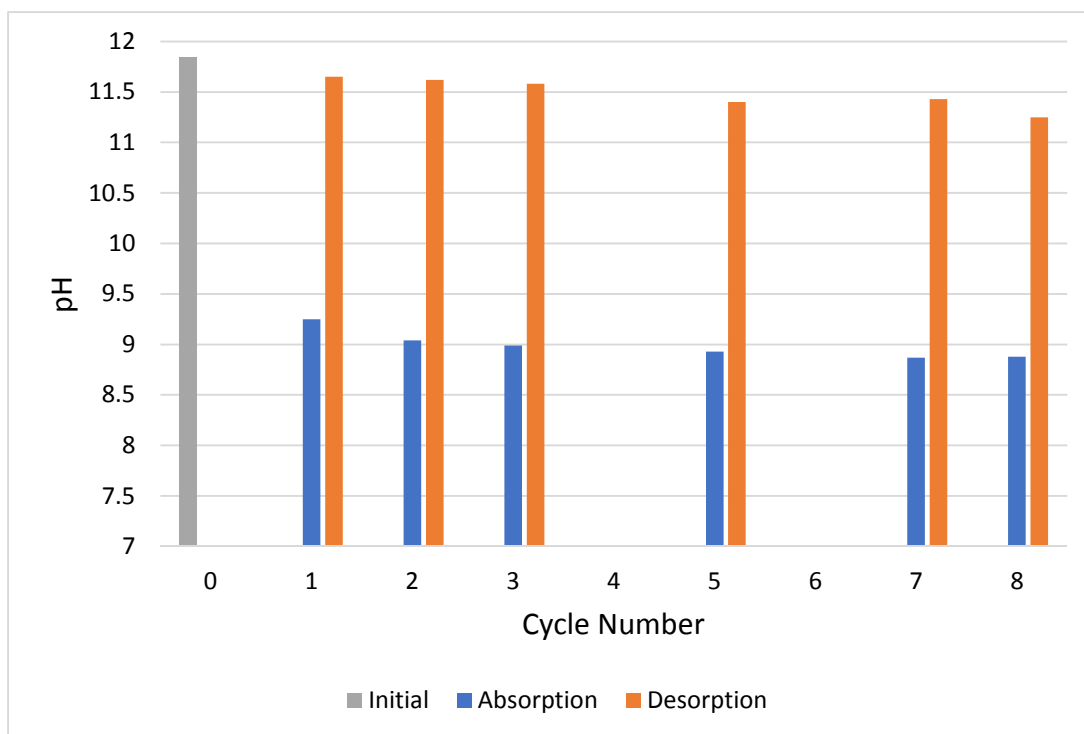


Figure 22: Algal Amino Acid Absorbent pH over Absorption and Desorption Cycles

The ATR-FTIR spectra in Figure 23 below are very similar to the synthetic absorbent spectra in Chapter 4. They both share peaks at wavenumbers 1630cm^{-1} and 1560cm^{-1} . Additionally, the same absorption and desorption trend is observed. After absorption, two additional peaks are observed at around 1350 and 1300cm^{-1} which correspond to bicarbonate and carbamate since they are generated during absorption and disappear after desorption. The peak at 1400cm^{-1} is assigned to the carboxylate in carbonate since it is present in both the desorbed and absorbed spectra⁵¹⁻⁵³. Overall, the spectra show that the absorbent regains a similar composition to itself prior to absorption. This suggests that the absorbent is highly regenerable as seen in Figure 21 and Figure 22 above.

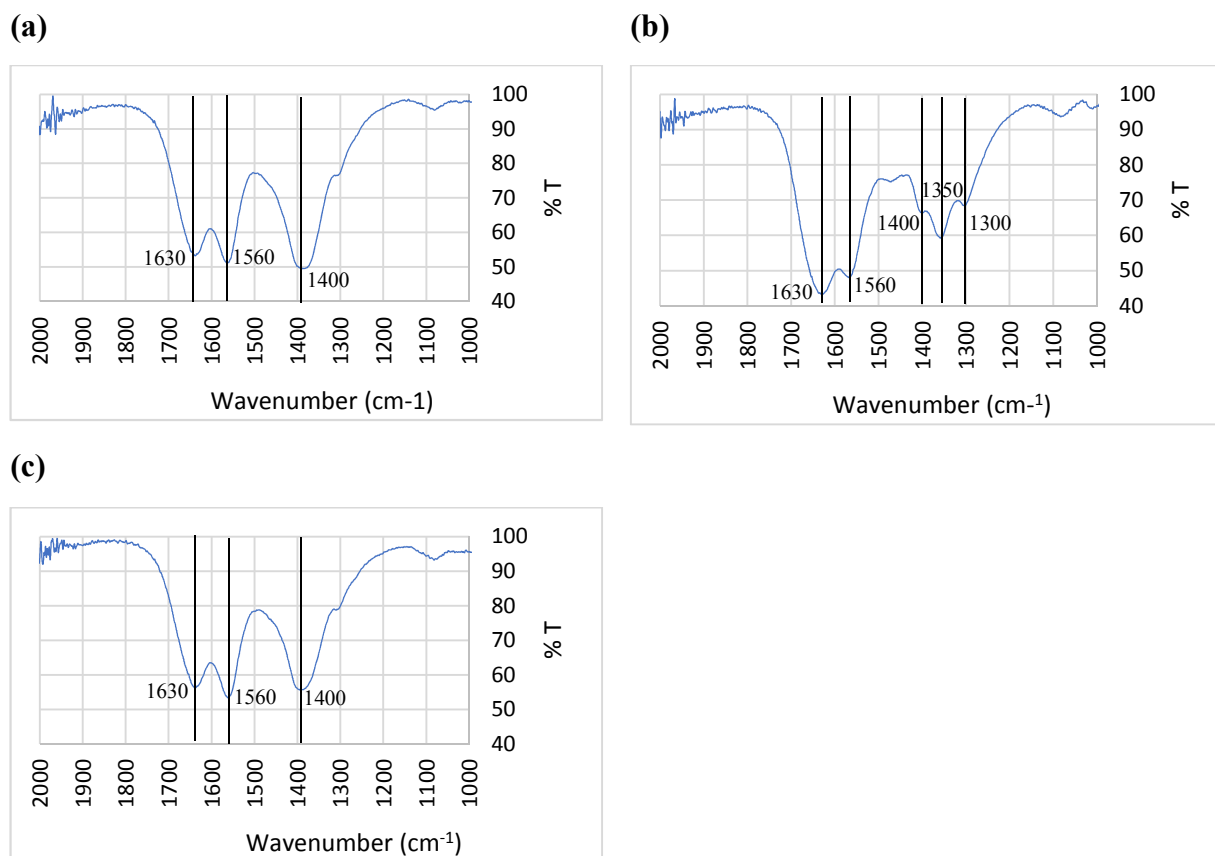


Figure 23: Algal Amino Acid Absorbent ATR-FTIR Spectra **a)** original **b)** after absorption **c)** after desorption

The final objective of this research was to compare the absorption capacity of the algal amino acid absorbent to that of a synthetic amino acid (GAPL) absorbent. Figure 24 below contains the absorption capacities of the two absorbents in mol/mol amine. Appendix C includes a table of the exact values along with a plot in mol/L. The algal amino acid absorbent had a significantly higher absorption capacity ($p < 0.05$) compared to the synthetic absorbent (1.27 to 0.747 mol CO₂/mol amine, respectively). This suggests that there are other factors increasing the absorption capacity. The algal absorbent has other components of the biomass remaining in the

solution such as carbohydrates⁵⁴, polypeptides, and lipids⁵⁵ that may have a synergistic effect with the amino acids when used for carbon dioxide absorption and desorption. This could be useful in the development of better absorbents for further reduced costs and environmental impact. Other studies have reported similar absorption capacities to those determined here. Figure 24 shows the average cyclic absorption capacity of some amino acid absorbents and MEA from the literature along with standard deviation error bars. Solutions of 1M glycine, alanine, and proline with KOH had cyclic absorption capacities of 0.465, 0.535, and 0.412 mol/mol amine, respectively²⁷. Another study that used an organic base with 2.5M glycine and alanine determined cyclic absorption capacities of 0.519 and 0.518 mol/mol amine, respectively²⁴. A 0.5M equimolar KOH and lysine solution captured 0.378 mol/mol amine³. Overall, the numbers reported in this study are similar to those found in related literature shown in Table 11. When looking to compare cyclic absorption capacity against the most common absorbent (MEA), the algal absorbent greatly outperforms by over 300%. MEA had a very comparable cyclic absorption capacity to the amino acid absorbents at around 0.385 mol/mol amine^{24,27,56}.

Table 11: Literature Absorption Capacities for Amino Acid and MEA Absorbents

| Absorbent | Absorbent Concentration (M) | Temperature (°C) | CO ₂ Concentration (kPa) | Absorption Capacity (mol/mol amine) | Cyclic Capacity (mol/mol amine) | Reference |
|----------------------------|-----------------------------|------------------|-------------------------------------|-------------------------------------|---------------------------------|---------------|
| MEA + KOH | 1.0 | 40 | 15 | 0.736 | 0.483 | ²⁷ |
| Glycine + KOH | 1.0 | 40 | 15 | 0.738 | 0.465 | ²⁷ |
| Alanine + KOH | 1.0 | 40 | 15 | 0.670 | 0.535 | ²⁷ |
| Proline + KOH | 1.0 | 40 | 15 | 0.746 | 0.412 | ²⁷ |
| MEA + KOH | 2.5 | 40 | 10 | 0.529 | 0.303 | ²⁴ |
| Glycine + MAPA | 2.5 | 40 | 10 | 0.519 | 0.338 | ²⁴ |
| Alanine + MAPA | 2.5 | 40 | 10 | 0.518 | 0.308 | ²⁴ |
| MEA + KOH | 2.5 | 22 | 4.8 | 0.5 | n/a | ²⁵ |
| Glycine + KOH | 2.5 | 22 | 4.8 | 0.49 | n/a | ²⁵ |
| Alanine + KOH | 2.5 | 22 | 4.8 | 0.52 | n/a | ²⁵ |
| Alanine + KOH + Piperizine | 1.5 | 40 | 9.6 | 0.7238 | n/a | ²¹ |
| Glycine + KOH | 1.0 | 20 | 5.6 | 0.689 | n/a | ⁵⁷ |
| MEA + KOH | 2.5 | 40 | 41 | 0.635 | n/a | ⁵⁷ |
| MEA + KOH | 1.0 | 40 | 9.5 | 0.593 | 0.368 | ⁵⁶ |

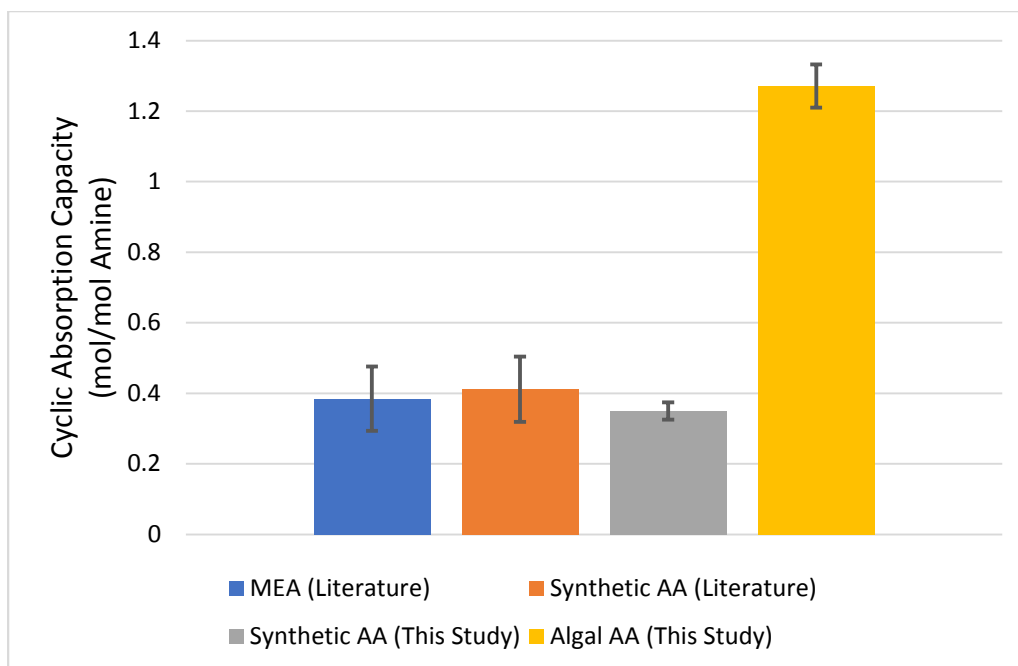


Figure 24: Cyclic Absorption Capacities for Absorbents in the Literature

Also, an energy balance was completed for the algal absorption and desorption cycle. Table 12 below shows the consumption during each process. The desorption process consumes about 4.5 times more energy than the absorption process per cycle. The desorption energy consumption was entirely composed of the cost for the heating mantle. For absorption, the only energy consuming piece of equipment was the metering pump. Energy consumption was calculated using the listed values on the equipment and are overestimates of the actual value.

Table 12: Energy Consumption for Algal Absorption and Desorption

| | Energy Consumption (kWh/cycle) | Energy Consumption (kWh/kg CO ₂) |
|-------------------|-----------------------------------|---|
| Absorption | 0.184 | 30.6 |
| Desorption | 0.833 | 139 |

CHAPTER 6: CONCLUSIONS AND FUTURE WORK

A novel process was used to convert microalgal biomass to an algal amino acid absorbent for post-combustion carbon dioxide capture using a trickling filter absorption column. The results show that the algal amino acid absorbent captures significantly more carbon dioxide than a synthetic amino acid absorbent (1.27 to 0.747 mol CO₂/mol amine, respectively). ATR-FTIR showed no significant change within the absorbents after multiple absorption cycles indicating high regenerability of the absorbents. A mass balance of the biomass conversion process shows that 168g of potassium carbonate can be recovered and recycled back into potassium hydroxide. This would greatly reduce the cost of the process and potentially provide a cheap alternative to synthetic amino acids allowing for increased implementation of amino acid absorbents in post-combustion carbon dioxide capture.

Future work should focus on investigating the interaction between algal amino acids and other algal compounds in the algal based amino acid solution on CO₂ absorption, and determining the economics of the process. A techno-economic analysis needs to be conducted on the process to determine the cost of producing the algal amino acid absorbent compared to synthetic absorbents. More work needs to be done to optimize the process and scale it up into a pilot scale operation as well. These steps would help determine the viability of mass implementation of algal amino acid absorbents for post-carbon dioxide capture and sequestration.

APPENDICES

APPENDIX A: CHAPTER 3 SUPPLEMENTAL INFORMATION

Table 13: Pairwise Comparisons of Mean Amino Acid Concentrations for Parr Reactor Conditions

| Comparison | Estimate | P-value |
|----------------------|----------|---------|
| KOH:Protein | | |
| 1:1 – 5:1 | -55.0 | 0.0012 |
| Temperature | | |
| 121 - 134 | 1.33 | 0.8396 |
| Reaction Time | | |
| 3 – 5 | -3.234 | 0.9361 |
| 3 – 7 | -3.998 | 0.8347 |
| 5 - 7 | -0.764 | 0.9918 |

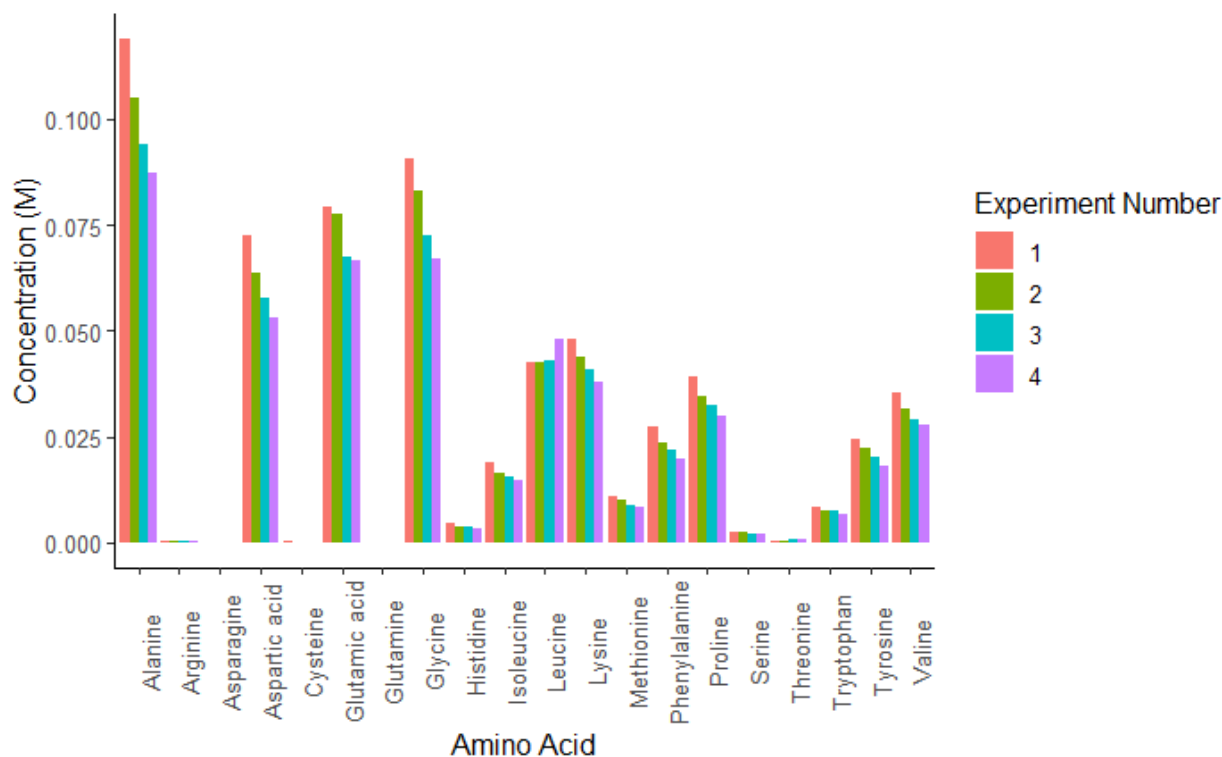


Figure 25: Amino Acid Concentrations after Parr Reactor for each Experiment

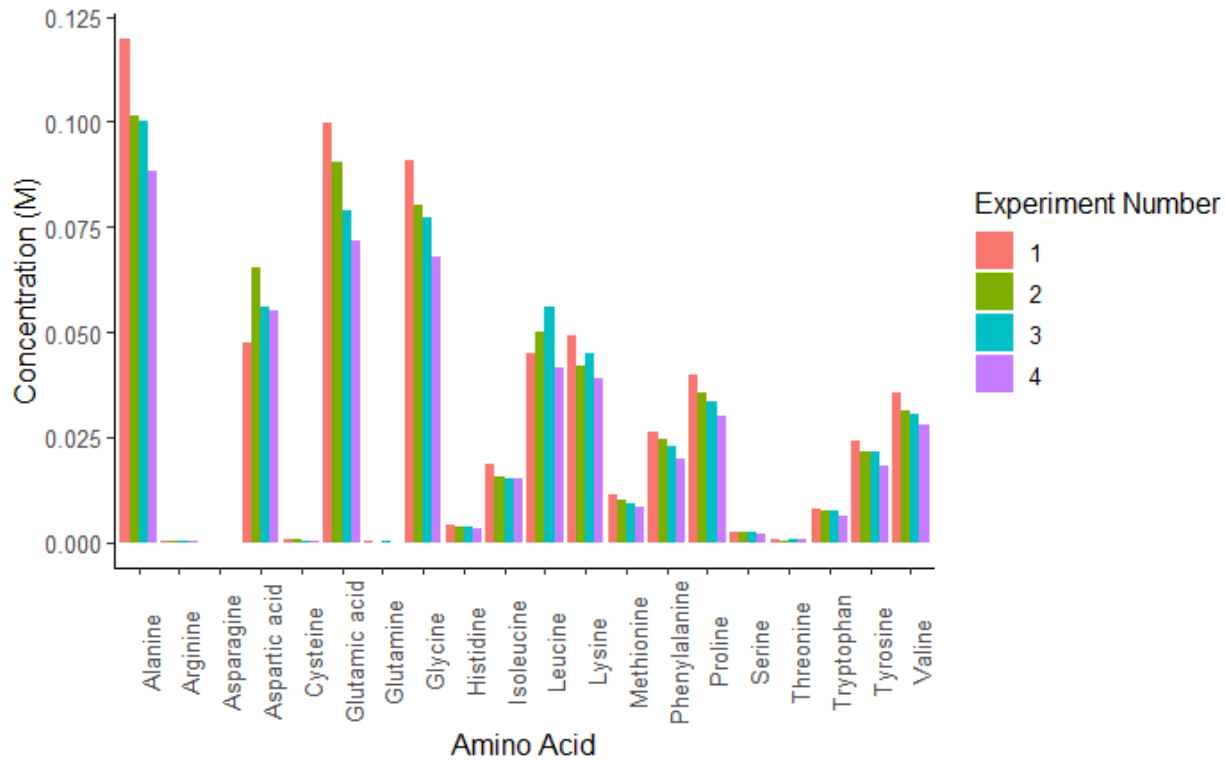


Figure 26: Amino Acid Concentrations after Centrifuge for each Experiment

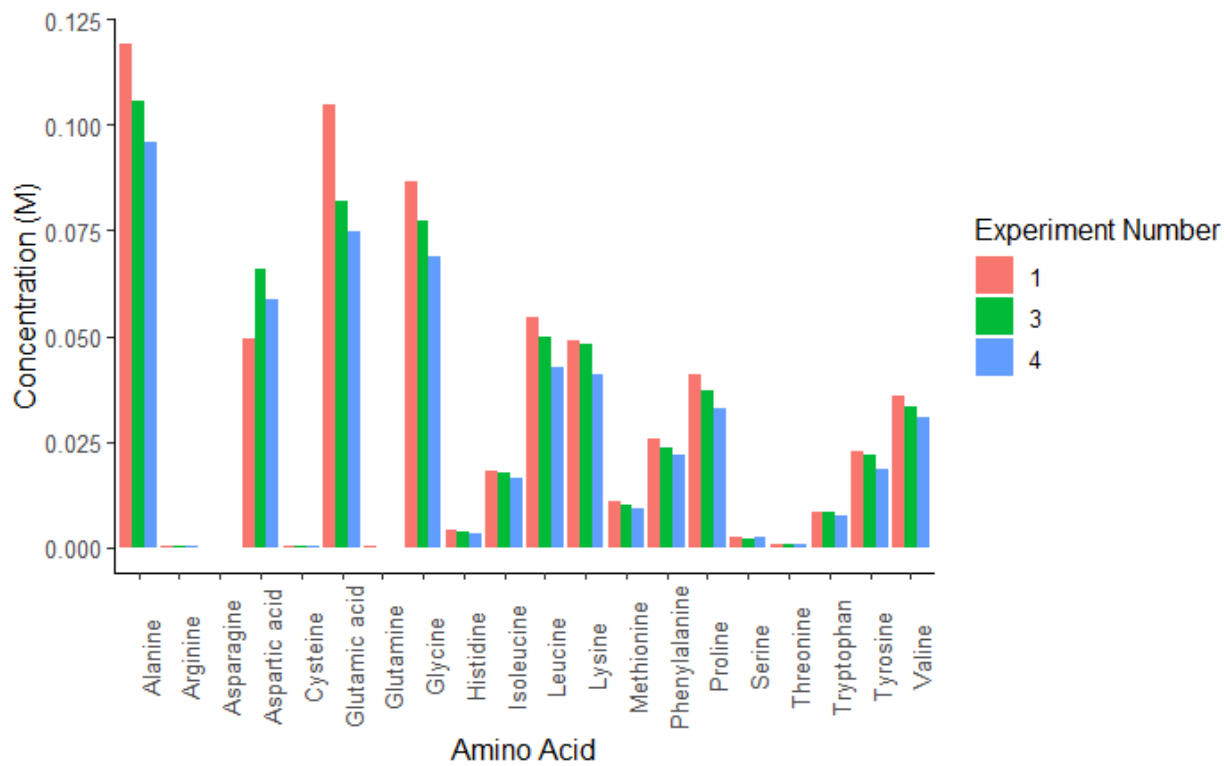


Figure 27: Amino Acid Concentrations after Acidification for each Experiment

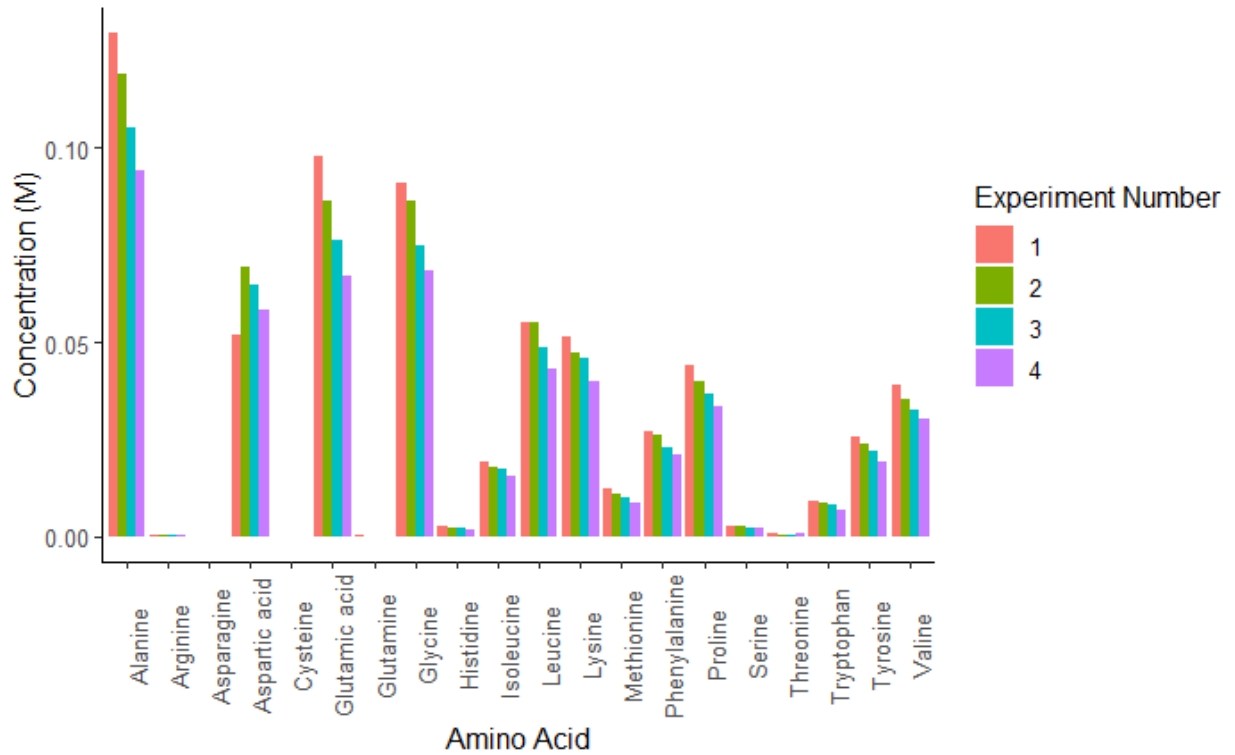


Figure 28: Amino Acid Concentrations after Desorption for each Experiment

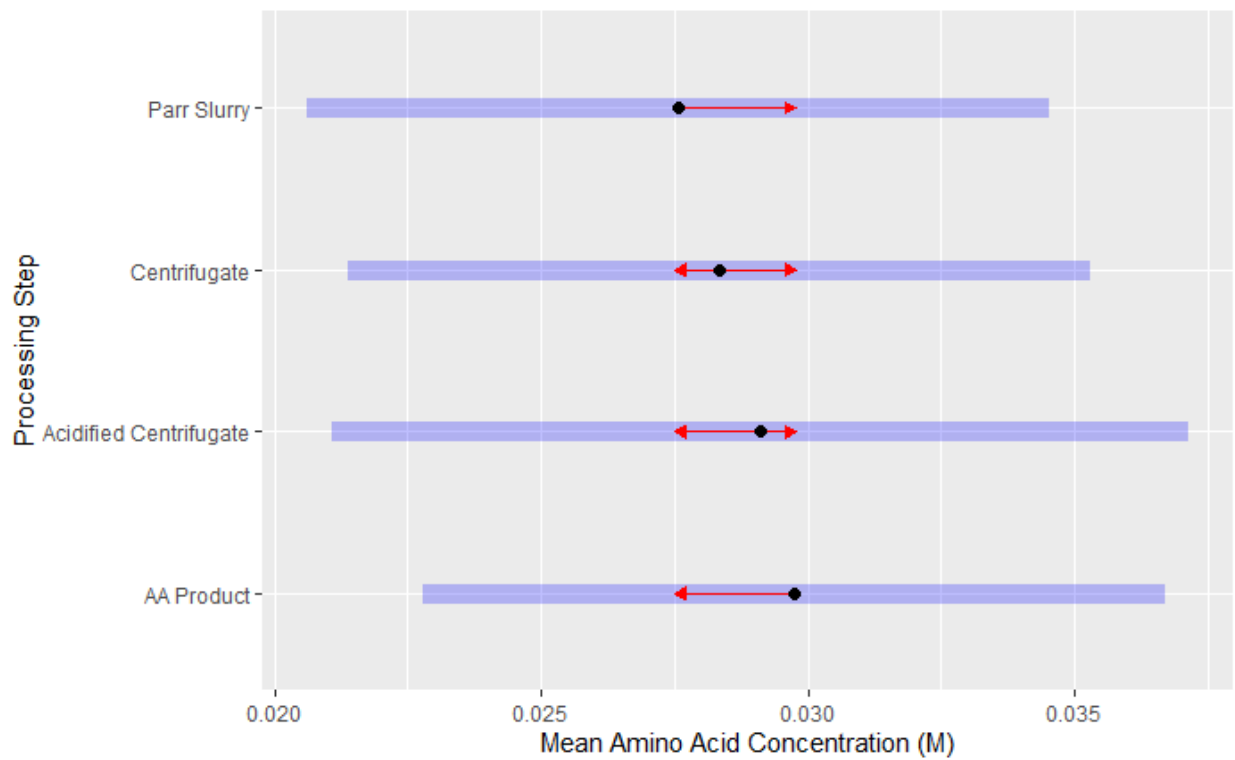


Figure 29: Pairwise Comparisons of Amino Acid Concentrations for the Algal Amino Acid Solution for each Processing Step

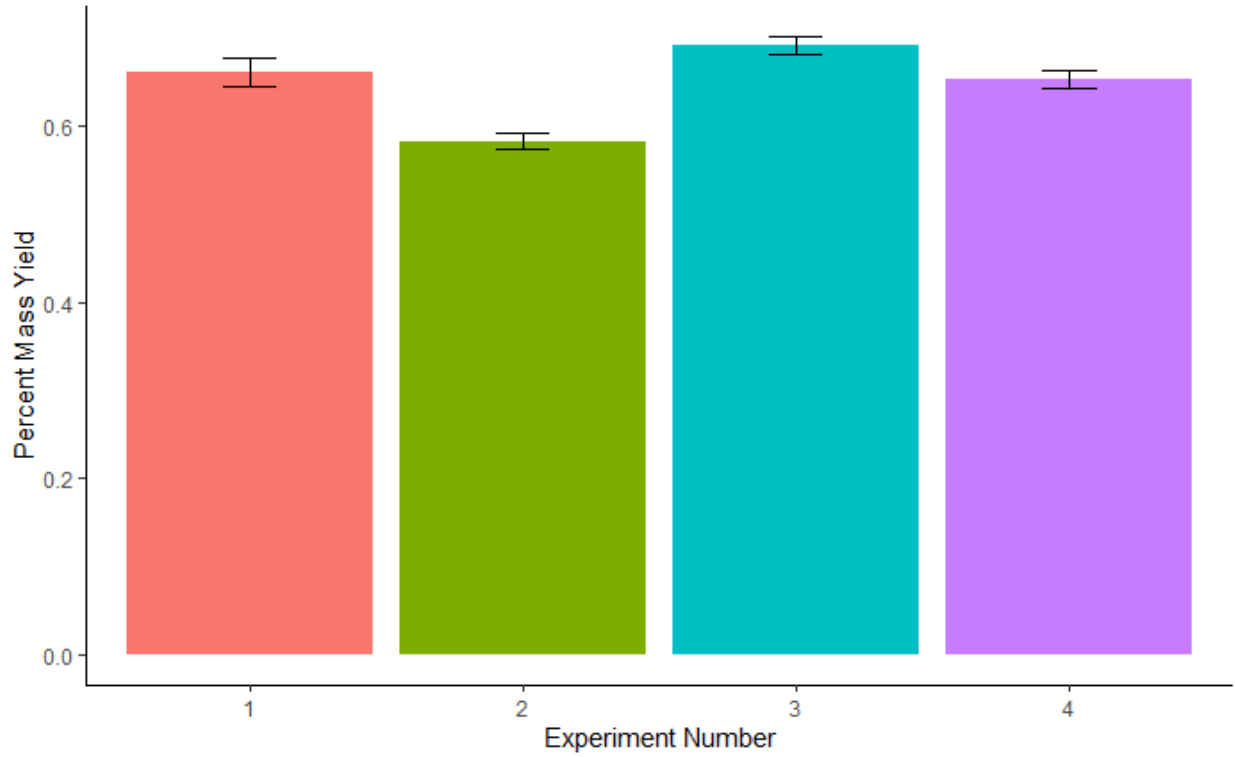


Figure 30: Algal Amino Acid Solution Percent Mass Liquid Yield after Centrifuge

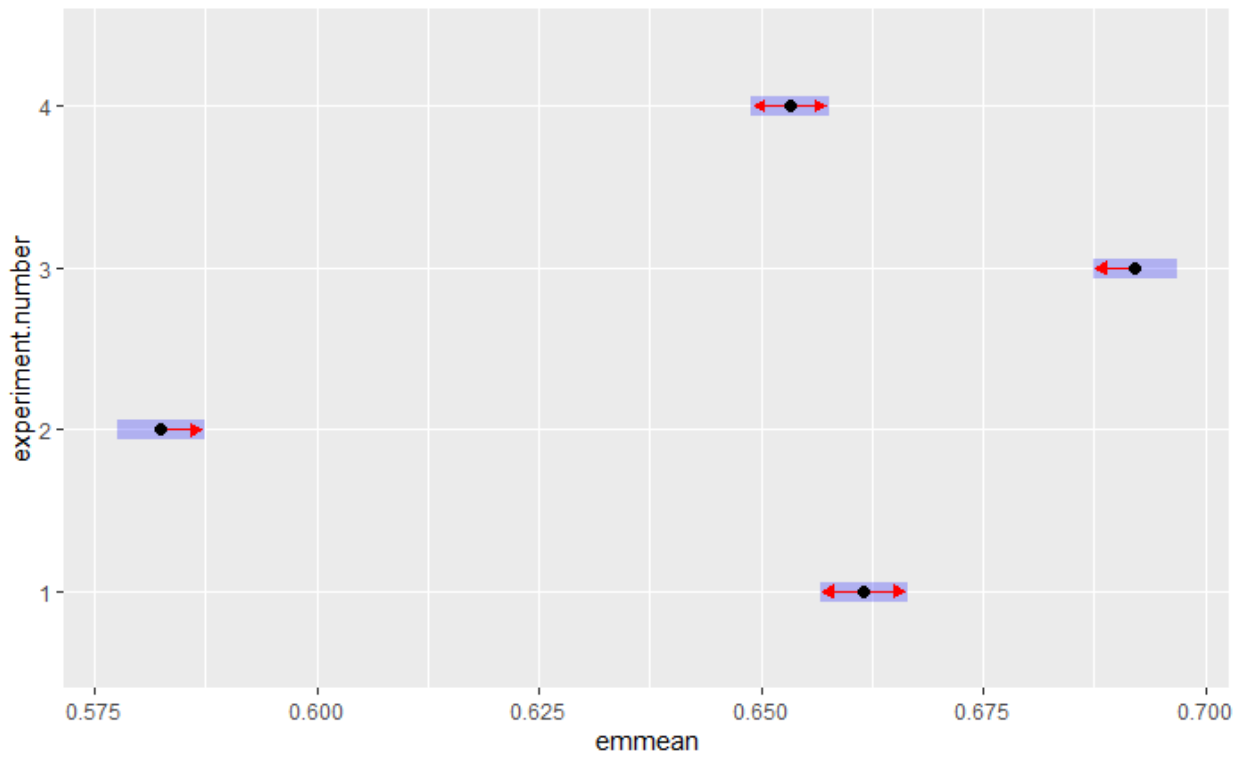


Figure 31: Algal Amino Acid Solution Percent Mass Liquid Yield Pairwise Comparisons

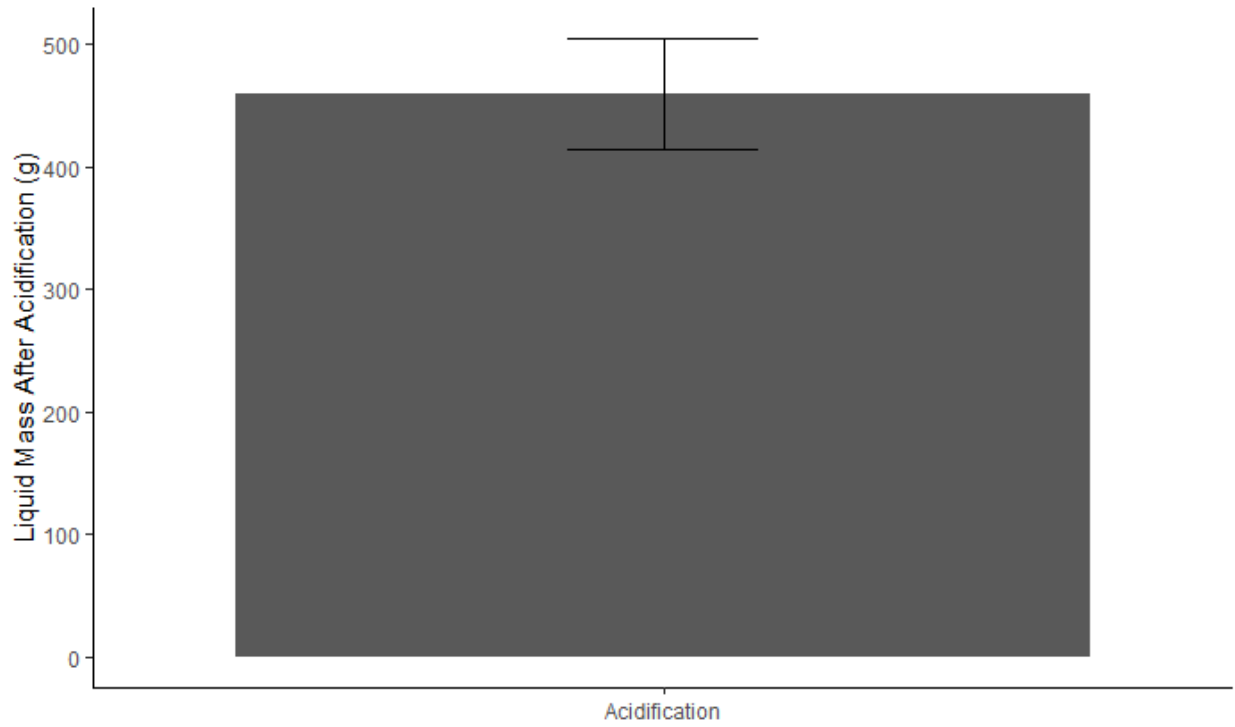


Figure 32: Algal Amino Acid Solution Liquid Mass after Acidification

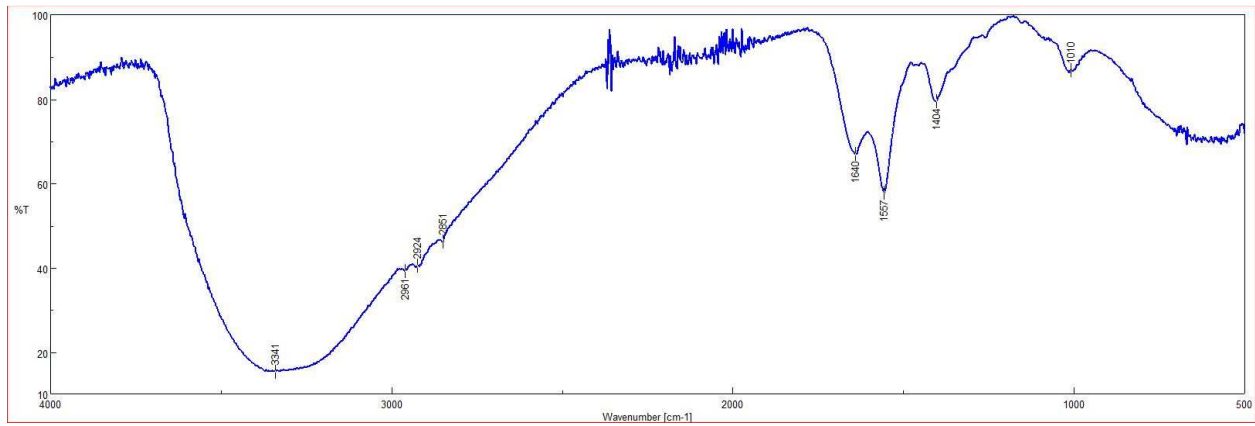


Figure 33: Parr Slurry 1 ATR-FTIR Spectrum

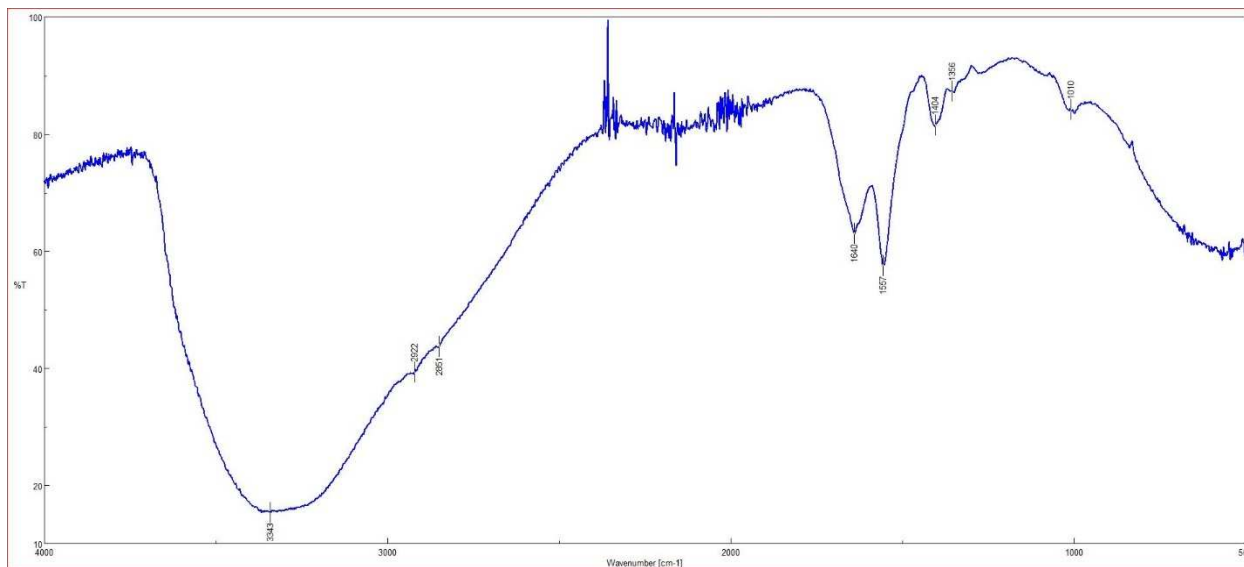


Figure 34: Parr Slurry 2 ATR-FTIR Spectrum

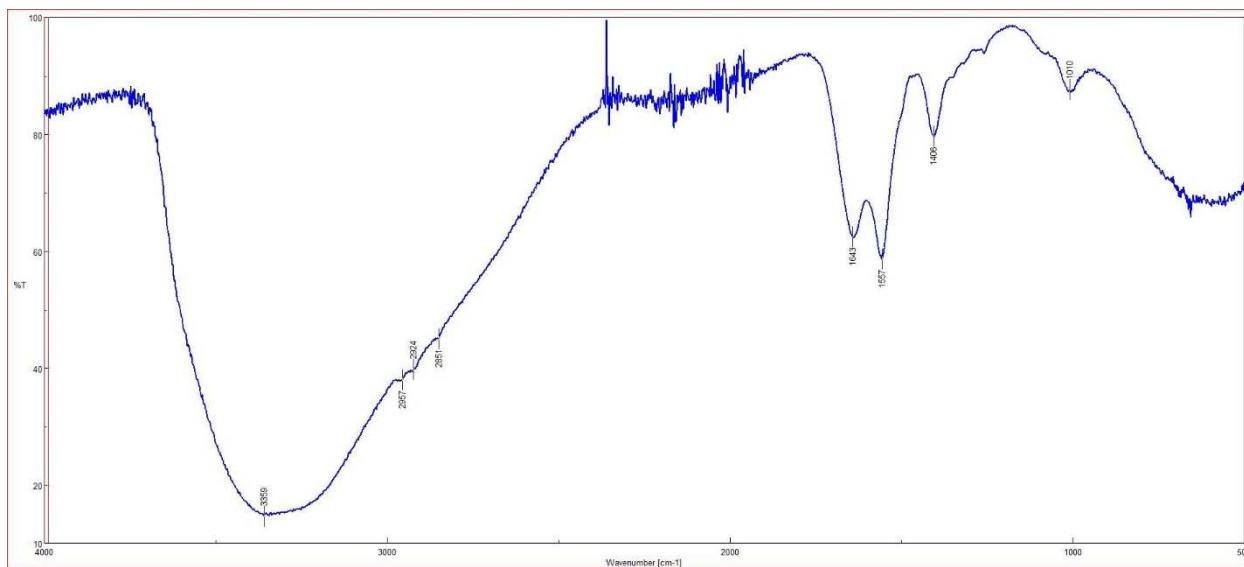


Figure 35: Parr Slurry 3 ATR-FTIR Spectrum

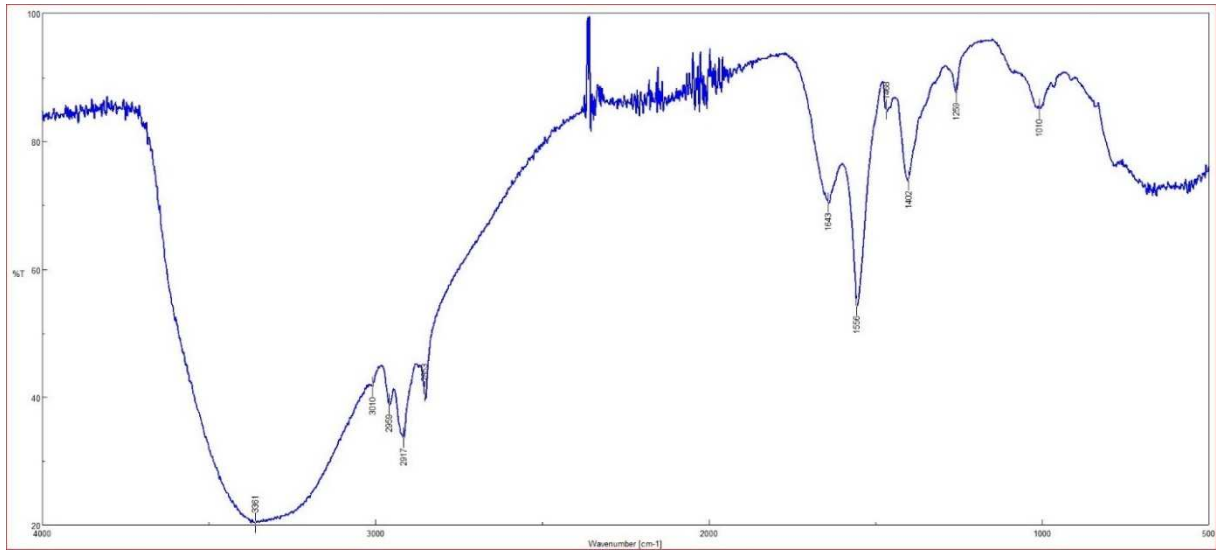


Figure 36: Parr Slurry 4 ATR-FTIR Spectrum

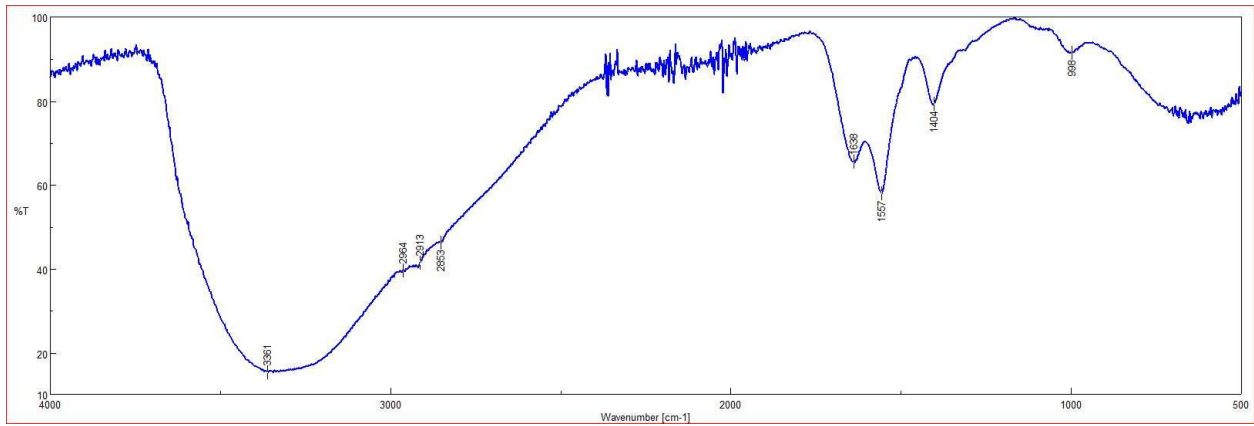


Figure 37: Parr Centrifugate 1 ATR-FTIR Spectrum

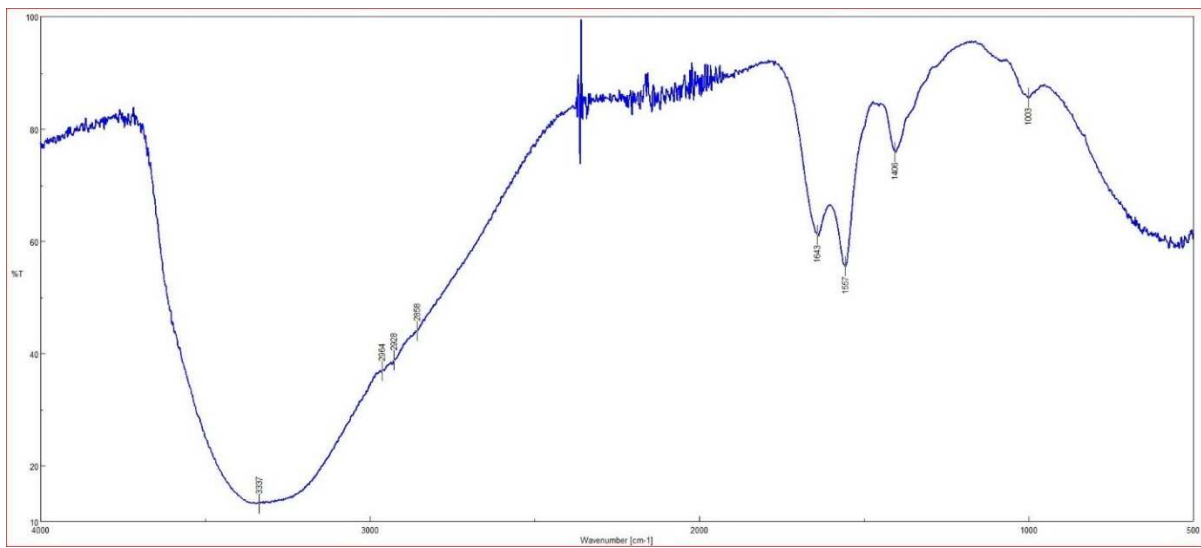


Figure 38: Parr Centrifugate 2 ATR-FTIR Spectrum

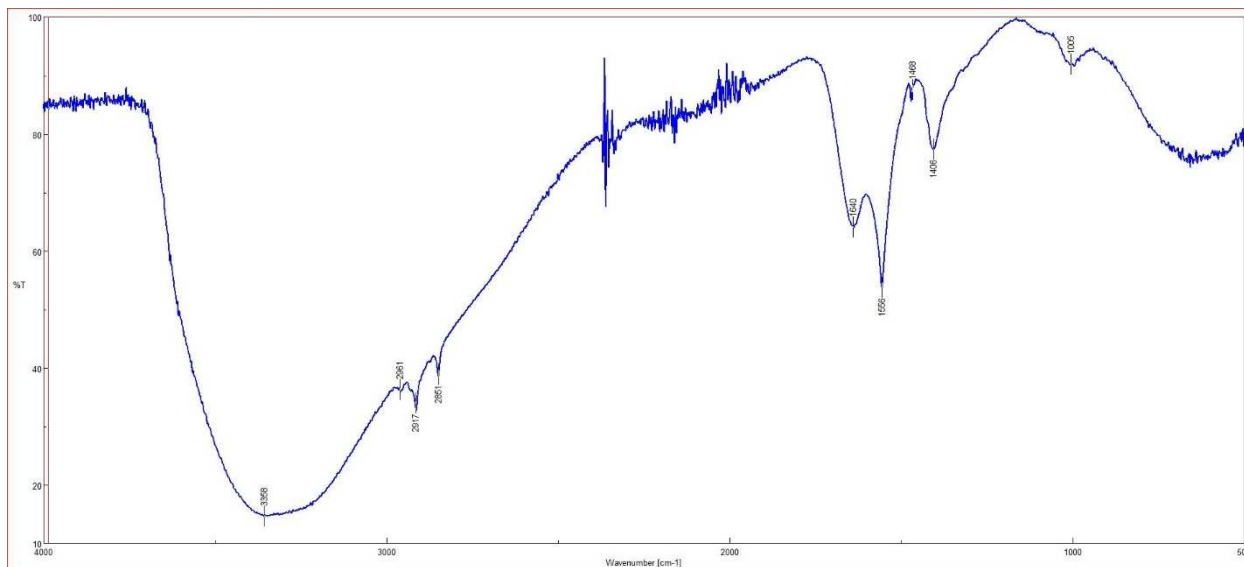


Figure 39: Parr Centrifugate 3 ATR-FTIR Spectrum

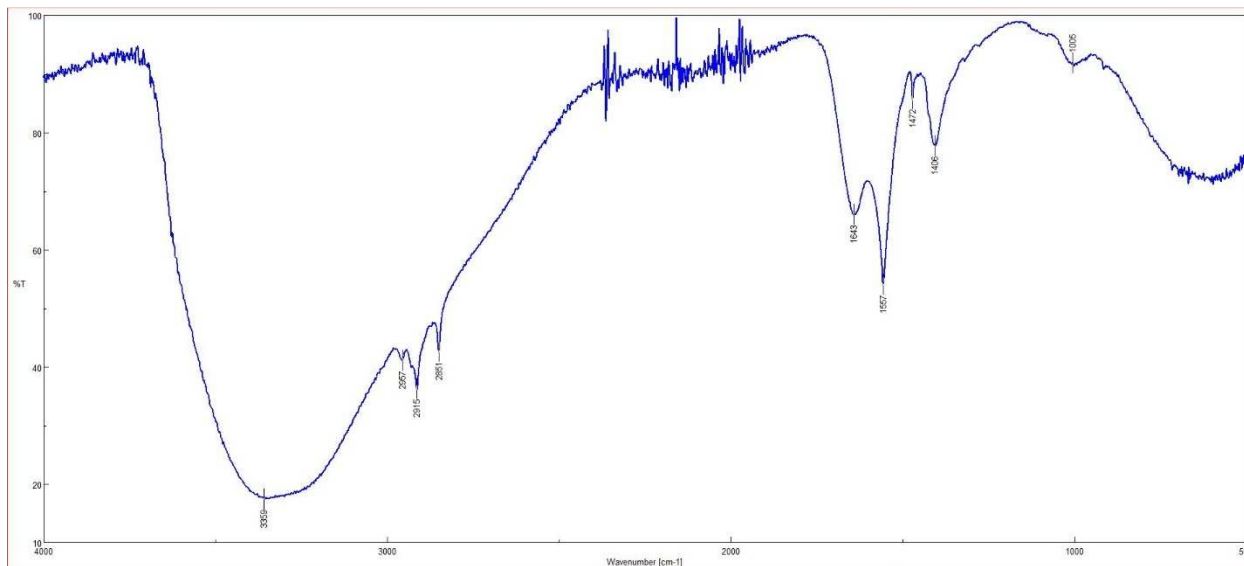


Figure 40: Parr Centrifugate 4 ATR-FTIR Spectrum

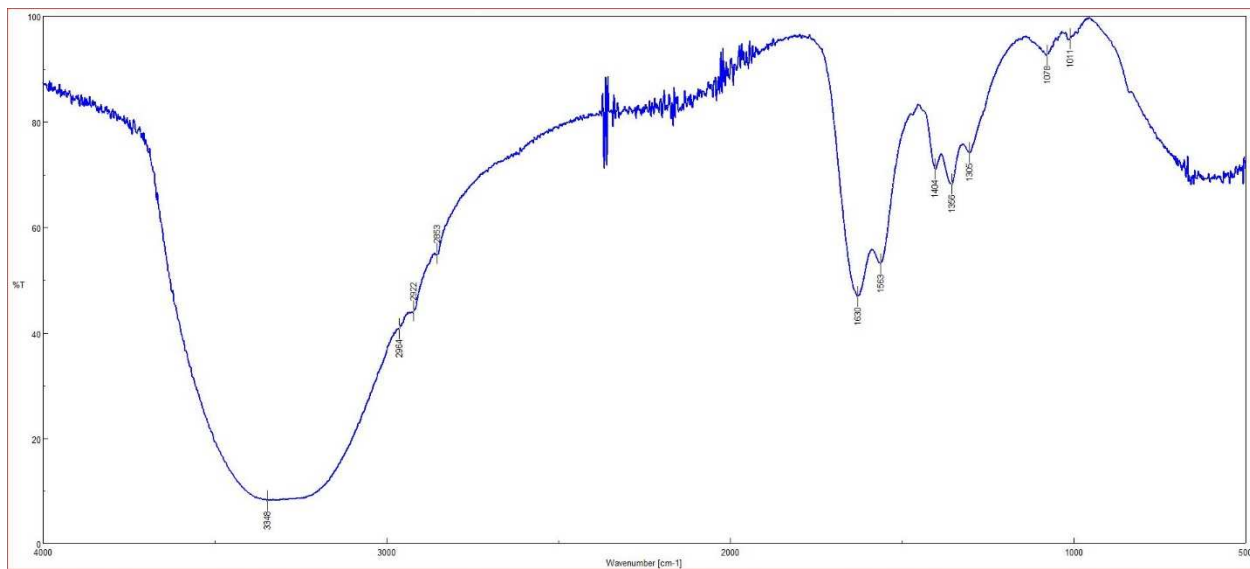


Figure 41: Acidified Centrifugate 1 ATR-FTIR Spectrum

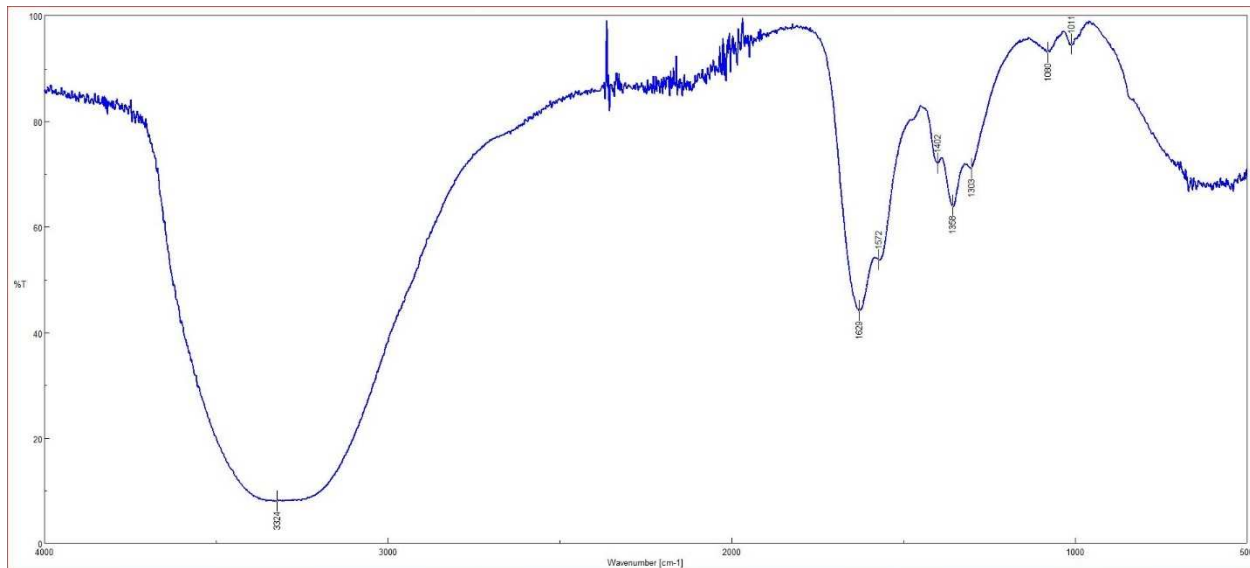


Figure 42: Acidified Centrifugate 3 ATR-FTIR Spectrum

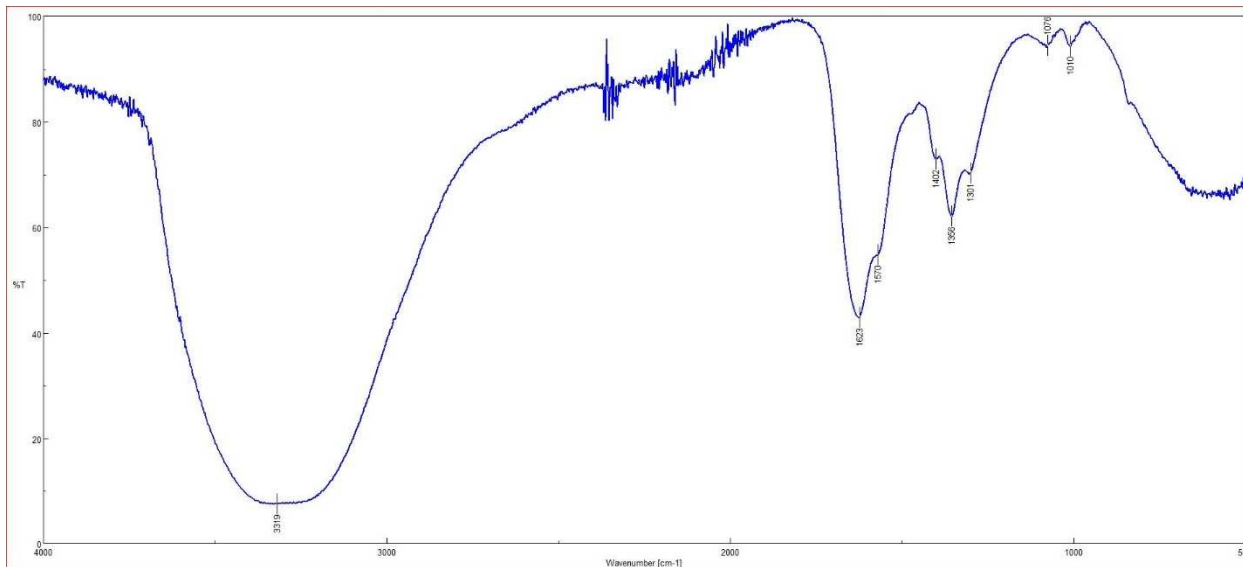


Figure 43: Acidified Centrifugate 4 ATR-FTIR Spectrum

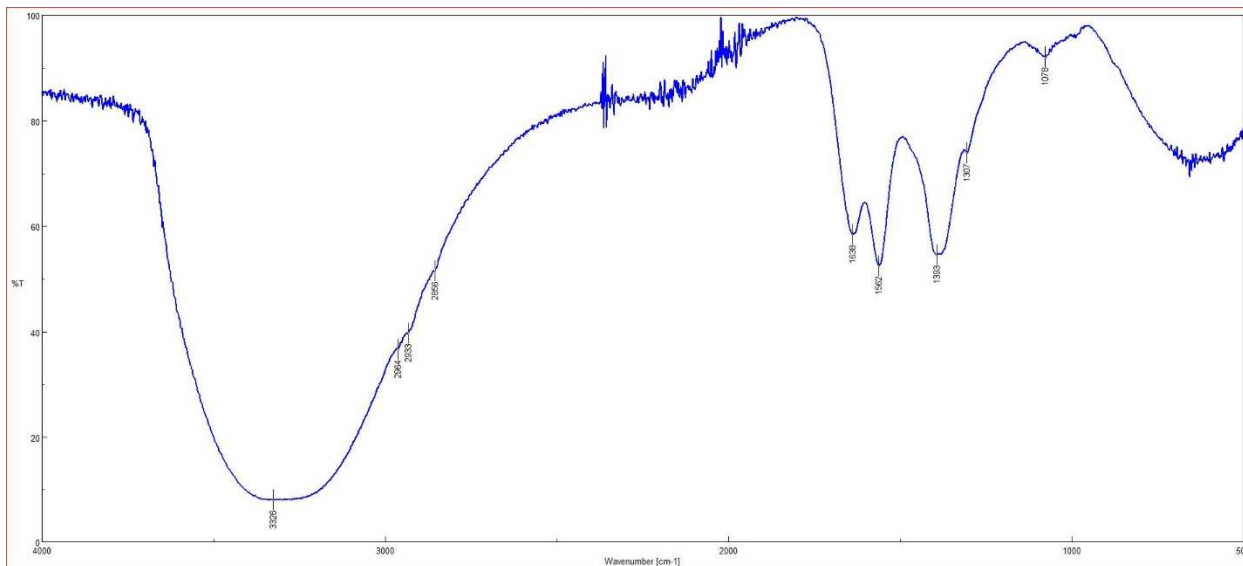


Figure 44: Algal Amino Acid Product 1 ATR-FTIR Spectrum

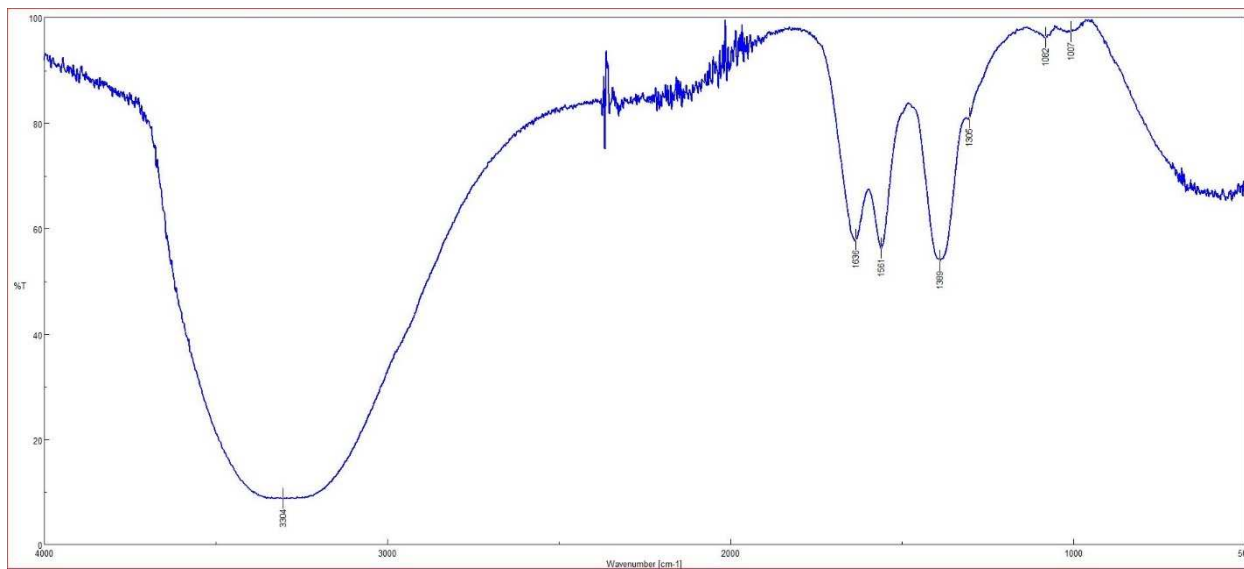


Figure 45: Algal Amino Acid Product 2 ATR-FTIR Spectrum

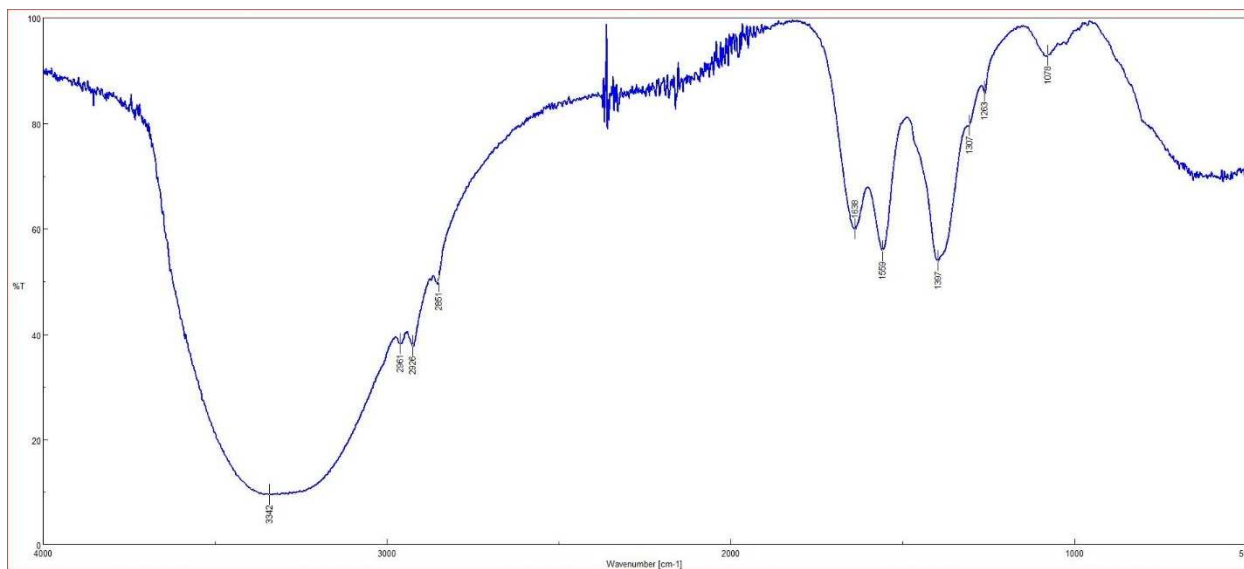


Figure 46: Algal Amino Acid Product 3 ATR-FTIR Spectrum

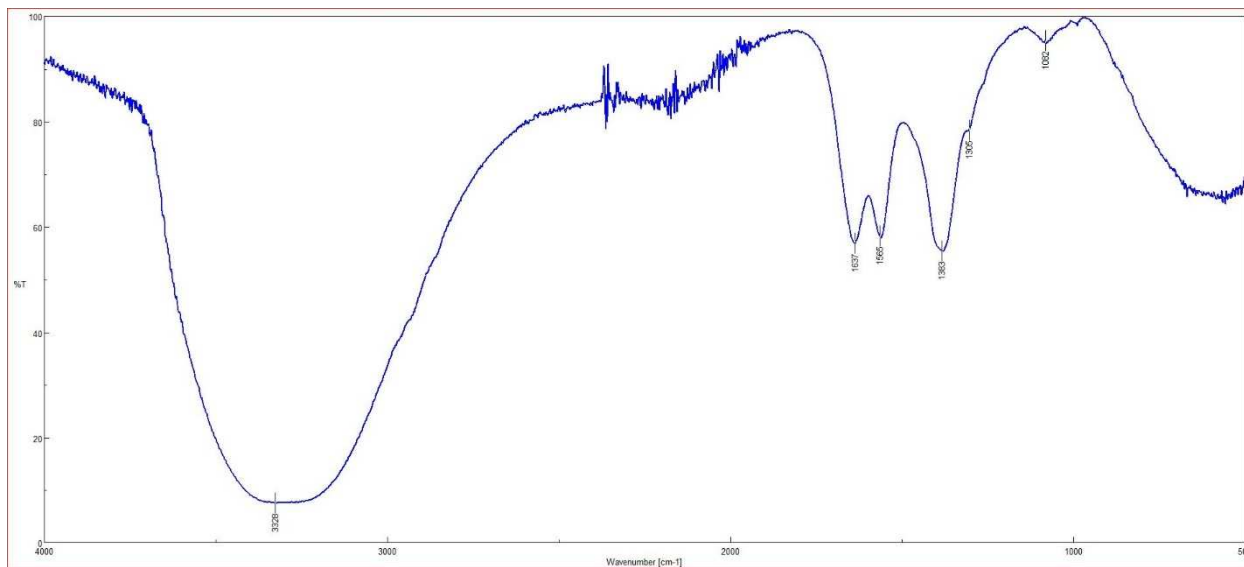


Figure 47: Algal Amino Acid Product 4 ATR-FTIR Spectrum

APPENDIX B: CHAPTER 4 SUPPLEMENTAL INFORMATION

Table 14: Pairwise Comparisons between Gas to Liquid Flow Ratios

| Contrast | Estimate | p-value |
|-------------|----------|---------|
| 0.5 - 1.875 | -0.439 | <0.01 |
| 0.5 - 2.5 | -0.464 | <0.01 |
| 0.5 - 3 | -0.523 | <0.01 |
| 0.5 - 4 | -0.312 | <0.01 |
| 1.875 - 2.5 | -0.025 | 0.887 |
| 1.875 - 3 | -0.084 | 0.131 |
| 1.875 - 4 | 0.127 | 0.029 |
| 2.5 - 3 | -0.059 | 0.330 |
| 2.5 - 4 | 0.152 | 0.014 |
| 3 - 4 | 0.211 | <0.01 |

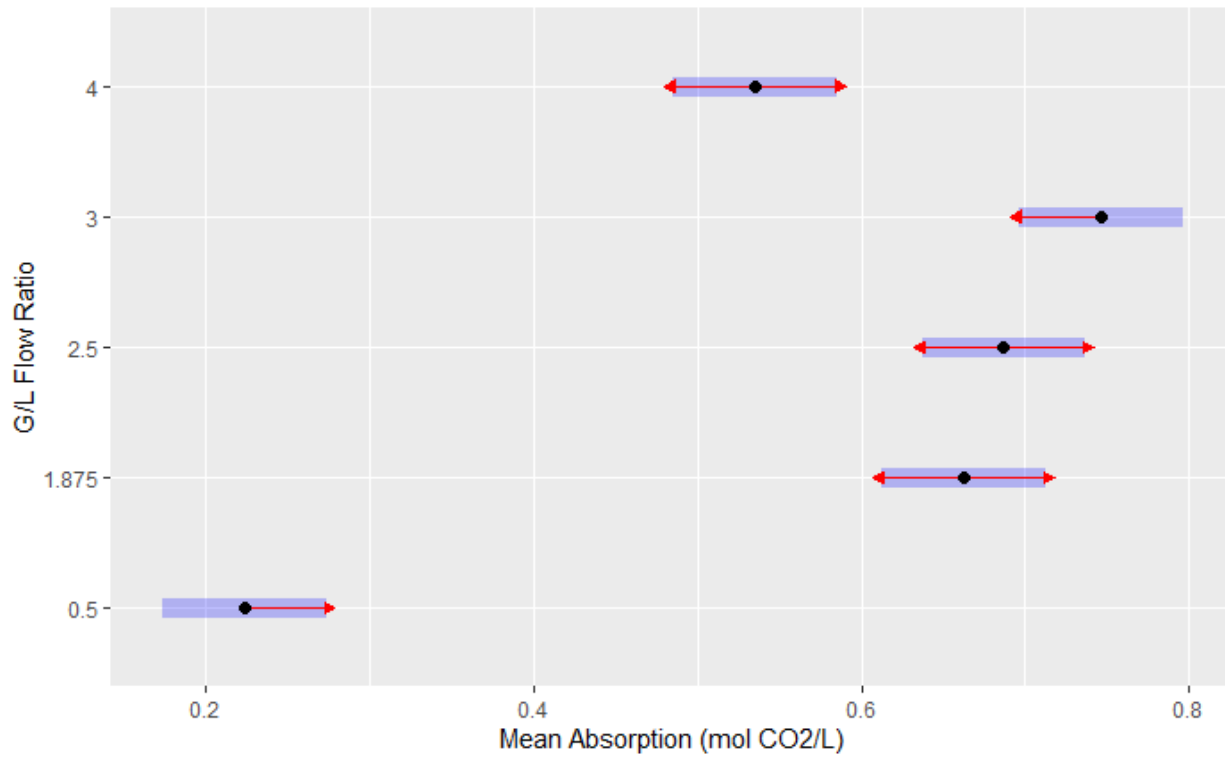


Figure 48: Mean comparisons for various Gas to Liquid Flow Ratios

Table 15: Synthetic Absorbent CO₂ Absorption and Desorption Capacities

| | Cycle Number | | | |
|--------------------------------|-----------------------------|----------------------------|----------------------------|-----------------------------|
| | 1 | 2 | 3 | 4 |
| Amount Absorbed (mol/L) | 0.470 ± 0.024 ^a | 0.352 ± 0.022 ^b | 0.341 ± 0.023 ^b | 0.357 ± 0.041 ^{ab} |
| Amount Desorbed (mol/L) | 0.290 ± 0.0002 ^a | 0.298 ± 0.024 ^a | 0.303 ± 0.015 ^a | 0.313 ± 0.027 ^a |

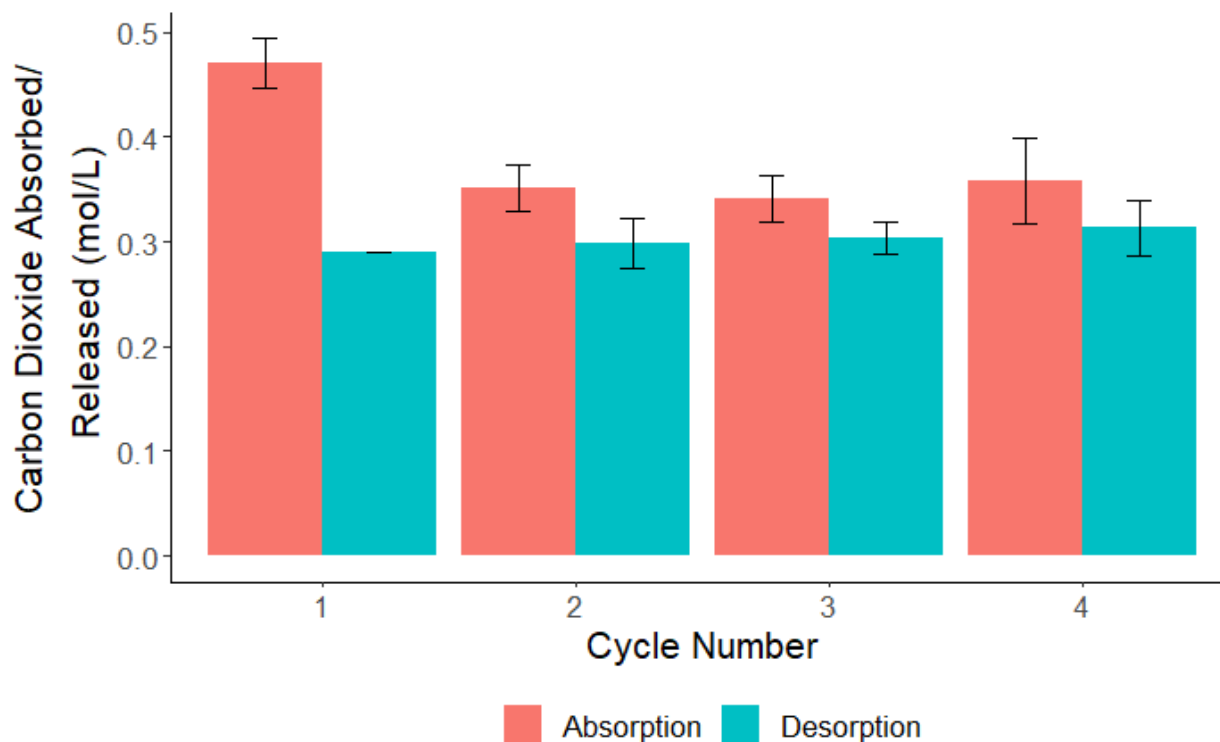


Figure 49: Synthetic Absorbent CO₂ Absorption and Desorption over Four Cycles in mol CO₂/L

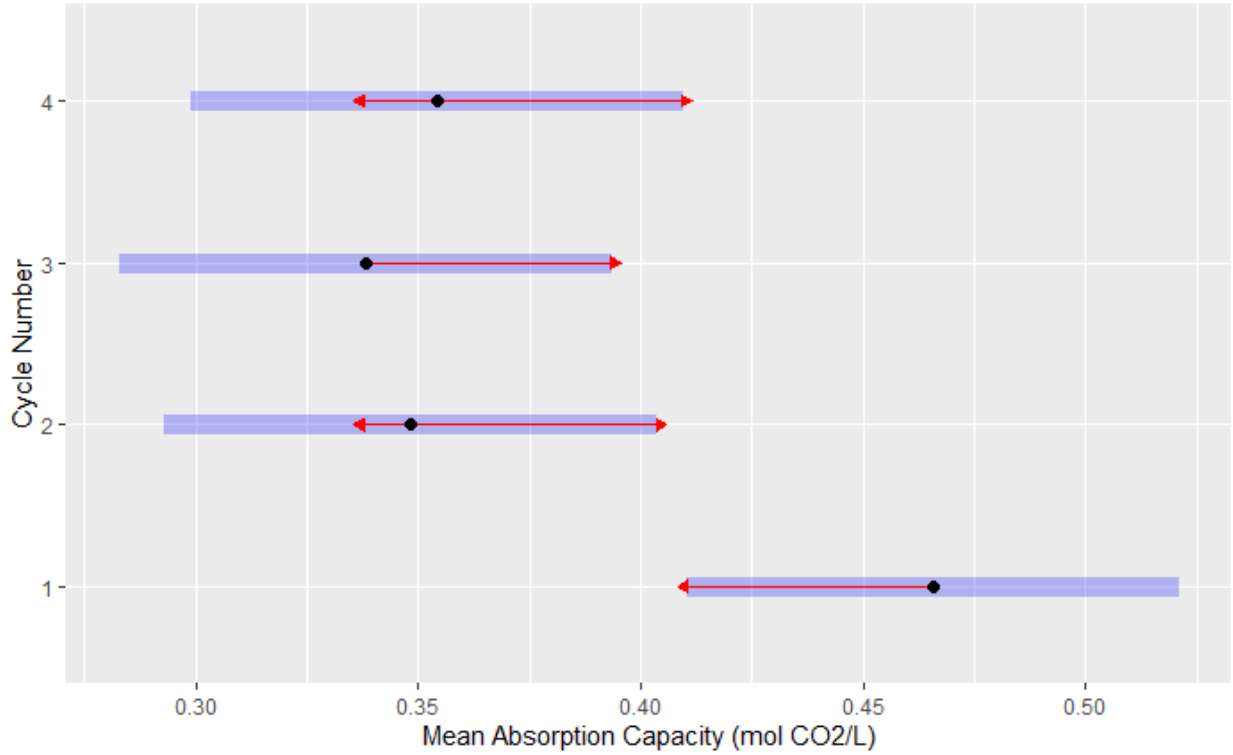


Figure 50: Pairwise Comparisons for Synthetic Amino Acid Absorbent Absorption Capacities for each Cycle

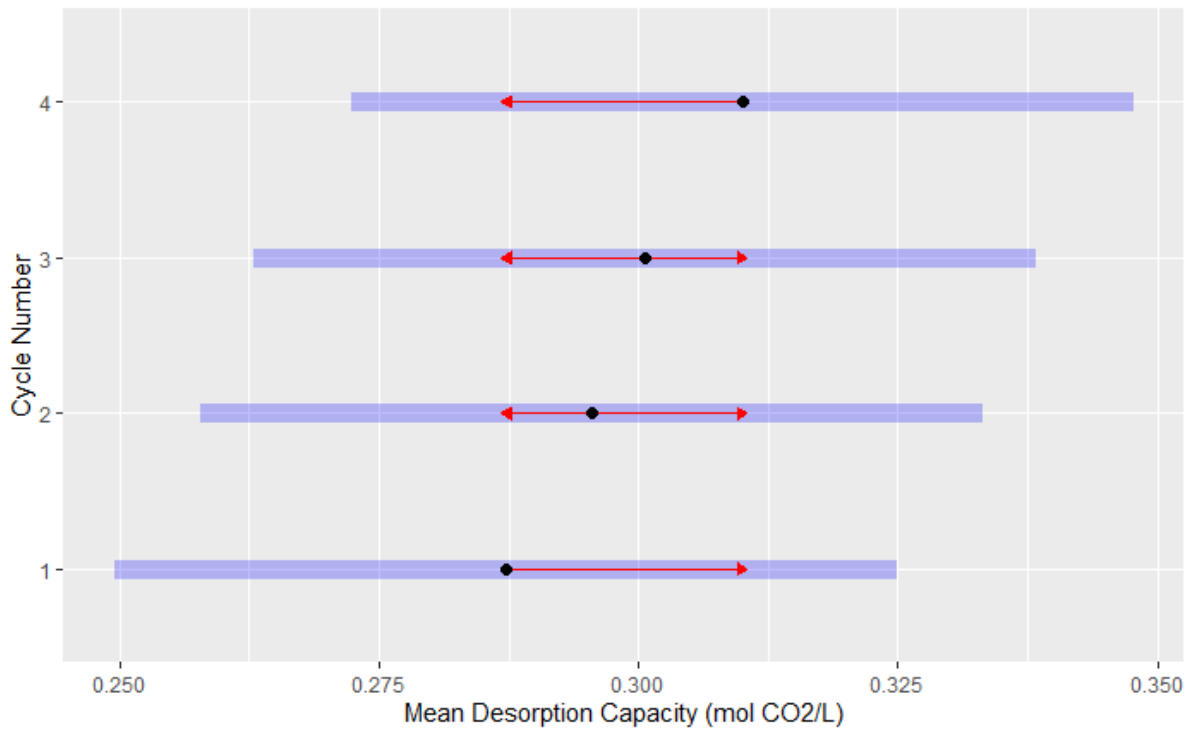


Figure 51: Pairwise Comparisons for Synthetic Amino Acid Absorbent Desorption Capacities for each Cycle

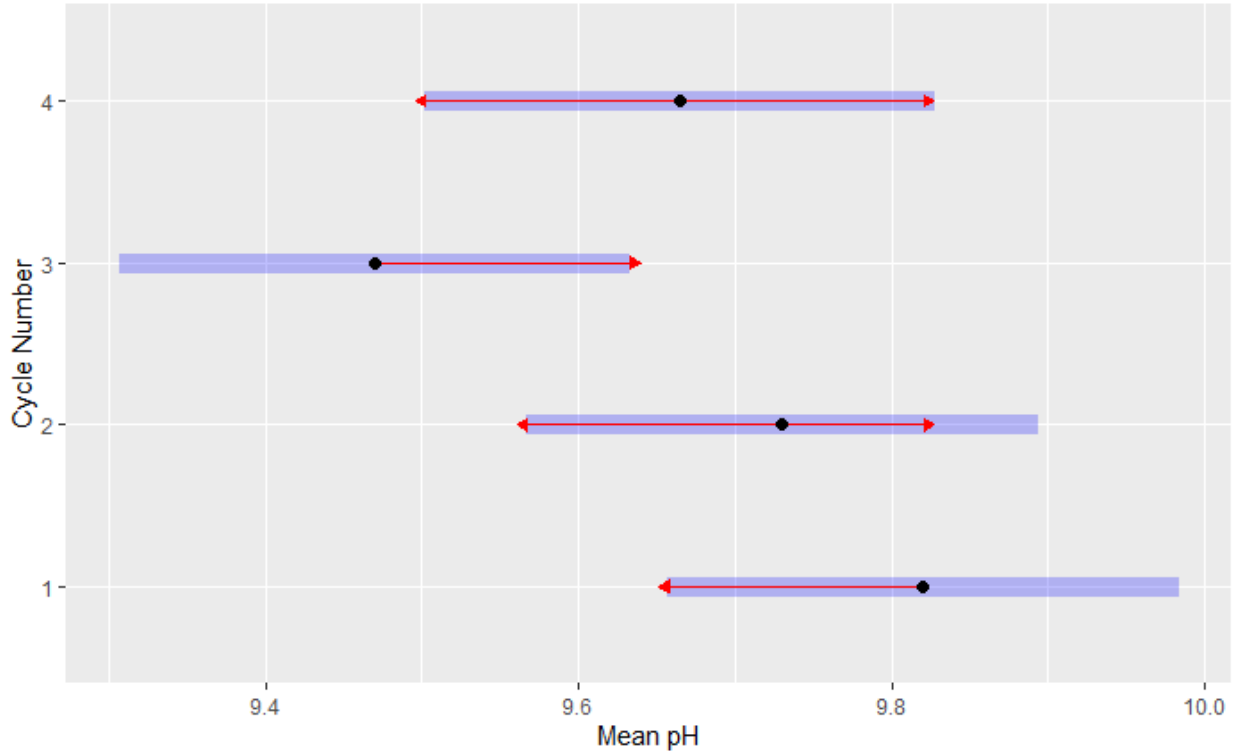


Figure 52: Pairwise Comparisons for Synthetic Amino Acid Absorbent Absorbed pH for each Cycle

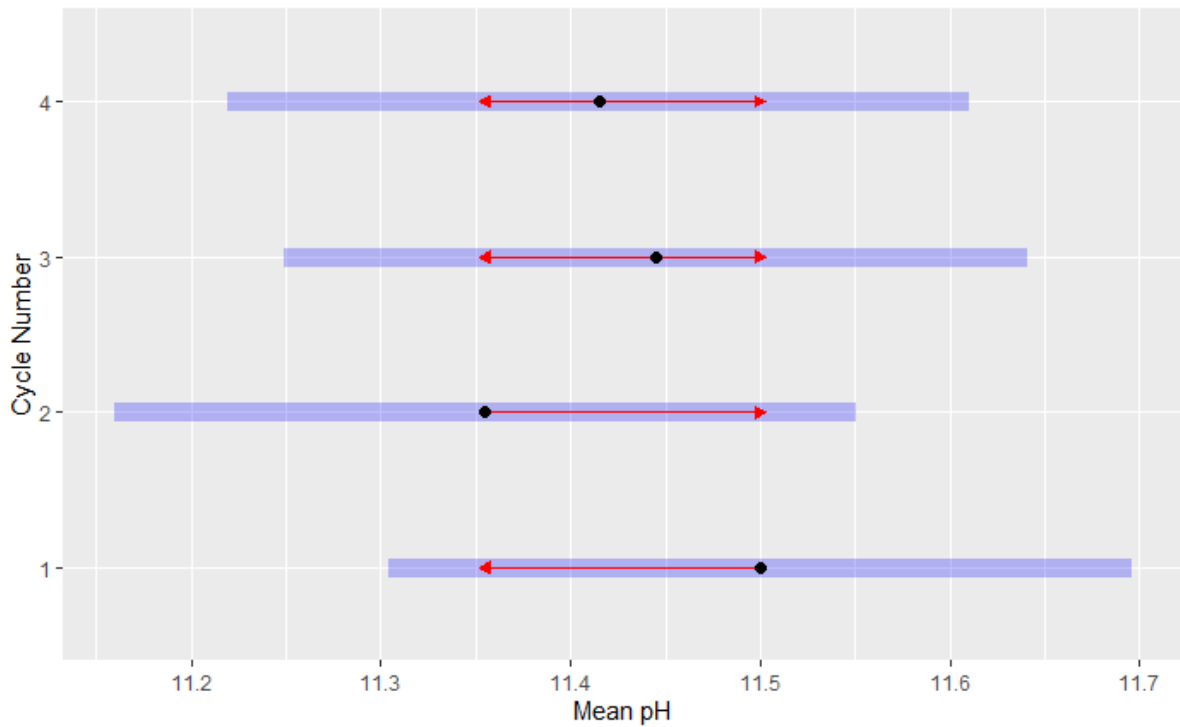
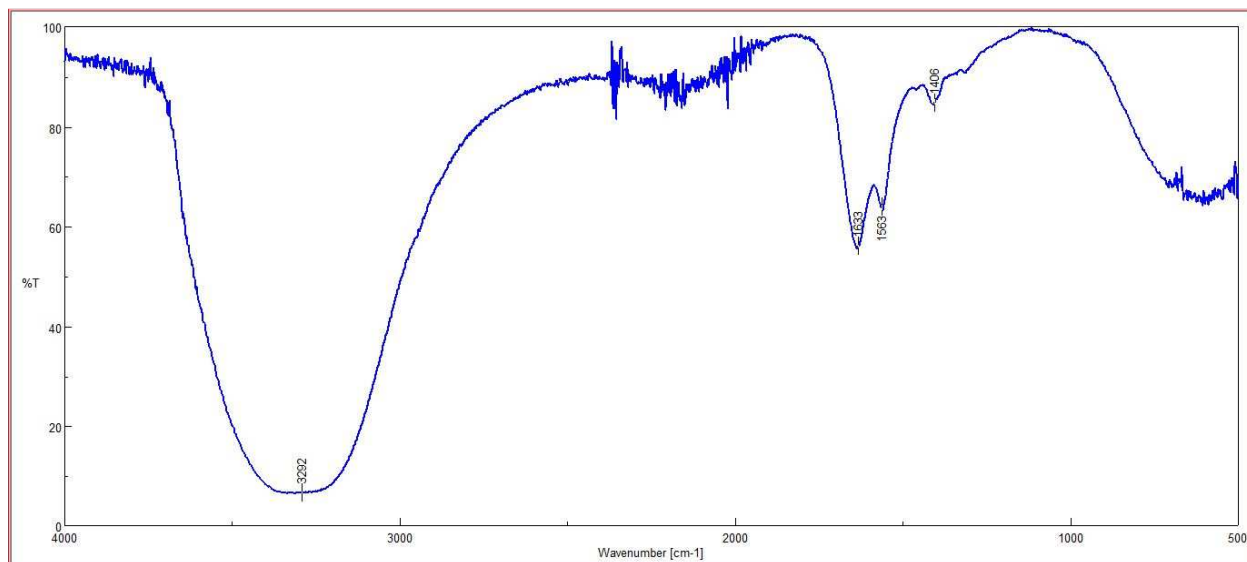
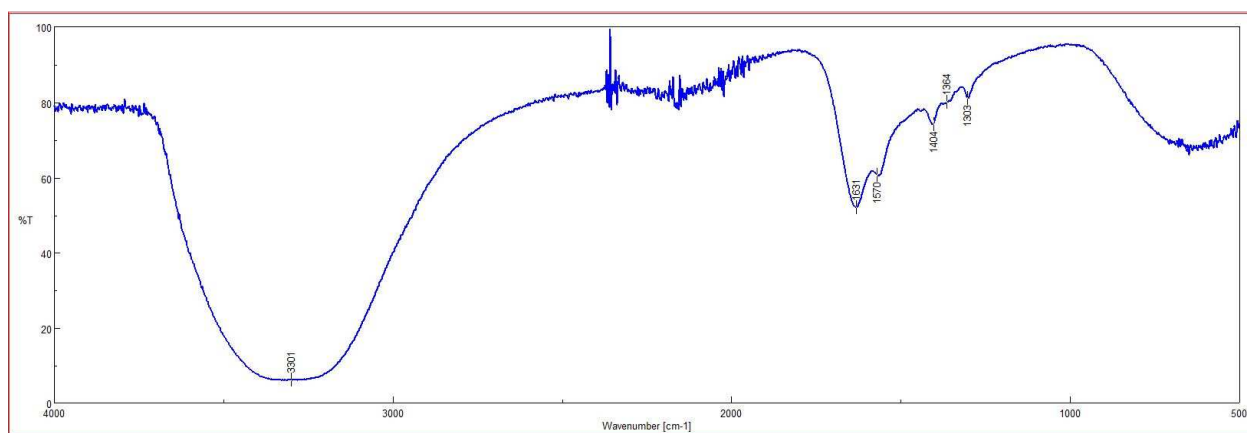


Figure 53: Pairwise Comparisons for Synthetic Amino Acid Absorbent Desorbed pH for each Cycle

(a)



(b)



(c)

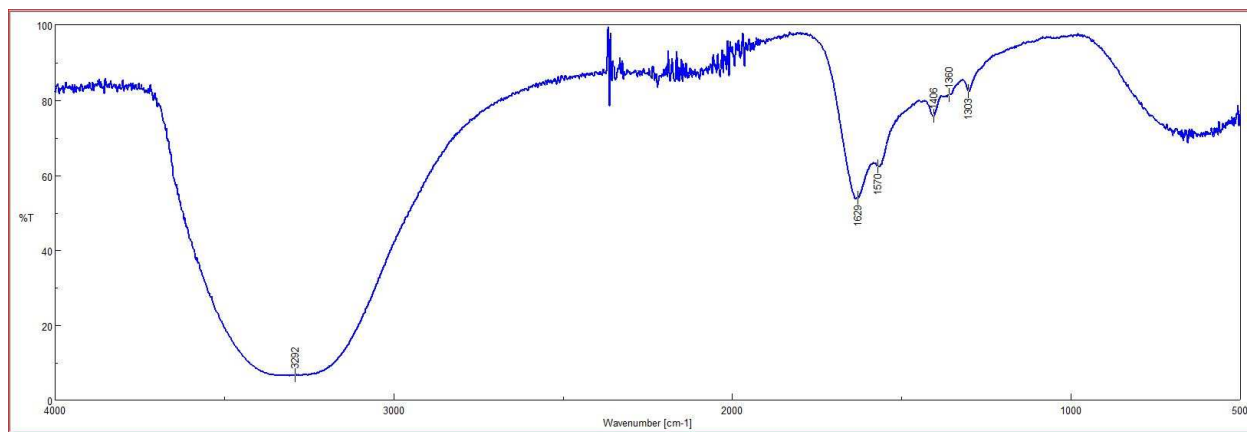
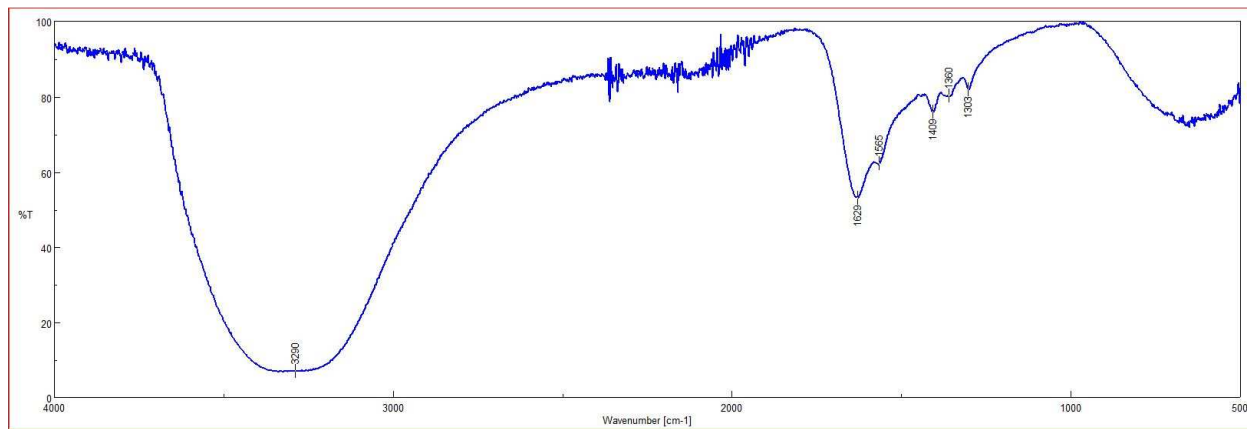


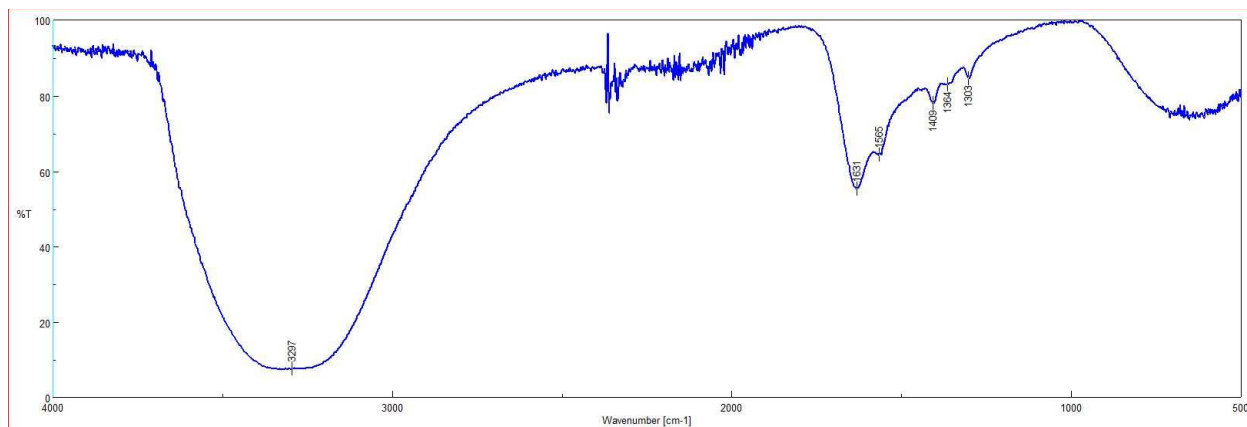
Figure 54: Synthetic Amino Acid Absorbent ATR-FTIR Spectrum **a)** prior to Absorption **b)** after Absorption 1 **c)** after Absorption 2 **d)** after Absorption 3 **e)** after Absorption 4

Figure 54 (cont'd)

(d)



(e)



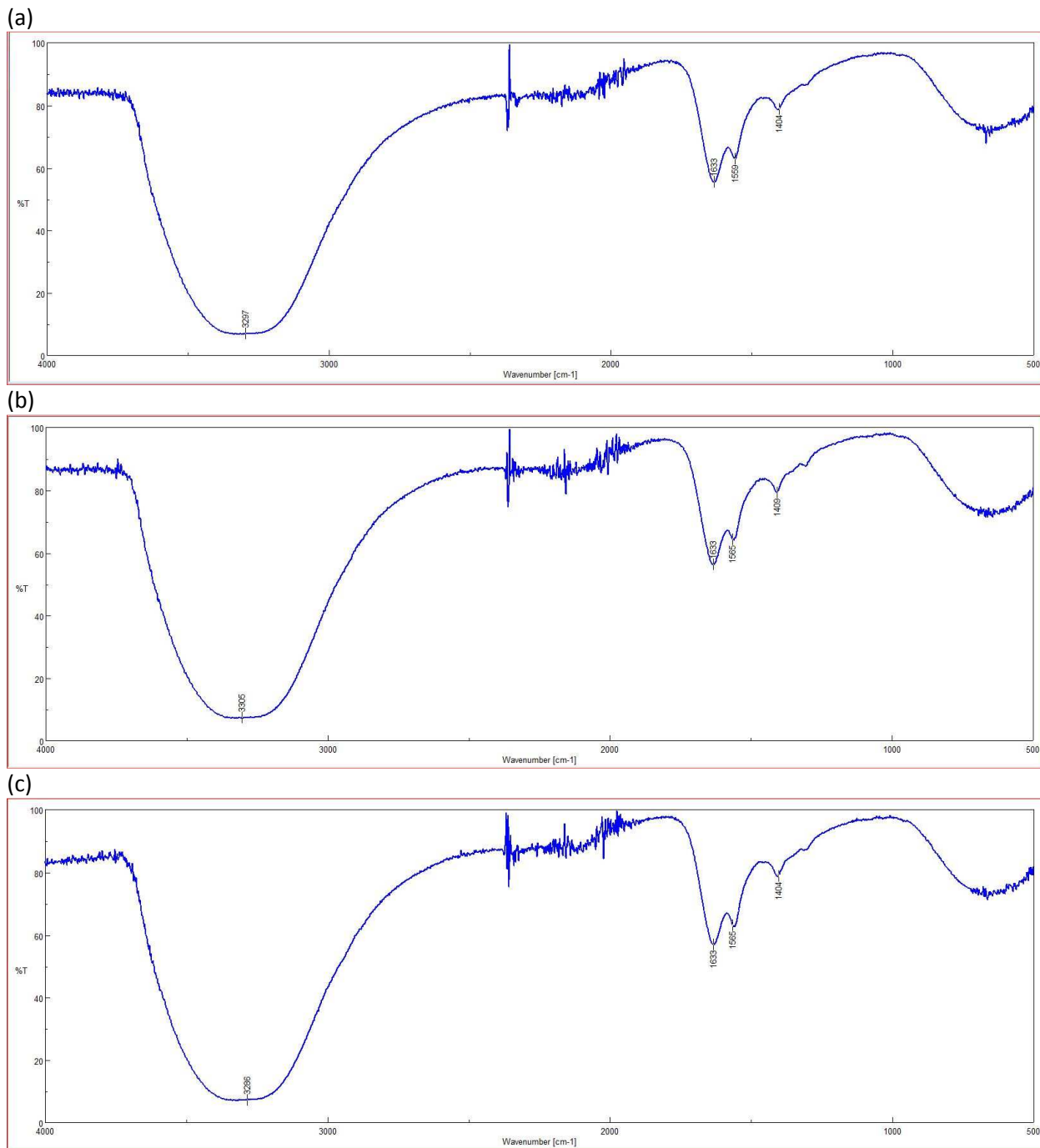
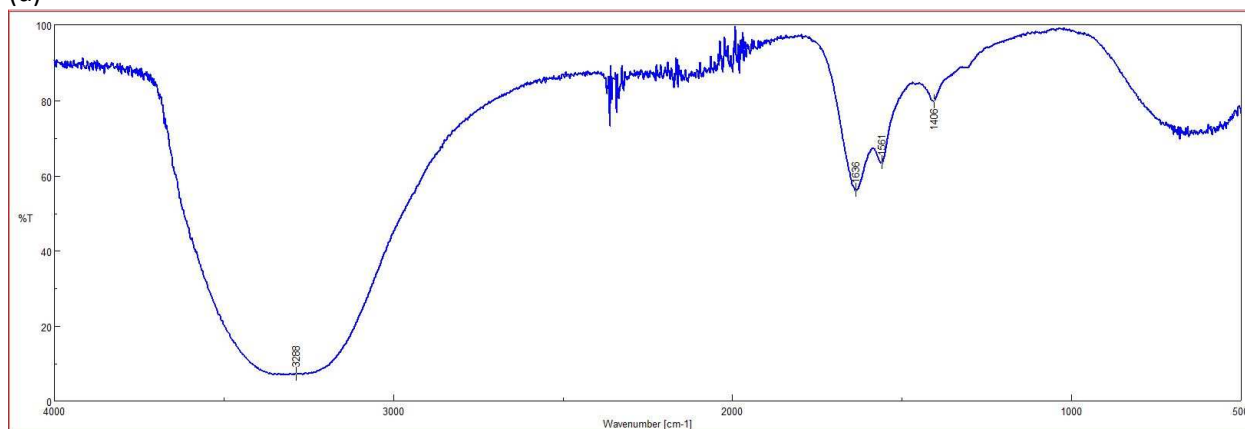
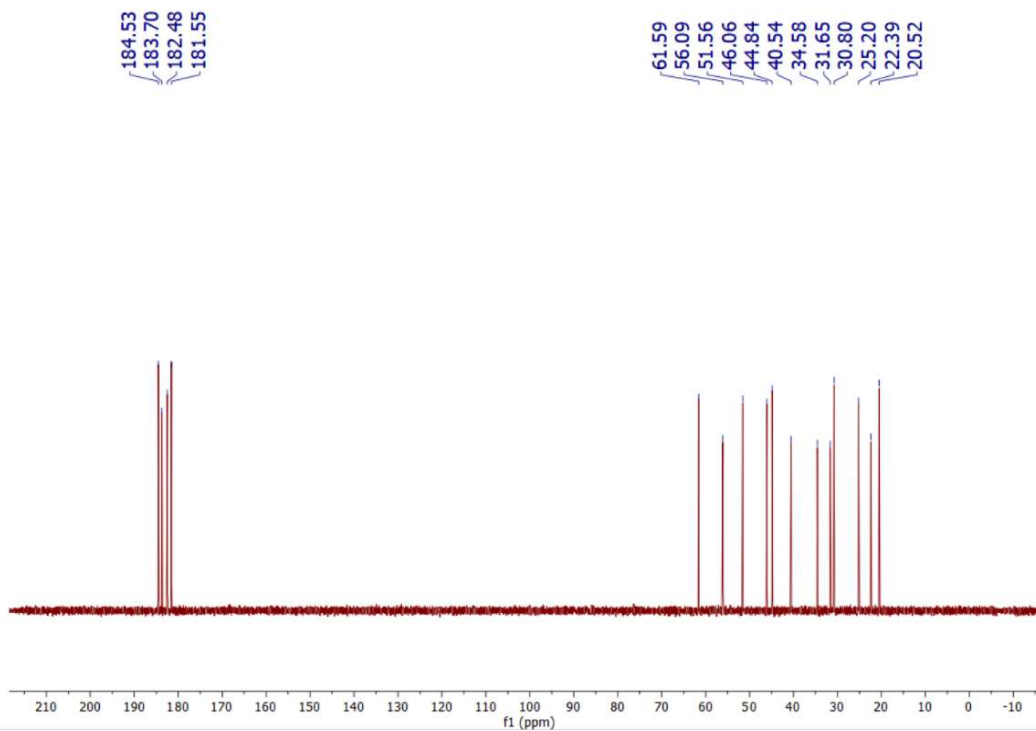


Figure 55: Synthetic Amino Acid Absorbent ATR-FTIR Spectrum **a)** after Desorption 1 **b)** after Desorption 2 **c)** after Absorption 3 **d)** after Desorption 4

Figure 55 (cont'd)
(d)



(a)



(b)

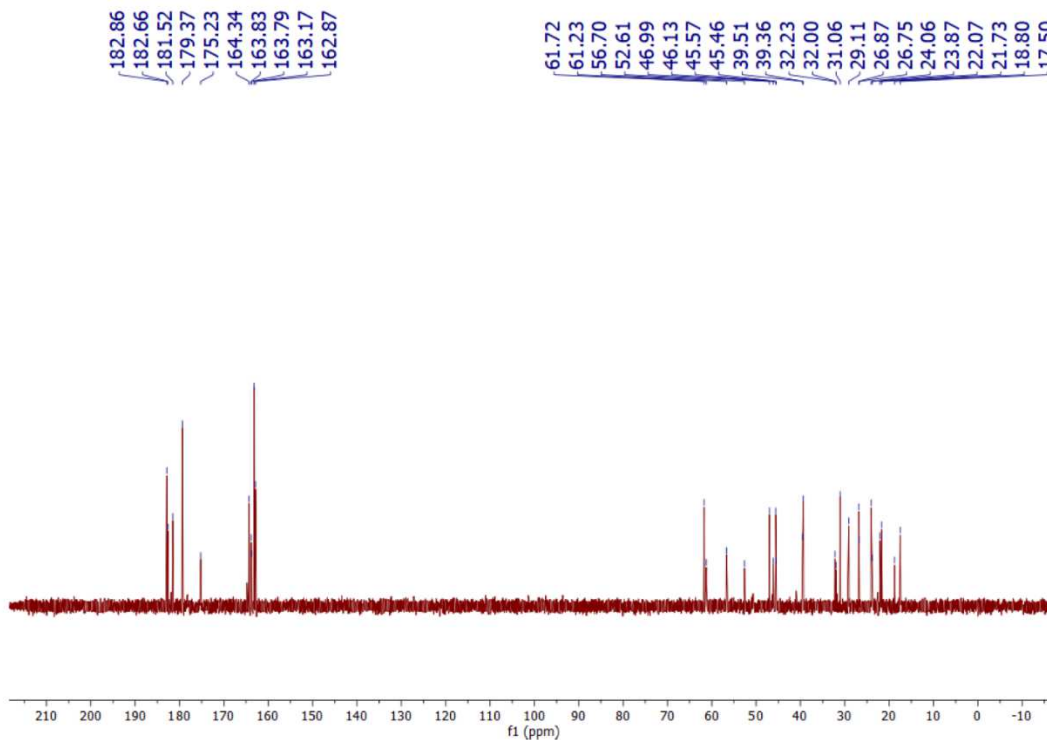
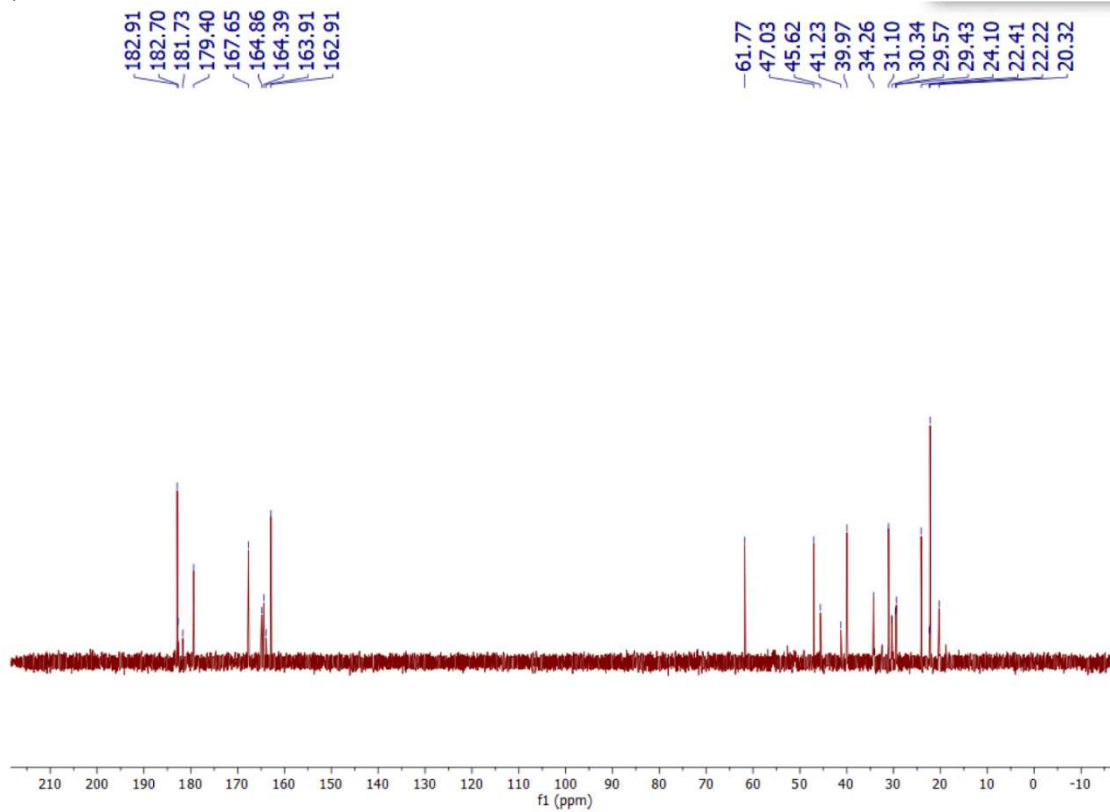


Figure 56: Synthetic Amino Acid Absorbent NMR Spectrum **a)** prior to Absorption **b)** after Absorption **4 c)** after Desorption **4**

Figure 56 (cont'd)

(c)



APPENDIX C: CHAPTER 5 SUPPLEMENTAL INFORMATION

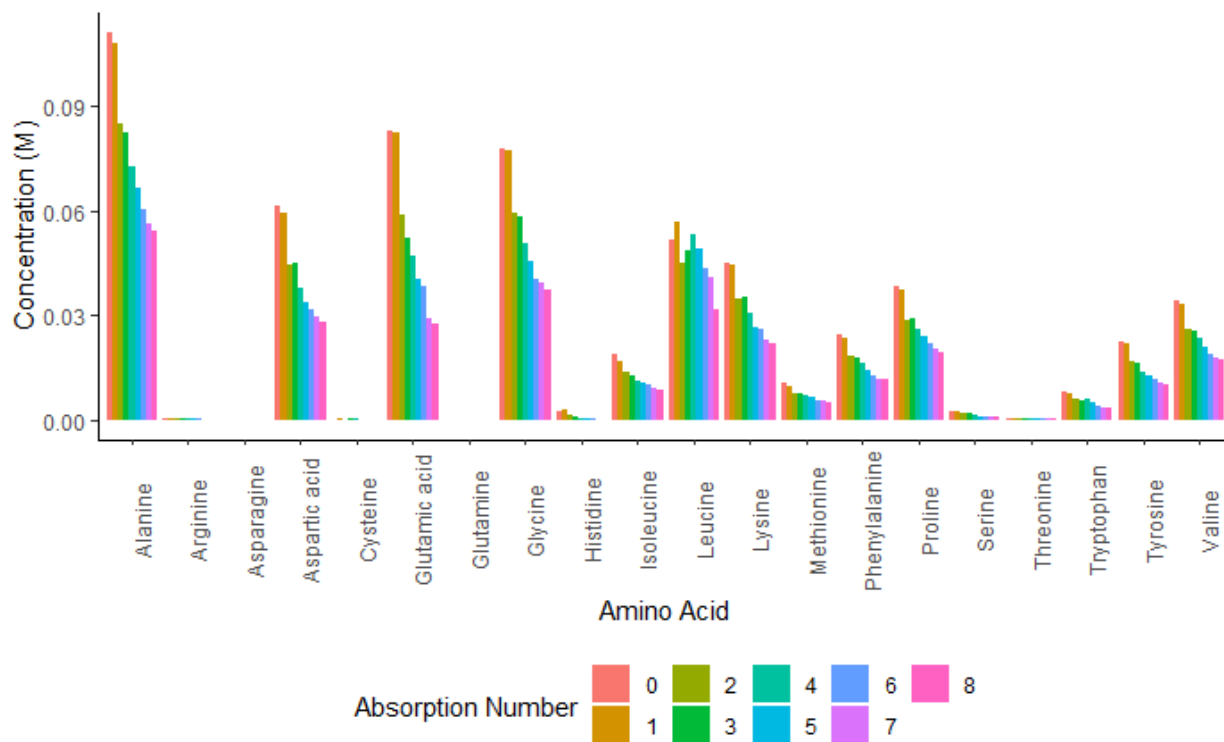


Figure 57: Amino Acid Concentration within the Algal Amino Acid Absorbent after Each Absorption

Table 16: Algal Amino Acid Absorbent CO₂ Absorption and Desorption Capacities

| | Cycle Number | | | | | |
|---|--------------|-------|-------|-------|-------|-------|
| | 1 | 2 | 3 | 5 | 7 | 8 |
| Amount Absorbed (mol/L) | 1.30 | 0.889 | 0.900 | 0.774 | 0.764 | 0.800 |
| Amount Desorbed (mol/L) | 0.615 | 0.697 | 0.739 | 0.728 | 0.728 | .742 |
| Amount Absorbed (mol/mol Amine) | 2.02 | 1.34 | 1.32 | 1.28 | 1.21 | 1.20 |
| Amount Desorbed (mol/mol Amine) | 0.967 | 1.09 | 1.08 | 1.30 | 1.21 | 1.20 |

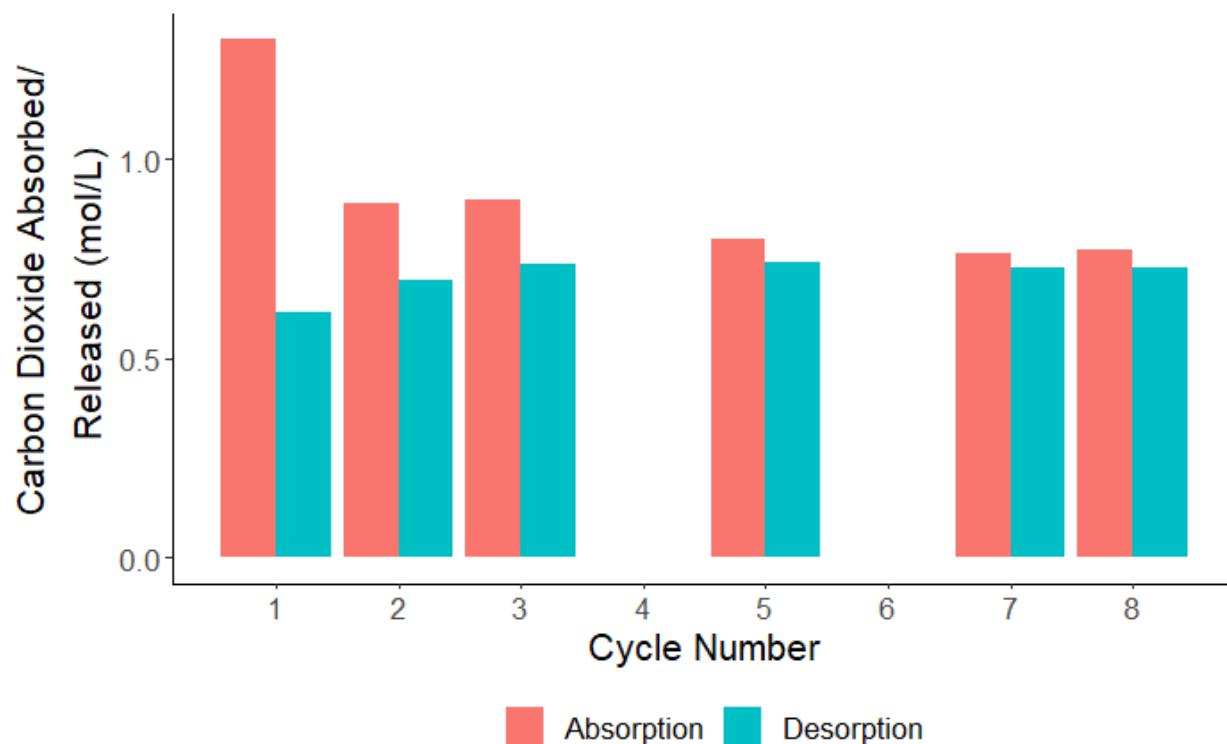


Figure 58: Algal Amino Acid Absorbent CO₂ Absorbed and Desorbed over 8 Cycles in mol/L

Table 17: Algal Amino Acid Absorbent pH over Absorption Cycles

| | Cycle Number | | | | | | | |
|--------------------|--------------|-------|-------|-------|------|-------|-------|-------|
| | 1 | 2 | 3 | 4 | 5 | 6 | 7 | 8 |
| Absorbed pH | 9.25 | 9.04 | 8.99 | 9.55 | 8.93 | 10.35 | 8.87 | 8.88 |
| Desorbed pH | 11.65 | 11.62 | 11.58 | 11.55 | 11.4 | 11.37 | 11.43 | 11.25 |

Table 18: Absorption Capacities for the Synthetic and Algal Amino Acid Absorbents

| | Synthetic AA Absorbent | Algal AA Absorbent |
|---|------------------------|--------------------|
| Amount CO₂ Absorbed (mol/L) | 0.754 ± 0.021 | 0.825 ± 0.065 |
| Amount CO₂ Absorbed (mol/mol Amine) | 0.747 ± 0.021 | 1.27 ± 0.061 |

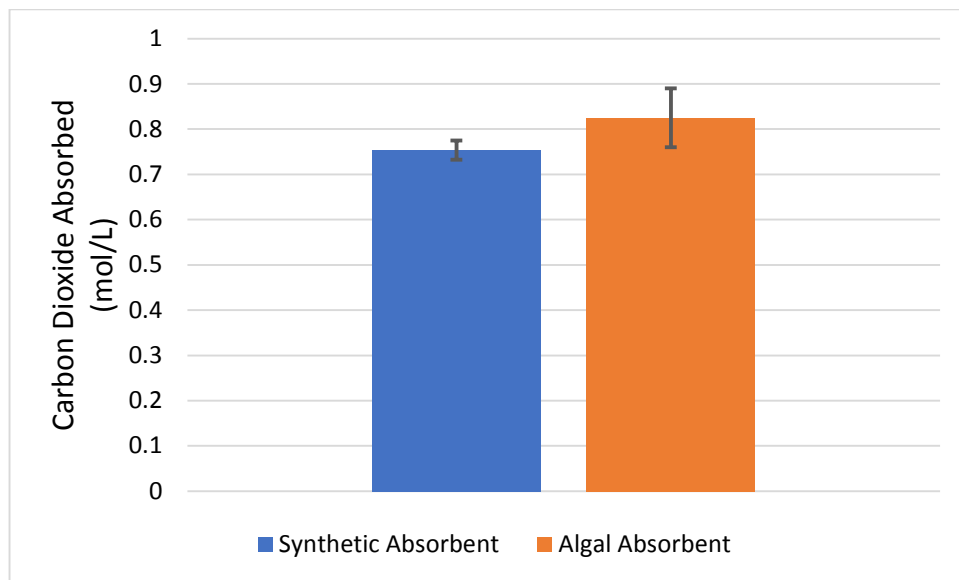


Figure 59: Absorption Capacities for the Synthetic and Algal Amino Acid Absorbents in mol/L

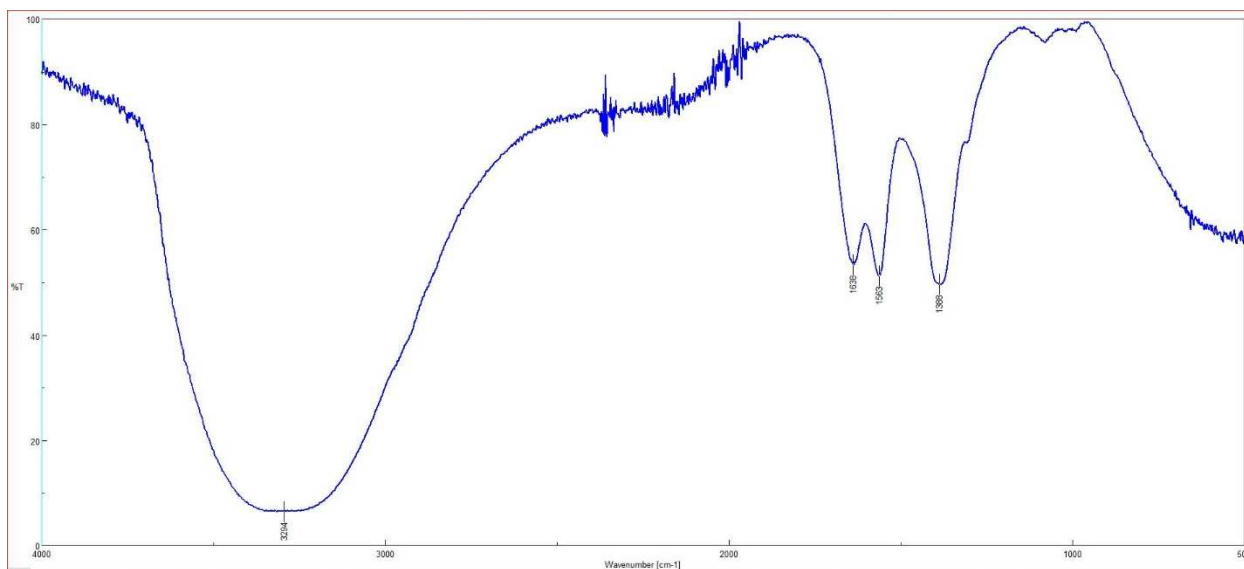


Figure 60: Algal Amino Acid Absorbent ATR-FTIR Spectrum prior to Absorption

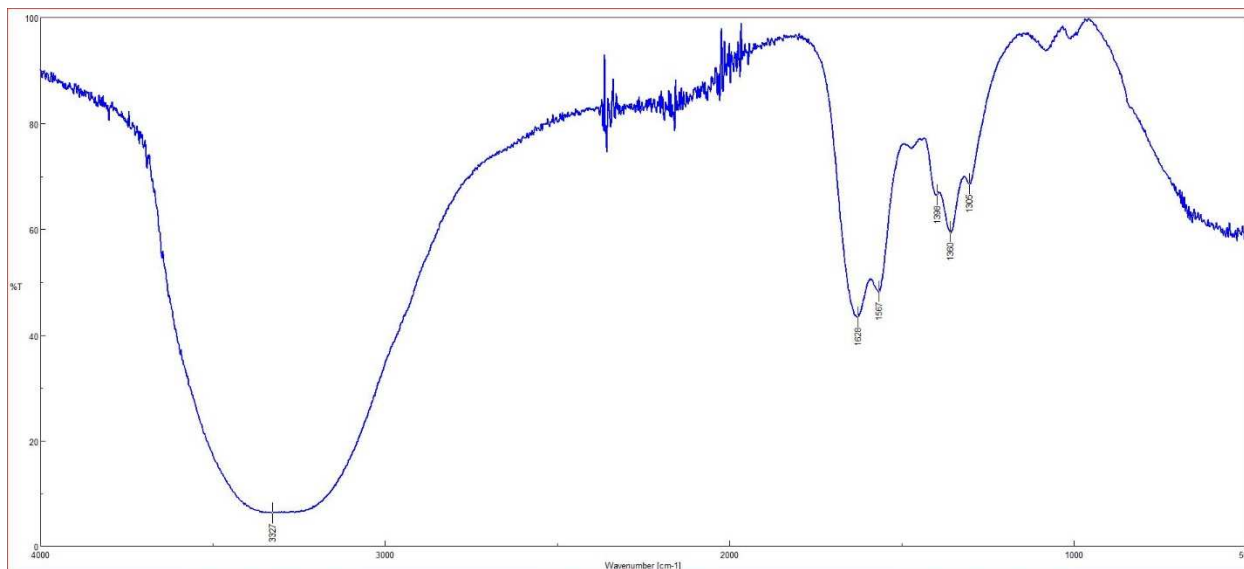


Figure 61: Algal Amino Acid Absorbent ATR-FTIR Spectrum after Absorption 1

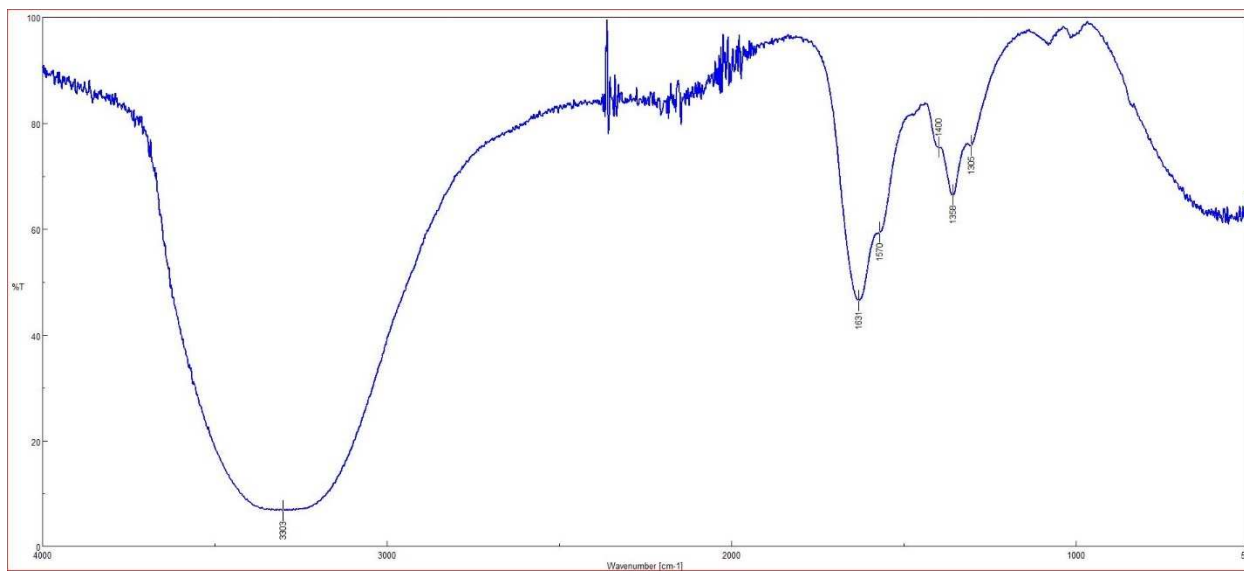


Figure 62: Algal Amino Acid Absorbent ATR-FTIR Spectrum after Absorption 2

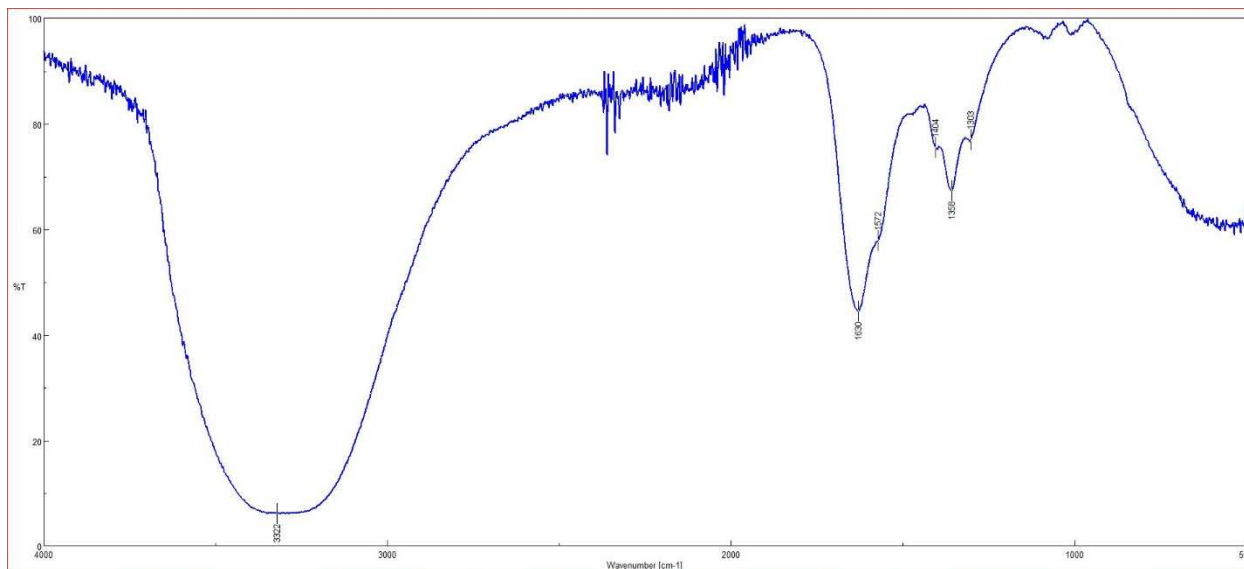


Figure 63: Algal Amino Acid Absorbent ATR-FTIR Spectrum after Absorption 3

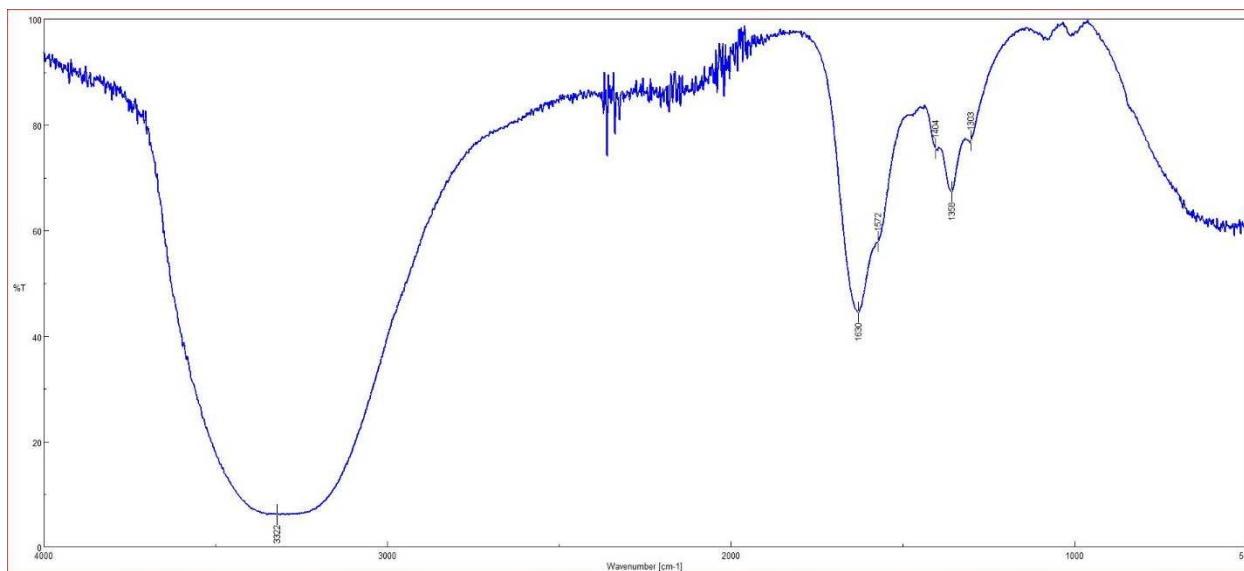


Figure 64: Algal Amino Acid Absorbent ATR-FTIR Spectrum after Absorption 4

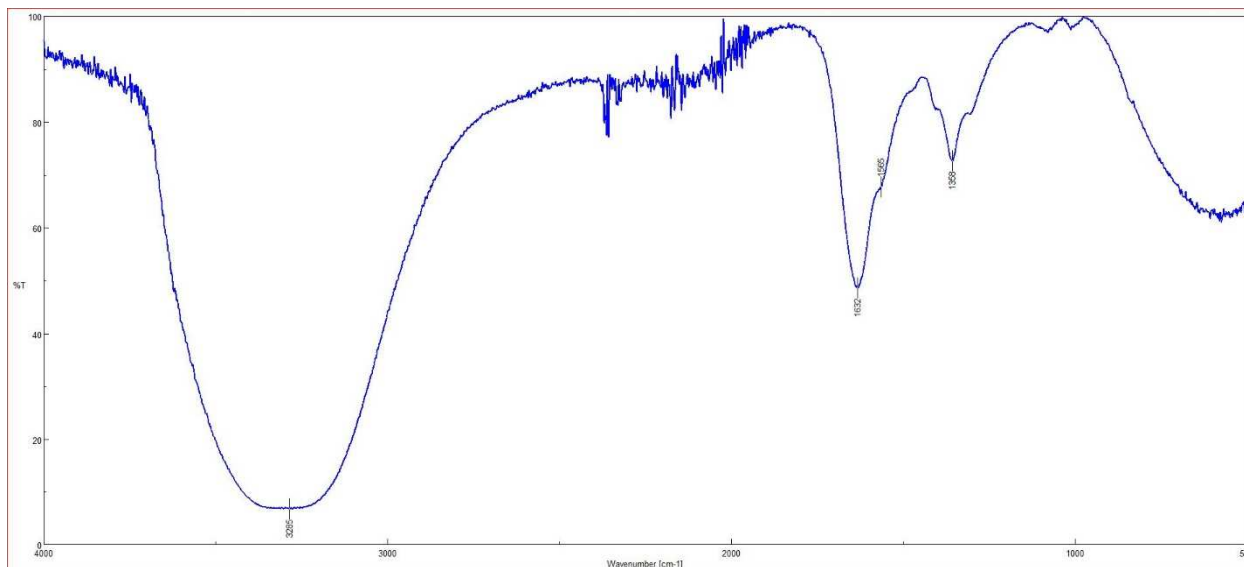


Figure 65: Algal Amino Acid Absorbent ATR-FTIR Spectrum after Absorption 5

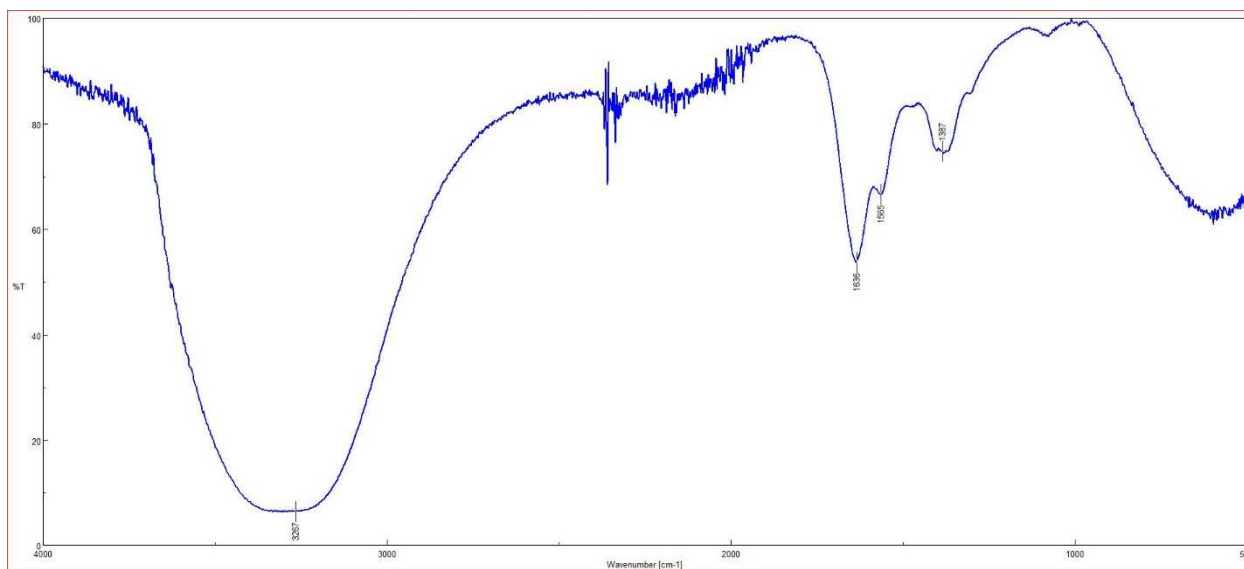


Figure 66: Algal Amino Acid Absorbent ATR-FTIR Spectrum after Absorption 6

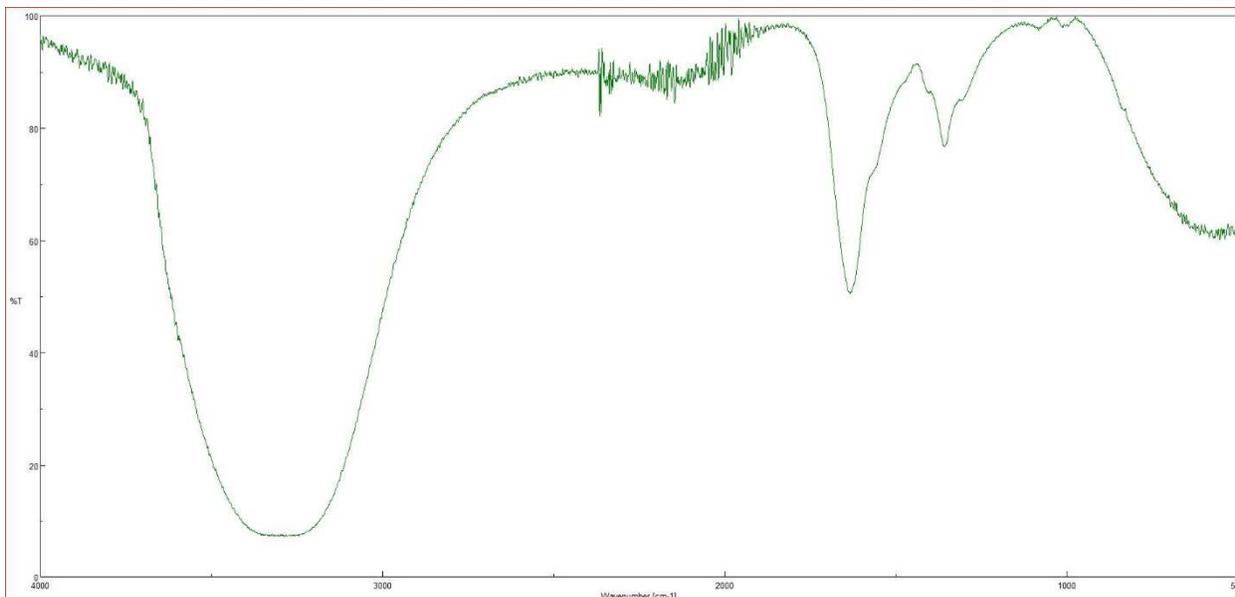


Figure 67: Algal Amino Acid Absorbent ATR-FTIR Spectrum after Absorption 7

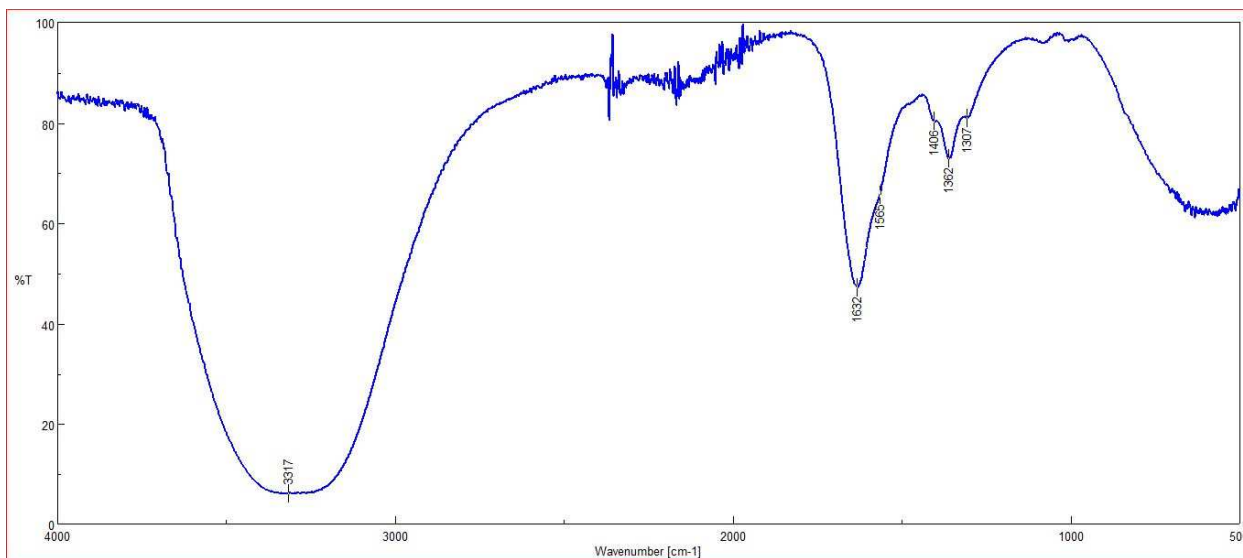


Figure 68: Algal Amino Acid Absorbent ATR-FTIR Spectrum after Absorption 8

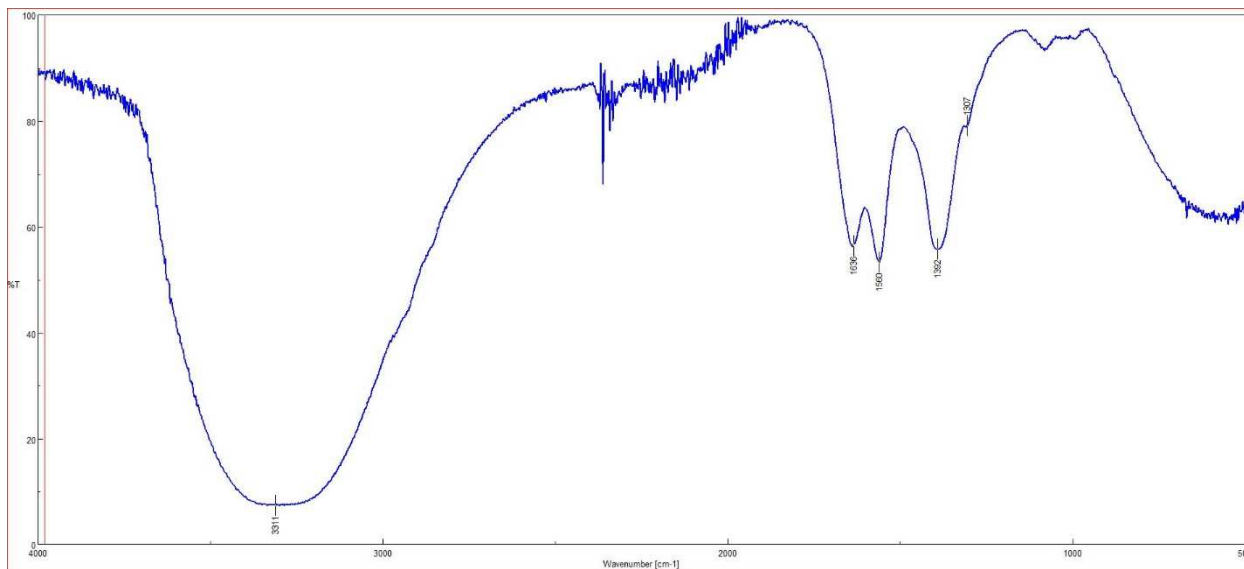


Figure 69: Algal Amino Acid Absorbent ATR-FTIR Spectrum after Desorption 1

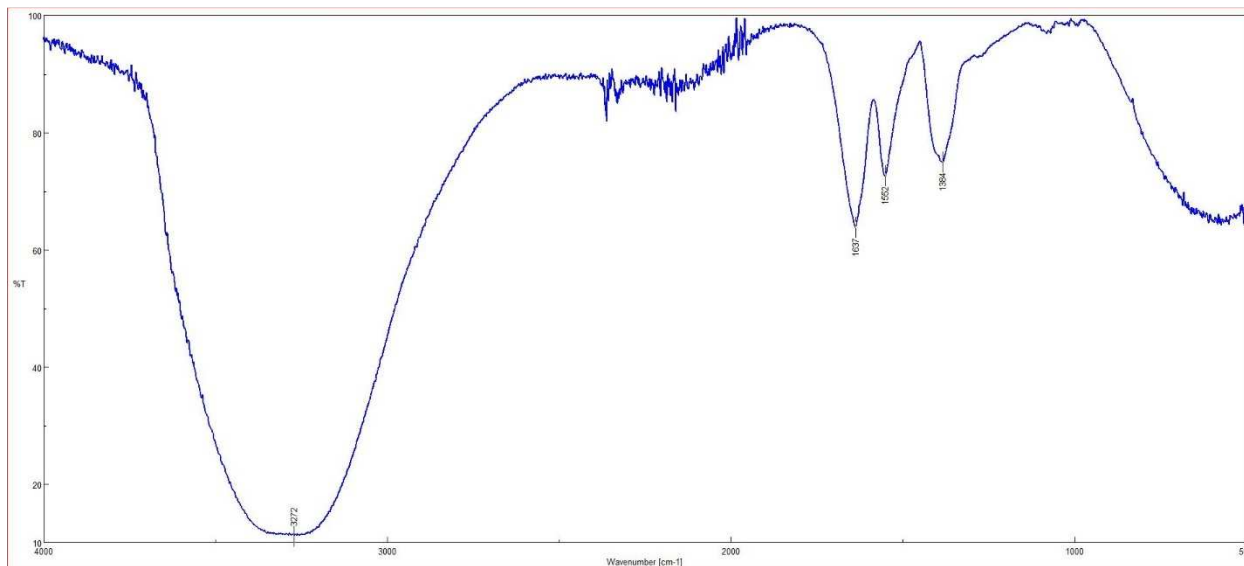


Figure 70: Algal Amino Acid Absorbent ATR-FTIR Spectrum after Desorption 2

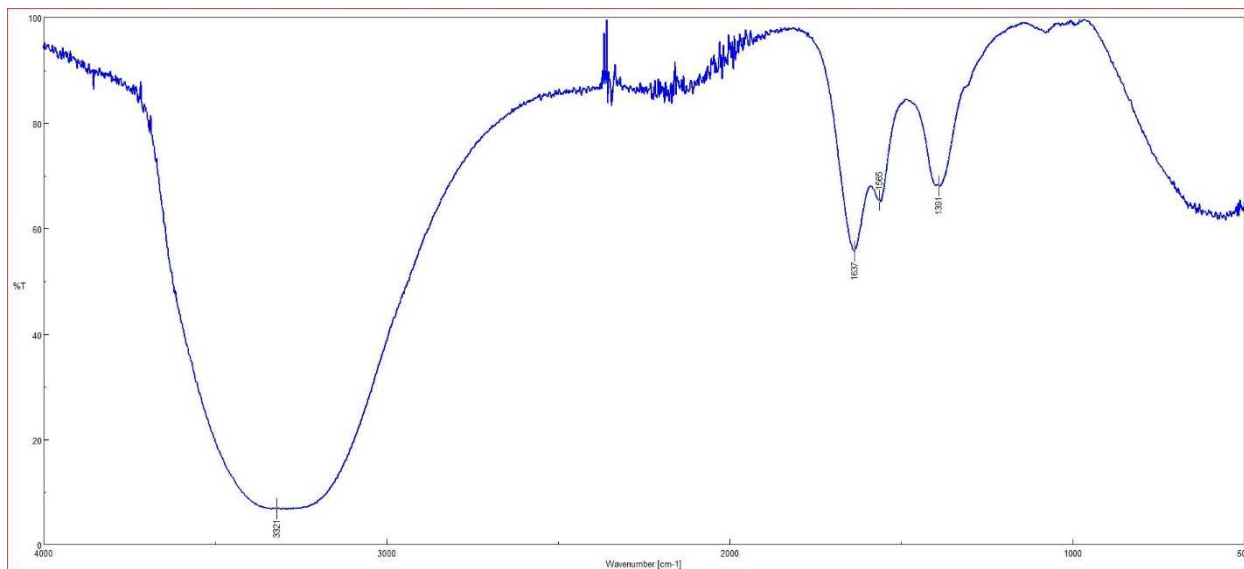


Figure 71: Algal Amino Acid Absorbent ATR-FTIR Spectrum after Desorption 4

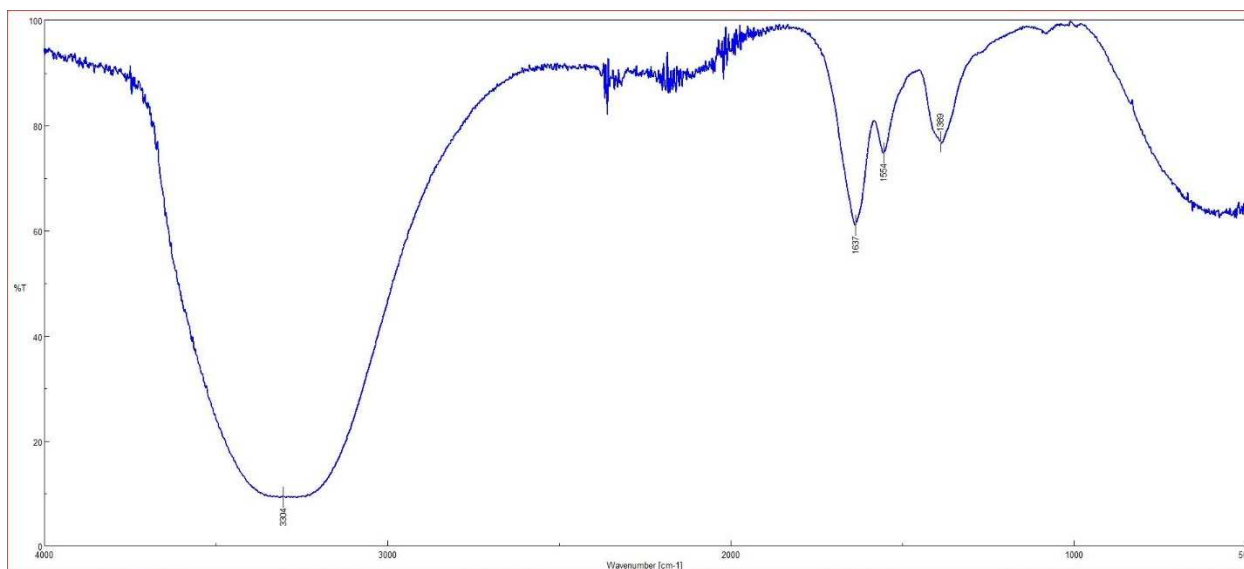


Figure 72: Algal Amino Acid Absorbent ATR-FTIR Spectrum after Desorption 5

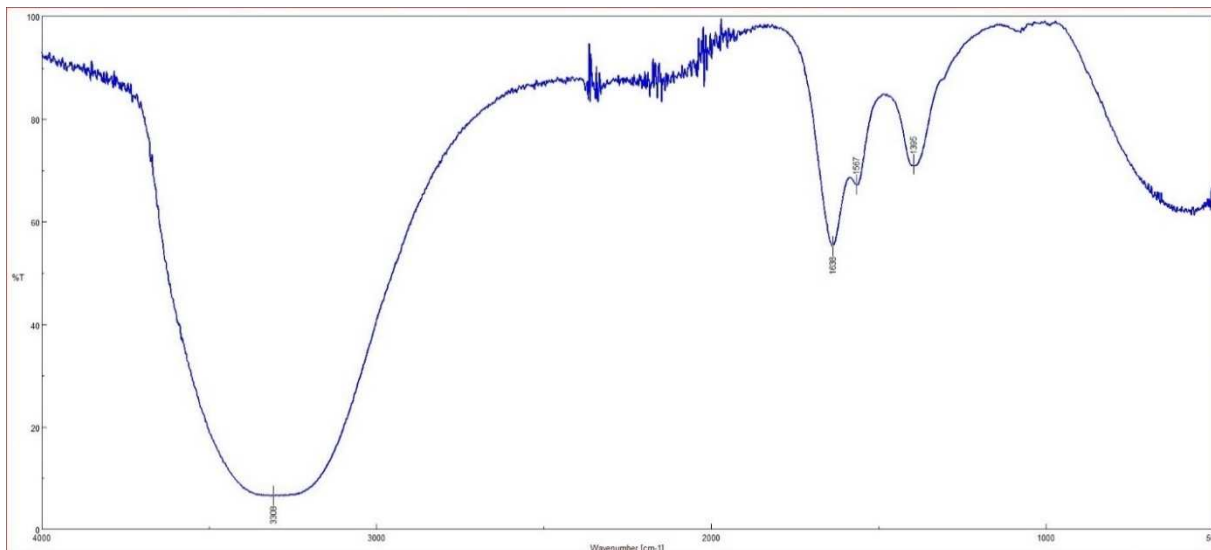


Figure 73: Algal Amino Acid Absorbent ATR-FTIR Spectrum after Desorption 6

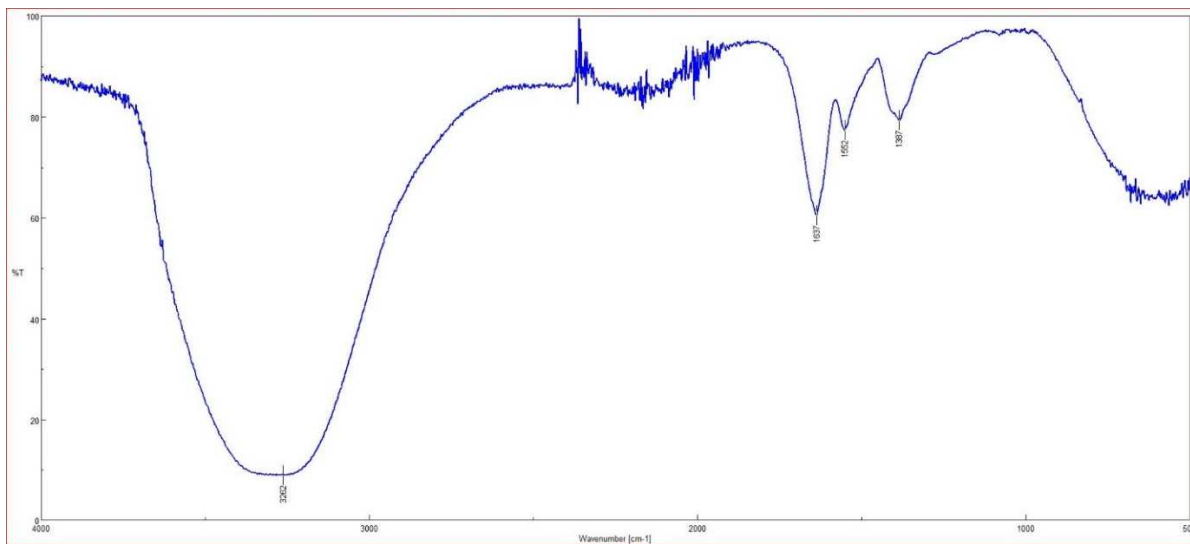


Figure 74: Algal Amino Acid Absorbent ATR-FTIR Spectrum after Desorption 7

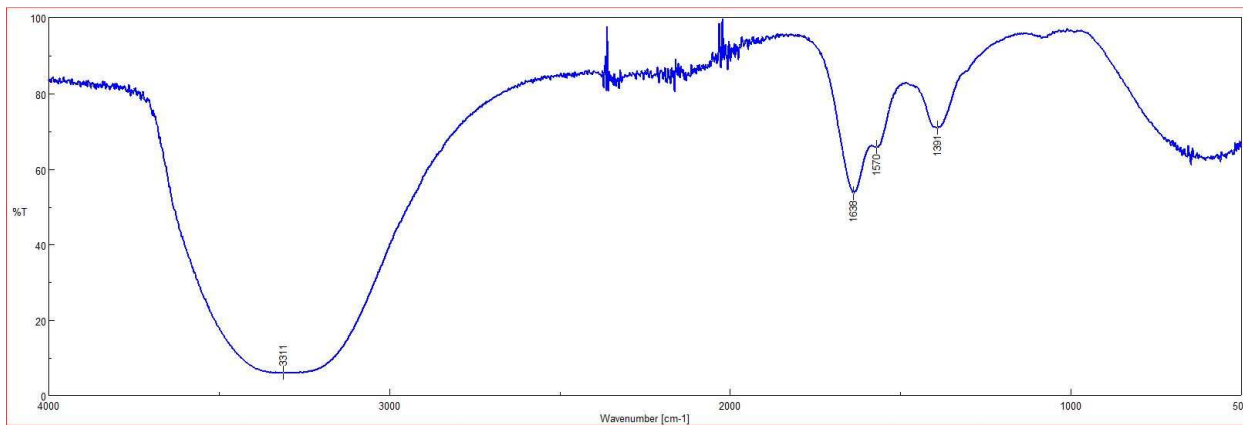


Figure 75: Algal Amino Acid Absorbent ATR-FTIR Spectrum after Desorption 8

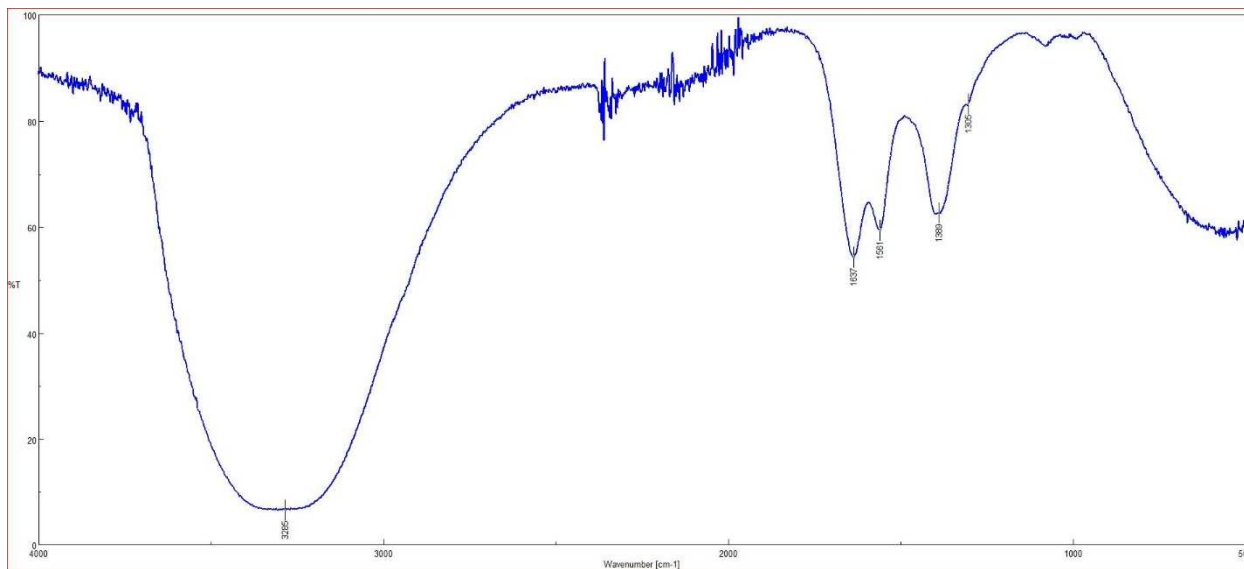


Figure 76: Algal Amino Acid Absorbent ATR-FTIR Spectrum after Desorption 1 after Dilution

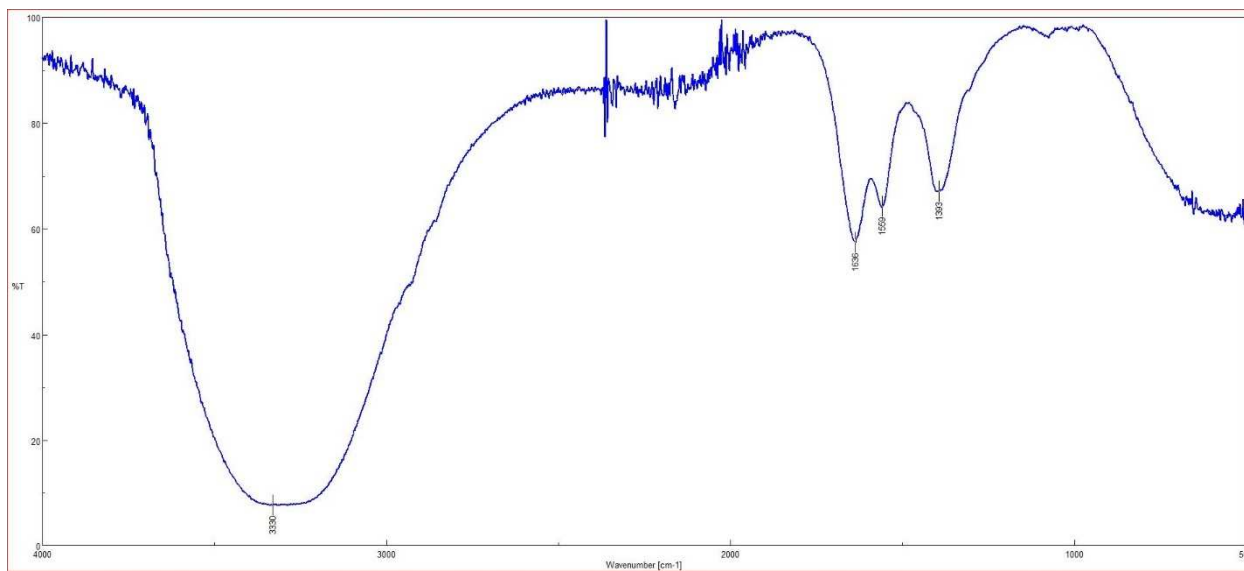


Figure 77: Algal Amino Acid Absorbent ATR-FTIR Spectrum after Desorption 2 after Dilution

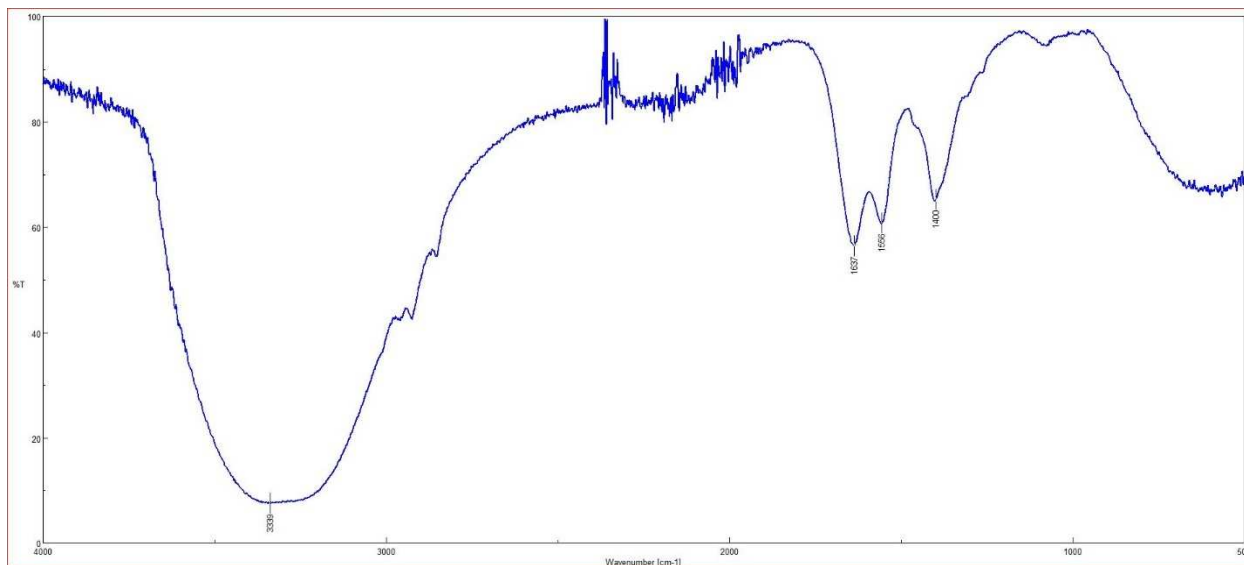


Figure 78: Algal Amino Acid Absorbent ATR-FTIR Spectrum after Desorption 3 after Dilution

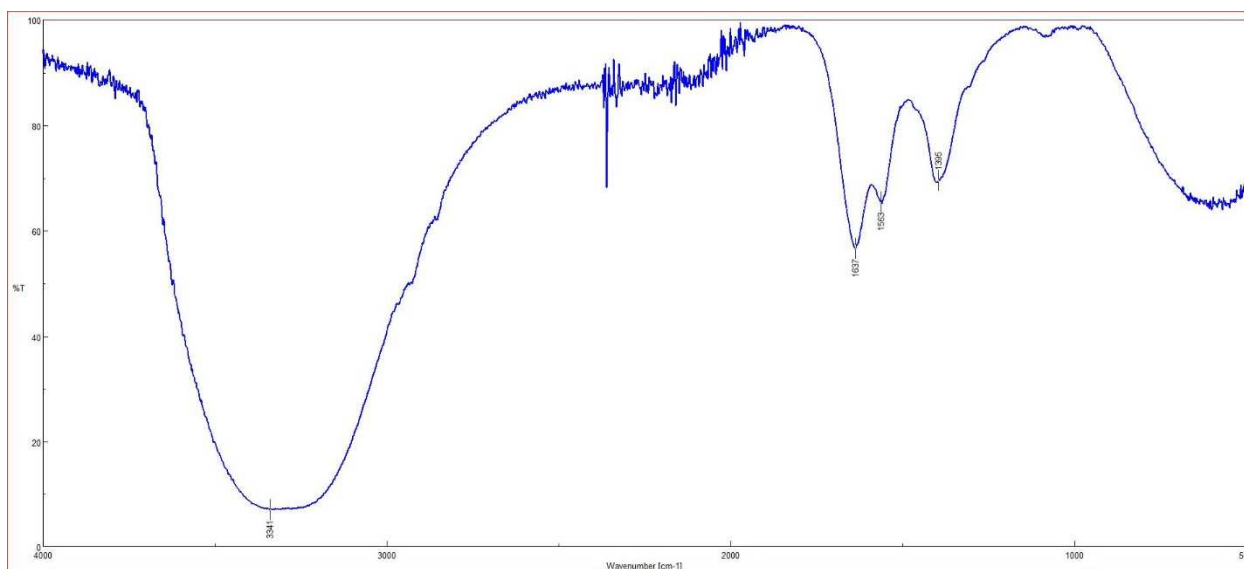


Figure 79: Algal Amino Acid Absorbent ATR-FTIR Spectrum after Desorption 4 after Dilution

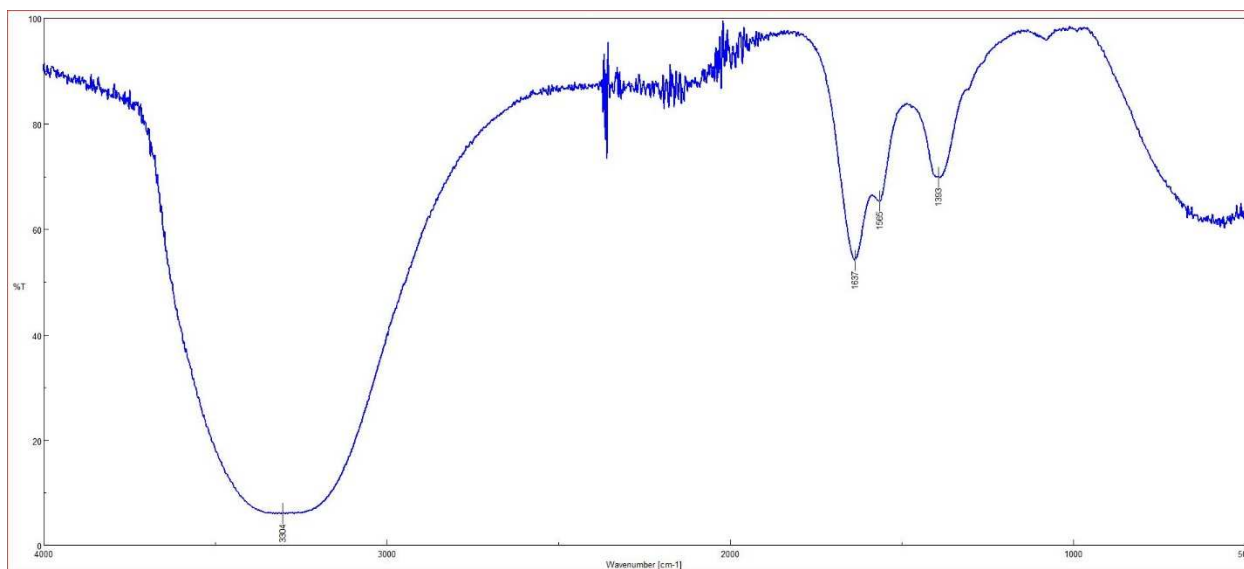


Figure 80: Algal Amino Acid Absorbent ATR-FTIR Spectrum after Desorption 5 after Dilution

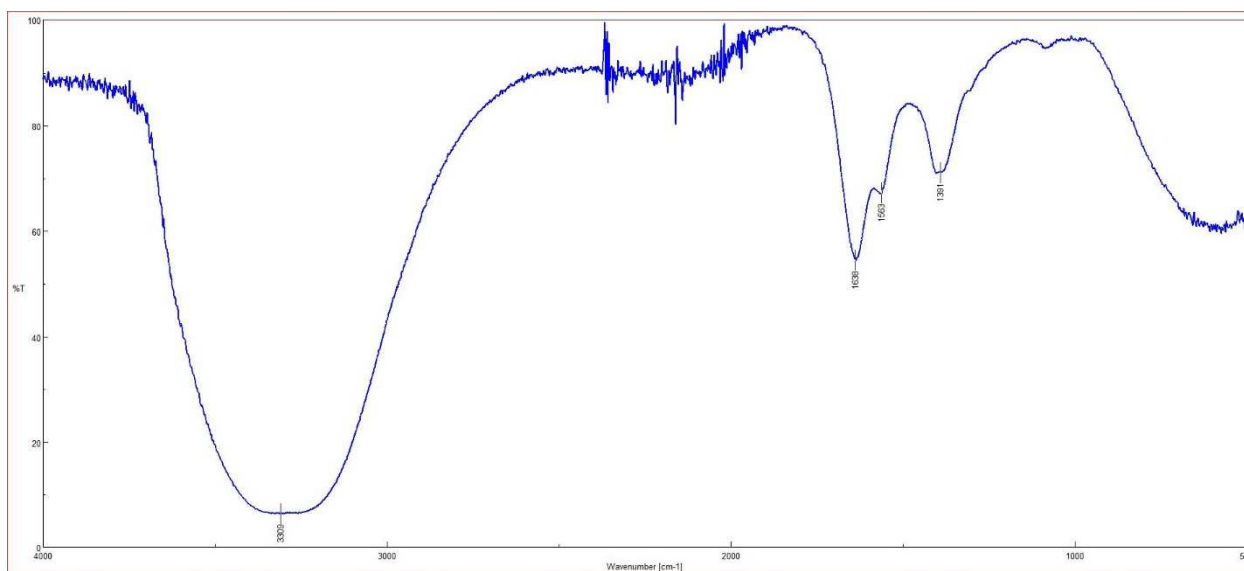


Figure 81: Algal Amino Acid Absorbent ATR-FTIR Spectrum after Desorption 6 after Dilution

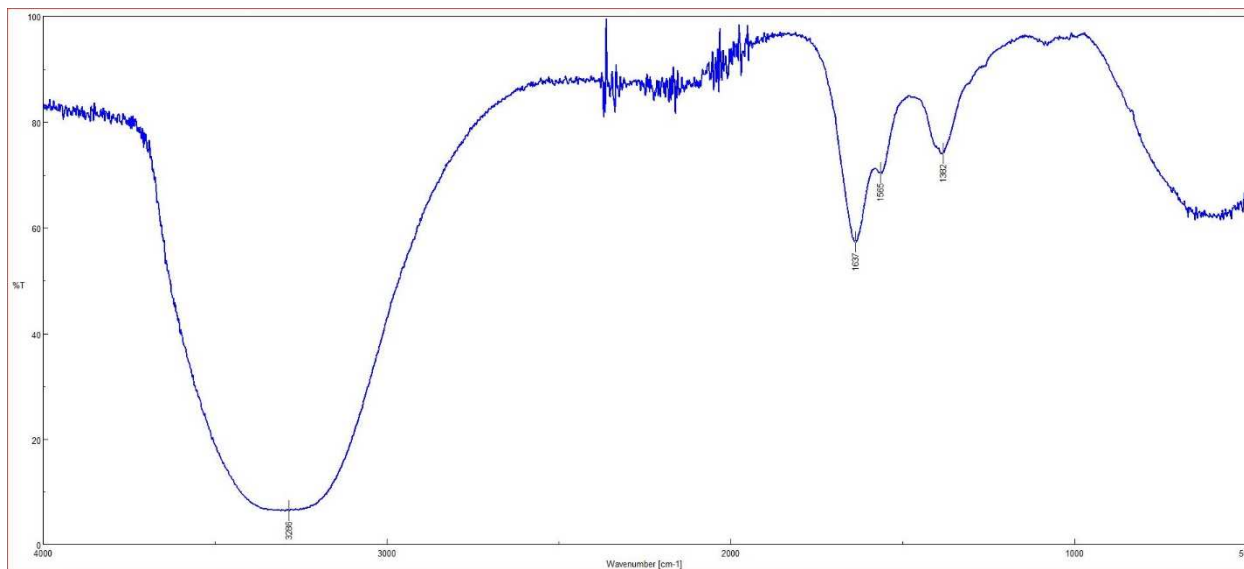


Figure 82: Algal Amino Acid Absorbent ATR-FTIR Spectrum after Desorption 7 after Dilution

Thesis Statistics

Adam Smerigan

07/27/2021

Clear the Environment

```
rm(List=ls())
```

Gather Packages and Data from Metadata Sheet

```
# Load Libraries
library(readxl)
library(ggplot2)

## Warning: package 'ggplot2' was built under R version 4.0.4

## Registered S3 methods overwritten by 'tibble':
##   method      from
##   format.tbl  pillar
##   print.tbl   pillar

library(dplyr)

##
## Attaching package: 'dplyr'

## The following objects are masked from 'package:stats':
##
##   filter, lag

## The following objects are masked from 'package:base':
##
##   intersect, setdiff, setequal, union

library(emmeans)

# Import Data from Metadata Sheet
g.l.ratio.data <- read_excel("Metadata_072621.xlsx", sheet = "g.l.rati
o")
GAPL.cycles.data <- read_excel("Metadata_072621.xlsx", sheet = "GAPL.c
ycles")
algae.cycles.data <- read_excel("Metadata_072621.xlsx", sheet = "algae
.cycles")
TS.data <- read_excel("Metadata_072621.xlsx", sheet = "TS")
```

```

centrifugate.data <- read_excel("Metadata_072621.xlsx", sheet = "Centrifugate")
acidification.data <- read_excel("Metadata_072621.xlsx", sheet = "Acidification")
desorption.data <- read_excel("Metadata_072621.xlsx", sheet = "Desorption")
LCMS.processing.data <- read_excel("Metadata_072621.xlsx", sheet = "LCMS.processing")
LCMS.algae.cycles.data <- read_excel("Metadata_072621.xlsx", sheet = "LCMS.algae.cycles")
Parr.Cond.data <- read_excel("Metadata_072621.xlsx", sheet = "Parr Conditions")

```

Microalgae Conversion and Processing

Parr Reactor Conditions Analysis

```

col <- c("protein.to.KOH", "temperature", "reaction.time")
Parr.Cond.data[col] <- lapply(Parr.Cond.data[col], factor)
summary(Parr.Cond.data)

```

| ## | sample.ID | protein.to.KOH | temperature | reaction.time | AA.conc |
|----|------------------|----------------|-------------|---------------|---------|
| ## | Length:10 | 1:4 | 121:2 | 3:5 | Min. |
| | :13.86 | | | | |
| ## | Class :character | 5:6 | 134:8 | 5:2 | 1st Qu |
| | .:15.19 | | | | |
| ## | Mode :character | | | 7:3 | Median |
| | :59.79 | | | | |
| ## | | | | | Mean |
| | :45.74 | | | | |
| ## | | | | | 3rd Qu |
| | .:67.76 | | | | |
| ## | | | | | Max. |
| | :75.95 | | | | |

```

parr.cond.lm <- lm(AA.conc ~ protein.to.KOH + temperature + reaction.time, Parr.Cond.data)
joint_tests(parr.cond.lm)

```

| ## | model term | df1 | df2 | F.ratio | p.value |
|----|----------------|-----|-----|---------|---------|
| ## | protein.to.KOH | 1 | 5 | 44.106 | 0.0012 |
| ## | temperature | 1 | 5 | 0.045 | 0.8396 |
| ## | reaction.time | 2 | 5 | 0.178 | 0.8424 |

```

lsmeans.parr.cond.koh = emmeans(parr.cond.lm, "protein.to.KOH")
pairs(lsmeans.parr.cond.koh)

```

```

## contrast estimate SE df t.ratio p.value
## 1 - 5 -55 8.28 5 -6.641 0.0012
##
## Results are averaged over the Levels of: temperature, reaction.time
multcomp::cld(Lsmeans.parr.cond.koh, by = NULL, Letters = "abcdefg", alpha = .05) # Tukey

## protein.to.KOH emmean SE df Lower.CL upper.CL .group
## 1 13.7 4.01 5 3.41 24.0 a
## 5 68.7 5.69 5 54.06 83.3 b
##
## Results are averaged over the Levels of: temperature, reaction.time
## Confidence Level used: 0.95
## significance level used: alpha = 0.05

Lsmeans.parr.cond.temp = emmeans(parr.cond.lm, "temperature")
pairs(Lsmeans.parr.cond.temp)

## contrast estimate SE df t.ratio p.value
## 121 - 134 1.33 6.26 5 0.213 0.8396
##
## Results are averaged over the Levels of: protein.to.KOH, reaction.time
ime
multcomp::cld(Lsmeans.parr.cond.temp, by = NULL, Letters = "abcdefg", alpha = .05) # Tukey

## temperature emmean SE df Lower.CL upper.CL .group
## 134 40.5 2.67 5 33.7 47.4 a
## 121 41.9 5.17 5 28.6 55.2 a
##
## Results are averaged over the Levels of: protein.to.KOH, reaction.time
ime
## Confidence Level used: 0.95
## significance level used: alpha = 0.05

Lsmeans.parr.cond.time = emmeans(parr.cond.lm, "reaction.time")
pairs(Lsmeans.parr.cond.time)

## contrast estimate SE df t.ratio p.value
## 3 - 5 -3.234 9.28 5 -0.348 0.9361
## 3 - 7 -3.998 6.86 5 -0.583 0.8347
## 5 - 7 -0.764 6.26 5 -0.122 0.9918
##
## Results are averaged over the Levels of: protein.to.KOH, temperature
e

```

```
## P value adjustment: tukey method for comparing a family of 3 estimates
multcomp::cld(Lsmeans.parr.cond.time, by = NULL, Letters = "abcdefg",
alpha = .05) # Tukey

## reaction.time emmean SE df Lower.CL upper.CL .group
## 3 38.8 5.00 5 26.0 51.6 a
## 5 42.0 6.06 5 26.5 57.6 a
## 7 42.8 4.14 5 32.2 53.4 a
##
## Results are averaged over the levels of: protein.to.KOH, temperature
## Confidence Level used: 0.95
## P value adjustment: tukey method for comparing a family of 3 estimates
## significance level used: alpha = 0.05

par(mfrow=c(2,2))
plot(Lsmeans.parr.cond.koh, comparisons=TRUE, xlab = "Mean AA Concentration (g/L)", ylab = "KOH:Protein Ratio")
```

```
plot(Lsmeans.parr.cond.temp, comparisons=TRUE, xlab = "Mean AA Concentration (g/L)", ylab = "Temperature (Celsius)")
```

```
plot(Lsmeans.parr.cond.time, comparisons=TRUE, xlab = "Mean AA Concentration (g/L)", ylab = "Reaction Time (Hours)")
```

```
par(mfrow=c(1,1))
```

Plot of Amino Acid Concentration after Each Processing Step

```
# Organize the Data for Plotting
parr.slurry.averaged <- LCMS.processing.data %>%
  group_by(Name) %>%
  filter(Type == "Parr Slurry") %>%
  summarize(m.1 = mean(AA.Conc.M), sd.1 = sd(AA.Conc.M), .groups = 'drop')

centrifugate.averaged <- LCMS.processing.data %>%
  group_by(Name) %>%
  filter(Type == "Centrifugate") %>%
  summarize(m.2 = mean(AA.Conc.M), sd.2 = sd(AA.Conc.M), .groups = 'drop')
```

```

op')

acid.cent.averaged <- LCMS.processing.data %>%
  group_by(Name) %>%
  filter(Type == "Acidified Centrifugate") %>%
  summarize(m.3 = mean(AA.Conc.M), sd.3 = sd(AA.Conc.M), .groups = 'dr
op')

prod.averaged <- LCMS.processing.data %>%
  group_by(Name) %>%
  filter(Type == "AA Product") %>%
  summarize(m.4 = mean(AA.Conc.M), sd.4 = sd(AA.Conc.M), .groups = 'dr
op')

y.proc.1 <- c(parr.slurry.averaged$m.1, centrifugate.averaged$m.2, aci
d.cent.averaged$m.3, prod.averaged$m.4)
x.proc.1 <- c(rep(sort(unique(LCMS.processing.data$Name)), 4))
error.proc.1 <- c(parr.slurry.averaged$sd.1, centrifugate.averaged$sd.
2, acid.cent.averaged$sd.3, prod.averaged$sd.4)
fill.proc.1 <- c(rep("Parr Slurry", 20), rep("Centrifugate", 20), rep(
"Acidified Centrifugate", 20), rep("AA Product", 20))
proc.data.frame <- as.data.frame(y.proc.1)
proc.plot.1 <- data.frame(x.proc.1, y.proc.1, error.proc.1, fill.proc.
1)

# Plot the Data
ggplot(proc.plot.1, aes(x= x.proc.1, y = y.proc.1, fill = fill.proc.1)
) +
  geom_bar(position = position_dodge(), stat = "identity") +
  geom_errorbar(aes(ymin=y.proc.1-error.proc.1, ymax=y.proc.1+error.pr
oc.1), width=0.2, position=position_dodge(0.9)) +
  labs(x = "Amino Acid", y = "Concentration (M)") +
  theme_classic() +
  theme(axis.text.x = element_text(angle = 90), legend.position="botto
m", text = element_text(size = 12)) +
  guides(fill=guide_legend(title=""))

```

Analysis of Algal Amino Acid Solution Amino Acid Concentrations after each Processing Step

```

# Organize Data for ANOVA
Lcms.processing.data <- LCMS.processing.data
Lcms.processing.data$Type <- factor(Lcms.processing.data$Type)
summary(Lcms.processing.data)

```

```

##      Column1                Type      Experiment      Name
## Min.      : 1  AA Product          :80  Min.      :1.000  Length:30
0
## 1st Qu.: 4  Acidified Centrifugate:60  1st Qu.:1.000  Class :ch
aracter
## Median : 8  Centrifugate                :80  Median :3.000  Mode  :ch
aracter
## Mean    : 8  Parr Slurry                  :80  Mean    :2.533
## 3rd Qu.:12                                     3rd Qu.:4.000
## Max.    :15                                     Max.    :4.000
##      MW g/mol          N      Raw Dilution  LCMS Dilution
## Min.      : 75.07  Min.      :1.00  Min.      :5000  Min.      :1
## 1st Qu.:118.60  1st Qu.:1.00  1st Qu.:5000  1st Qu.:1
## Median :132.60  Median :1.00  Median :5000  Median :1
## Mean    :136.90  Mean    :1.40  Mean    :5000  Mean    :1
## 3rd Qu.:150.70  3rd Qu.:1.25  3rd Qu.:5000  3rd Qu.:1
## Max.    :204.20  Max.    :4.00  Max.    :5000  Max.    :1
## Diluted Conc. (uM) Undiluted Conc. (uM) AA.Conc.gperL      AA.Con
c.M
## Min.      : 0.0000  Min.      : 0      Min.      : 0.0000  Min.      :
0.000000
## 1st Qu.: 0.3267  1st Qu.: 1634      1st Qu.: 0.1855  1st Qu.:
0.001634
## Median : 3.7105  Median : 18553      Median : 2.9021  Median :
0.018552
## Mean    : 5.7316  Mean    : 28658      Mean    : 3.5012  Mean    :
0.028658
## 3rd Qu.: 9.0510  3rd Qu.: 45255      3rd Qu.: 5.7940  3rd Qu.:
0.045255
## Max.    :25.9380  Max.    :129690      Max.    :15.4220  Max.    :
0.129690

# Conduct ANOVA and Pairwise Comparisons
algae.proc.lm <- lm(AA.Conc.M ~ Type, lcms.processing.data)
joint_tests(algae.proc.lm) #Type 3 ANOVA Table

## model term df1 df2 F.ratio p.value
## Type          3 296    0.07 0.9758

Lsmeans.algae.proc = emmeans(algae.proc.lm, "Type")
summary(Lsmeans.algae.proc)

## Type          emmean      SE  df Lower.CL upper.CL
## AA Product      0.0297 0.00353 296  0.0228  0.0367
## Acidified Centrifugate 0.0291 0.00408 296  0.0211  0.0371
## Centrifugate     0.0283 0.00353 296  0.0214  0.0353
## Parr Slurry      0.0276 0.00353 296  0.0206  0.0345

```

```
##
## Confidence Level used: 0.95
plot(Lsmeans.algae.proc, comparisons=TRUE, xlab = "Mean Amino Acid Con
centration (M)", ylab = "Processing Step")
```

```
pairs(Lsmeans.algae.proc)

## contrast                estimate      SE  df t.ratio
p.value
## AA Product - Acidified Centrifugate  0.000613 0.0054 296 0.114
0.9995
## AA Product - Centrifugate           0.001399 0.0050 296 0.280
0.9923
## AA Product - Parr Slurry            0.002174 0.0050 296 0.435
0.9724
## Acidified Centrifugate - Centrifugate 0.000786 0.0054 296 0.146
0.9989
## Acidified Centrifugate - Parr Slurry  0.001561 0.0054 296 0.289
0.9916
## Centrifugate - Parr Slurry           0.000775 0.0050 296 0.155
0.9987
##
## P value adjustment: tukey method for comparing a family of 4 estima
tes

multcomp::cld(Lsmeans.algae.proc, by = NULL, Letters = "abcdefg", alph
a = .05) # Tukey
```

```
## Type                emmean      SE  df Lower.CL upper.CL .group
## Parr Slurry         0.0276 0.00353 296  0.0206  0.0345  a
## Centrifugate        0.0283 0.00353 296  0.0214  0.0353  a
## Acidified Centrifugate 0.0291 0.00408 296  0.0211  0.0371  a
## AA Product          0.0297 0.00353 296  0.0228  0.0367  a
##
## Confidence Level used: 0.95
## P value adjustment: tukey method for comparing a family of 4 estima
tes
## significance level used: alpha = 0.05
```

Percent Mass Liquid Yield after Centrifuge Plot and Analysis

```
# Organize data for plotting
cent.exp.1 <- centrifugate.data %>%
  group_by(experiment.number) %>%
```

```

  summarize(m = mean(perc.mass.Liquid, na.rm = T), stdev = sd(perc.mass.Liquid, na.rm = T))
## `summarise()` ungrouping output (override with `.groups` argument)
cent.exp.1$experiment.number <- as.factor(cent.exp.1$experiment.number)

# Plot Percent Mass Liquid Yield after Centrifuge Data
ggplot(cent.exp.1, aes(fill = experiment.number, x= experiment.number, y = m)) +
  geom_bar(position = position_dodge(), stat = "identity") +
  geom_errorbar(aes(ymin=m-stdev, ymax=m+stdev), width=0.2, position=position_dodge(0.9)) +
  labs(x = "Experiment Number", y = "Percent Mass Yield") +
  theme_classic() +
  theme(legend.position = "none")

```

```

# ANOVA Analysis
summary(aov(perc.mass.Liquid~as.factor(experiment.number), data = centrifugate.data))

##
##              Df  Sum Sq Mean Sq F value Pr(>F)
## as.factor(experiment.number)  3 0.14588 0.04863   359.4 <2e-16 ***
## Residuals                    92 0.01245 0.00014
## ---
## Signif. codes:  0 '***' 0.001 '**' 0.01 '*' 0.05 '.' 0.1 ' ' 1
## 16 observations deleted due to missingness

cent.mass.sas <- lm(perc.mass.Liquid~as.factor(experiment.number), data = centrifugate.data)
summary(cent.mass.sas)

##
## Call:
## lm(formula = perc.mass.Liquid ~ as.factor(experiment.number),
##     data = centrifugate.data)
##
## Residuals:
##      Min       1Q   Median       3Q      Max
## -0.042226 -0.007986  0.001870  0.009704  0.021917
##
## Coefficients:
##              Estimate Std. Error t value Pr(>|t|)
## (Intercept)    0.661556   0.002480  266.759 < 2e-16
## ***

```

```

## as.factor(experiment.number)2 -0.079112 0.003507 -22.557 < 2e-16
***
## as.factor(experiment.number)3 0.030482 0.003433 8.878 5.23e-14
***
## as.factor(experiment.number)4 -0.008276 0.003314 -2.497 0.0143
*
## ---
## Signif. codes: 0 '***' 0.001 '**' 0.01 '*' 0.05 '.' 0.1 ' ' 1
##
## Residual standard error: 0.01163 on 92 degrees of freedom
## (16 observations deleted due to missingness)
## Multiple R-squared: 0.9214, Adjusted R-squared: 0.9188
## F-statistic: 359.4 on 3 and 92 DF, p-value: < 2.2e-16

Lsmeans_cent.mass = emmeans(cent.mass.sas, "experiment.number")
summary(Lsmeans_cent.mass)

## experiment.number emmean SE df Lower.CL upper.CL
## 1 0.662 0.00248 92 0.657 0.666
## 2 0.582 0.00248 92 0.578 0.587
## 3 0.692 0.00237 92 0.687 0.697
## 4 0.653 0.00220 92 0.649 0.658
##
## Confidence Level used: 0.95

plot(Lsmeans_cent.mass, comparisons=TRUE)

```

```

pairs(Lsmeans_cent.mass) # Shows which comparison has the most significant
difference between means. All except 1-4 are very significant

## contrast estimate SE df t.ratio p.value
## 1 - 2 0.07911 0.00351 92 22.557 <.0001
## 1 - 3 -0.03048 0.00343 92 -8.878 <.0001
## 1 - 4 0.00828 0.00331 92 2.497 0.0670
## 2 - 3 -0.10959 0.00343 92 -31.920 <.0001
## 2 - 4 -0.07084 0.00331 92 -21.375 <.0001
## 3 - 4 0.03876 0.00324 92 11.978 <.0001
##
## P value adjustment: tukey method for comparing a family of 4 estimates

```

Algal Amino Acid Solution Liquid Mass after Acidification

```

# Calculate mean and standard deviation for plotting
mean(acidification.data$mass.Liquid[c(1,4)])

```

```
## [1] 459.05
sd(acidification.data$mass.Liquid[c(1,4)])
## [1] 45.32554
# Plot the mean liquid mass after acidification with error bars
ggplot(data = acidification.data, aes(x = "Acidification", y = mean(mass.Liquid[c(1,4)]))) +
  geom_bar(position = position_dodge(), stat = "identity") +
  geom_errorbar(aes(ymin=mean(mass.Liquid[c(1,4)])-sd(mass.Liquid[c(1,4)]), ymax=mean(mass.Liquid[c(1,4)])+sd(mass.Liquid[c(1,4)])), width=0.2, position=position_dodge(0.9)) +
  labs(x = "", y = "Liquid Mass After Acidification (g)") +
  theme_classic()
```

```
theme(legend.position = "none")
```

```
## List of 1
## $ legend.position: chr "none"
## - attr(*, "class")= chr [1:2] "theme" "gg"
## - attr(*, "complete")= logi FALSE
## - attr(*, "validate")= logi TRUE
```

Plot of Amino Acid Concentrations (M) after each Processing Step for Each Experimental Replicate

```
# Plot Amino Acid Concentrations after Parr Reactor for each Experiment
ggplot(filter(select(LCMS.processing.data, Type, Experiment, Name, AA.Conc.M), Type == "Parr Slurry"), aes(fill = as.factor(Experiment), x = Name, y = AA.Conc.M)) +
  geom_bar(position = position_dodge(), stat = "identity") +
  theme_classic() +
  theme(axis.text.x = element_text(angle = 90), text = element_text(size = 12))+
  labs(x = "Amino Acid", y = "Concentration (M)") +
  scale_fill_discrete(name = "Experiment Number")
```

```
# Plot Amino Acid Concentrations after Centrifuge for each Experiment
ggplot(filter(select(LCMS.processing.data, Type, Experiment, Name, AA.Conc.M), Type == "Centrifugate"), aes(fill = as.factor(Experiment), x = Name, y = AA.Conc.M)) +
  geom_bar(position = position_dodge(), stat = "identity") +
  theme_classic() +
  theme(axis.text.x = element_text(angle = 90), text = element_text(size = 12))+
```

```
ze = 12)) +
  labs(x = "Amino Acid", y = "Concentration (M)") +
  scale_fill_discrete(name = "Experiment Number")
```

```
# Plot Amnio Acid Concentrations after Acidification for each Experiment
ggplot(filter(select(LCMS.processing.data, Type, Experiment, Name, AA.
Conc.M), Type == "Acidified Centrifugate"), aes(fill = as.factor(Exper
iment), x = Name, y = AA.Conc.M)) +
  geom_bar(position = position_dodge(), stat = "identity") +
  theme_classic() +
  theme(axis.text.x = element_text(angle = 90), text = element_text(si
ze = 12)) +
  labs(x = "Amino Acid", y = "Concentration (M)") +
  scale_fill_discrete(name = "Experiment Number")
```

```
# Plot Amnio Acid Concentrations after Desorption for each Experiment
ggplot(filter(select(LCMS.processing.data, Type, Experiment, Name, AA.
Conc.M), Type == "AA Product"), aes(fill = as.factor(Experiment), x =
Name, y = AA.Conc.M)) +
  geom_bar(position = position_dodge(), stat = "identity") +
  theme_classic() +
  theme(axis.text.x = element_text(angle = 90), text = element_text(si
ze = 12)) +
  labs(x = "Amino Acid", y = "Concentration (M)") +
  scale_fill_discrete(name = "Experiment Number")
```

Synthetic Amino Acid Plots and Analysis

Gas to Liquid Flow Ratio (G/L) Analysis

```
# Convert G/L ratio as factor
g.l.ratio.data$g.l.ratio <- as.factor(g.l.ratio.data$g.l.ratio)
summary(g.l.ratio.data)
```

| ## | row.number | covariate.value | g.l.ratio | CO2.abs. | initia |
|----|---------------|-----------------|-----------|----------------|---------|
| ## | Min. : 1.00 | Min. :1 | 0.5 :2 | Min. :0.2176 | Min. |
| ## | 1st Qu.: 3.25 | 1st Qu.:2 | 1.875:2 | 1st Qu.:0.5316 | 1st Qu. |
| ## | Median : 5.50 | Median :3 | 2.5 :2 | Median :0.6603 | Median |

```

:12.88
## Mean : 5.50 Mean :3 3 :2 Mean :0.5762 Mean
:12.88
## 3rd Qu.: 7.75 3rd Qu.:4 4 :2 3rd Qu.:0.7032 3rd Qu.
:12.93
## Max. :10.00 Max. :5 Max. :0.7678 Max.
:12.96
## abs.ph.
## Min. :8.020
## 1st Qu.:8.605
## Median :8.670
## Mean :8.695
## 3rd Qu.:8.845
## Max. :9.580

```

Conduct ANOVA Analysis

```

g.l.ratio.lm <- lm(CO2.abs./1.009356 ~ g.l.ratio, g.l.ratio.data)
joint_tests(g.l.ratio.lm) #Type 3 ANOVA Table

```

```

## model term df1 df2 F.ratio p.value
## g.l.ratio 4 5 115.047 <.0001

```

Look at Pairwise Comparisons

```

lsmeans.g.l.ratio = emmeans(g.l.ratio.lm, "g.l.ratio")
summary(lsmeans.g.l.ratio)

```

```

## g.l.ratio emmean SE df Lower.CL upper.CL
## 0.5 0.223 0.0195 5 0.173 0.274
## 1.875 0.662 0.0195 5 0.612 0.712
## 2.5 0.687 0.0195 5 0.637 0.737
## 3 0.746 0.0195 5 0.696 0.796
## 4 0.535 0.0195 5 0.485 0.586
##
## Confidence Level used: 0.95

```

```

par(cex.lab=2, cex.axis=2)
plot(lsmeans.g.l.ratio, comparisons=TRUE, xlab = "Mean Absorption (mol
CO2/L)", ylab = "G/L Flow Ratio")

```

pairs(lsmeans.g.l.ratio)

```

## contrast estimate SE df t.ratio p.value
## 0.5 - 1.875 -0.4389 0.0275 5 -15.939 0.0001
## 0.5 - 2.5 -0.4635 0.0275 5 -16.835 0.0001
## 0.5 - 3 -0.5225 0.0275 5 -18.975 <.0001
## 0.5 - 4 -0.3120 0.0275 5 -11.330 0.0005

```

```
## 1.875 - 2.5 -0.0247 0.0275 5 -0.897 0.8870
## 1.875 - 3 -0.0836 0.0275 5 -3.036 0.1305
## 1.875 - 4 0.1269 0.0275 5 4.608 0.0292
## 2.5 - 3 -0.0589 0.0275 5 -2.140 0.3302
## 2.5 - 4 0.1516 0.0275 5 5.505 0.0140
## 3 - 4 0.2105 0.0275 5 7.645 0.0033
##
## P value adjustment: tukey method for comparing a family of 5 estimates
multcomp::cld(lsmmeans.g.l.ratio, by = NULL, Letters = "abcdefg", alpha = .05) # Tukey

## g.l.ratio emmean SE df Lower.CL upper.CL .group
## 0.5 0.223 0.0195 5 0.173 0.274 a
## 4 0.535 0.0195 5 0.485 0.586 b
## 1.875 0.662 0.0195 5 0.612 0.712 c
## 2.5 0.687 0.0195 5 0.637 0.737 c
## 3 0.746 0.0195 5 0.696 0.796 c
##
## Confidence Level used: 0.95
## P value adjustment: tukey method for comparing a family of 5 estimates
## significance level used: alpha = 0.05
```

Synthetic Amino Acid Absorption Cycle Plots

```
GAPL.amine.conc <- 1.009356 # from LCMS data (averaging the results for each AA)

GAPL.cycles.data$cycle.number <- factor(GAPL.cycles.data$cycle.number)
# make cycle number a factor

# Organize Synthetic Absorption Cycle data for mol/mol Amine plot
GAPL.averaged <- GAPL.cycles.data %>%
  group_by(cycle.number) %>%
  summarize(m.abs = mean(CO2.abs/GAPL.amine.conc), m.des = mean(CO2.des/GAPL.amine.conc),
            sd.abs = sd(CO2.abs/GAPL.amine.conc), sd.des = sd(CO2.des/GAPL.amine.conc),
            .groups = 'drop')

x.GAPL <- GAPL.cycles.data$cycle.number
y.GAPL <- c(GAPL.averaged$m.abs, GAPL.averaged$m.des)
error.GAPL <- c(GAPL.averaged$sd.abs, GAPL.averaged$sd.des)
fill.GAPL <- c(rep("Absorption", 4), rep("Desorption", 4))
GAPL.plot.1 <- data.frame(x.GAPL, y.GAPL, error.GAPL, fill.GAPL)

# Plot Absorption Cycle Data for Synthetic AA Absorbent in mol/mol Amine
```

```

ne
ggplot(GAPL.plot.1, aes(x= x.GAPL, y = y.GAPL, fill = fill.GAPL)) +
  geom_bar(position = position_dodge(), stat = "identity") +
  geom_errorbar(aes(ymin=y.GAPL-error.GAPL, ymax=y.GAPL+error.GAPL), w
  idth=0.2, position=position_dodge(0.9)) +
  labs(x = "Cycle Number") +
  theme_classic() +
  theme(legend.position="bottom", text = element_text(size = 16)) +
  guides(fill=guide_legend(title="")) +
  ylab(expression(atop("Carbon Dioxide Absorbed/", paste("Released (mo
L/mol Amine)"))))

```

```

# Organize Synthetic Absorption Cycle data for mol/L plot
GAPL.averaged.2 <- GAPL.cycles.data %>%
  group_by(cycle.number) %>%
  summarize(m.abs = mean(CO2.abs), m.des = mean(CO2.des), sd.abs = sd(
CO2.abs), sd.des = sd(CO2.des), .groups = 'drop')

```

```

x.GAPL.2 <- GAPL.cycles.data$cycle.number
y.GAPL.2 <- c(GAPL.averaged.2$m.abs, GAPL.averaged.2$m.des)
error.GAPL.2 <- c(GAPL.averaged.2$sd.abs, GAPL.averaged.2$sd.des)
fill.GAPL.2 <- c(rep("Absorption", 4), rep("Desorption", 4))
GAPL.plot.2 <- data.frame(x.GAPL.2, y.GAPL.2, error.GAPL.2, fill.GAPL.
2)

```

```

# Plot Absorption Cycle Data for Synthetic AA Absorbent in mol/L
ggplot(GAPL.plot.2, aes(x= x.GAPL.2, y = y.GAPL.2, fill = fill.GAPL.2)
) +
  geom_bar(position = position_dodge(), stat = "identity") +
  geom_errorbar(aes(ymin=y.GAPL.2-error.GAPL.2, ymax=y.GAPL.2+error.GA
PL.2), width=0.2, position=position_dodge(0.9)) +
  labs(x = "Cycle Number") +
  theme_classic() +
  theme(legend.position="bottom", text = element_text(size = 16)) +
  guides(fill=guide_legend(title="")) +
  ylab(expression(atop("Carbon Dioxide Absorbed/", paste("Released (mo
L/L)"))))

```

Synthetic Amino Acid Absorbent Absorption Cycle Analysis

```

# Convert cycle number to a factor
GAPL.cycles.data$cycle.number <- as.factor(GAPL.cycles.data$cycle.numb

```

```

er)
summary(GAPL.cycles.data)

##      row.number  cycle.number  CO2.abs          CO2.des          pH
.initial
## Min.      :1.00    1:2          Min.      :0.3252    Min.      :0.2814    Min.
:11.24
## 1st Qu.:2.75    2:2          1st Qu.:0.3340    1st Qu.:0.2899    1st
Qu.:11.45
## Median :4.50    3:2          Median :0.3623    Median :0.2935    Medi
an :11.49
## Mean    :4.50    4:2          Mean    :0.3801    Mean     :0.3011    Mean
:11.82
## 3rd Qu.:6.25          3rd Qu.:0.4030    3rd Qu.:0.3143    3rd
Qu.:11.87
## Max.     :8.00          Max.     :0.4867    Max.     :0.3317    Max.
:13.01
##      pH.abs          pH.des
## Min.      :9.370    Min.      :11.24
## 1st Qu.:9.615    1st Qu.:11.38
## Median :9.710    Median :11.46
## Mean    :9.671    Mean     :11.43
## 3rd Qu.:9.748    3rd Qu.:11.49
## Max.     :9.870    Max.     :11.52

# Conduct ANOVA and Pairwise Comparisons for Absorption Capacity across Cycles
GAPL.cycles.lm <- lm(CO2.abs/GAPL.amine.conc ~ cycle.number, GAPL.cycles.data)
joint_tests(GAPL.cycles.lm) #Type 3 ANOVA Table

## model term  df1 df2 F.ratio p.value
## cycle.number  3  4    8.99 0.0299

lsmeans.GAPL.cycles.abs = emmeans(GAPL.cycles.lm, "cycle.number")
summary(lsmeans.GAPL.cycles.abs)

## cycle.number emmean      SE df Lower.CL upper.CL
## 1            0.466 0.0199  4    0.410    0.521
## 2            0.348 0.0199  4    0.293    0.404
## 3            0.338 0.0199  4    0.283    0.393
## 4            0.354 0.0199  4    0.299    0.409
##
## Confidence Level used: 0.95

```

```
par(cex.lab=2, cex.axis=2)
plot(Lsmeans.GAPL.cycles.abs, comparisons=TRUE, xlab = "Mean Absorption Capacity (mol CO2/L)", ylab = "Cycle Number")
```

```
pairs(Lsmeans.GAPL.cycles.abs)
```

```
## contrast estimate SE df t.ratio p.value
## 1 - 2 0.11720 0.0282 4 4.159 0.0466
## 1 - 3 0.12753 0.0282 4 4.526 0.0353
## 1 - 4 0.11149 0.0282 4 3.957 0.0547
## 2 - 3 0.01033 0.0282 4 0.367 0.9809
## 2 - 4 -0.00571 0.0282 4 -0.203 0.9966
## 3 - 4 -0.01604 0.0282 4 -0.569 0.9363
```

```
##
## P value adjustment: tukey method for comparing a family of 4 estimates
```

```
multcomp::cld(Lsmeans.GAPL.cycles.abs, by = NULL, Letters = "abcdefg", alpha = .05) # Tukey
```

```
## cycle.number emmean SE df Lower.CL upper.CL .group
## 3 0.338 0.0199 4 0.283 0.393 a
## 2 0.348 0.0199 4 0.293 0.404 a
## 4 0.354 0.0199 4 0.299 0.409 ab
## 1 0.466 0.0199 4 0.410 0.521 b
```

```
##
## Confidence Level used: 0.95
## P value adjustment: tukey method for comparing a family of 4 estimates
## significance level used: alpha = 0.05
```

```
# Conduct ANOVA and Pairwise Comparisons for Desorption Capacity across Cycles
```

```
GAPL.cycles.des.Lm <- lm(CO2.des/GAPL.amine.conc ~ cycle.number, GAPL.cycles.data)
```

```
joint_tests(GAPL.cycles.des.Lm) #Type 3 ANOVA Table
```

```
## model term df1 df2 F.ratio p.value
## cycle.number 3 4 0.494 0.7056
```

```
Lsmeans.GAPL.cycles.des = emmeans(GAPL.cycles.des.Lm, "cycle.number")
summary(Lsmeans.GAPL.cycles.des)
```

```
## cycle.number emmean SE df Lower.CL upper.CL
## 1 0.287 0.0136 4 0.249 0.325
## 2 0.296 0.0136 4 0.258 0.333
```

```
## 3          0.301 0.0136 4    0.263    0.338
## 4          0.310 0.0136 4    0.272    0.348
##
## Confidence Level used: 0.95

par(cex.lab=2, cex.axis=2)
plot(Lsmeans.GAPL.cycles.des, comparisons=TRUE, xlab = "Mean Desorption Capacity (mol CO2/L)", ylab = "Cycle Number")
```

```
pairs(Lsmeans.GAPL.cycles.des)

## contrast estimate      SE df t.ratio p.value
## 1 - 2      -0.00837 0.0192 4 -0.436 0.9690
## 1 - 3      -0.01343 0.0192 4 -0.700 0.8924
## 1 - 4      -0.02281 0.0192 4 -1.188 0.6642
## 2 - 3      -0.00507 0.0192 4 -0.264 0.9926
## 2 - 4      -0.01444 0.0192 4 -0.752 0.8718
## 3 - 4      -0.00937 0.0192 4 -0.488 0.9577
##
## P value adjustment: tukey method for comparing a family of 4 estimates

multcomp::cld(Lsmeans.GAPL.cycles.des, by = NULL, Letters = "abcdefg", alpha = .05) # Tukey

## cycle.number emmean      SE df Lower.CL upper.CL .group
## 1              0.287 0.0136 4    0.249    0.325  a
## 2              0.296 0.0136 4    0.258    0.333  a
## 3              0.301 0.0136 4    0.263    0.338  a
## 4              0.310 0.0136 4    0.272    0.348  a
##
## Confidence Level used: 0.95
## P value adjustment: tukey method for comparing a family of 4 estimates
## significance level used: alpha = 0.05

# Conduct ANOVA and Pairwise Comparisons for Absorption pH across Cycles
GAPL.cycles.abs.ph.lm <- lm(pH.abs ~ cycle.number, GAPL.cycles.data)
joint_tests(GAPL.cycles.abs.ph.lm) #Type 3 ANOVA Table

## model term  df1 df2 F.ratio p.value
## cycle.number  3  4  6.377 0.0527
```

```

Lsmeans.GAPL.cycles.abs.ph = emmeans(GAPL.cycles.abs.ph.Lm, "cycle.number")
summary(Lsmeans.GAPL.cycles.abs.ph)

```

```

## cycle.number emmean SE df Lower.CL upper.CL
## 1 9.82 0.0588 4 9.66 9.98
## 2 9.73 0.0588 4 9.57 9.89
## 3 9.47 0.0588 4 9.31 9.63
## 4 9.66 0.0588 4 9.50 9.83
##
## Confidence Level used: 0.95

```

```

par(cex.lab=2, cex.axis=2)
plot(Lsmeans.GAPL.cycles.abs.ph, comparisons=TRUE, xlab = "Mean pH", ylab = "Cycle Number")

```

```

pairs(Lsmeans.GAPL.cycles.abs.ph)

```

```

## contrast estimate SE df t.ratio p.value
## 1 - 2 0.090 0.0831 4 1.082 0.7174
## 1 - 3 0.350 0.0831 4 4.210 0.0449
## 1 - 4 0.155 0.0831 4 1.864 0.3666
## 2 - 3 0.260 0.0831 4 3.127 0.1109
## 2 - 4 0.065 0.0831 4 0.782 0.8595
## 3 - 4 -0.195 0.0831 4 -2.345 0.2306
##

```

```

## P value adjustment: tukey method for comparing a family of 4 estimates

```

```

multcomp::cld(Lsmeans.GAPL.cycles.abs.ph, by = NULL, Letters = "abcdefg", alpha = .05) # Tukey

```

```

## cycle.number emmean SE df Lower.CL upper.CL .group
## 3 9.47 0.0588 4 9.31 9.63 a
## 4 9.66 0.0588 4 9.50 9.83 ab
## 2 9.73 0.0588 4 9.57 9.89 ab
## 1 9.82 0.0588 4 9.66 9.98 b
##

```

```

## Confidence Level used: 0.95

```

```

## P value adjustment: tukey method for comparing a family of 4 estimates

```

```

## significance level used: alpha = 0.05

```

```

# Conduct ANOVA and Pairwise Comparisons for Desorption pH across Cycles

```

```

GAPL.cycles.des.ph.lm <- lm(pH.des ~ cycle.number, GAPL.cycles.data)
joint_tests(GAPL.cycles.des.ph.lm) #Type 3 ANOVA Table

## model term    df1 df2 F.ratio p.value
## cycle.number  3   4   0.736 0.5829

Lsmeans.GAPL.cycles.des.ph = emmeans(GAPL.cycles.des.ph.lm, "cycle.number")
summary(Lsmeans.GAPL.cycles.des.ph)

## cycle.number emmean      SE df Lower.CL upper.CL
## 1             11.5 0.0705  4     11.3     11.7
## 2             11.4 0.0705  4     11.2     11.6
## 3             11.4 0.0705  4     11.2     11.6
## 4             11.4 0.0705  4     11.2     11.6
##
## Confidence Level used: 0.95

par(cex.lab=2, cex.axis=2)
plot(Lsmeans.GAPL.cycles.des.ph, comparisons=TRUE, xlab = "Mean pH", y
lab = "Cycle Number")

```

```

pairs(Lsmeans.GAPL.cycles.des.ph)

## contrast estimate      SE df t.ratio p.value
## 1 - 2          0.145 0.0997  4   1.455 0.5340
## 1 - 3          0.055 0.0997  4   0.552 0.9413
## 1 - 4          0.085 0.0997  4   0.853 0.8286
## 2 - 3         -0.090 0.0997  4  -0.903 0.8054
## 2 - 4         -0.060 0.0997  4  -0.602 0.9264
## 3 - 4          0.030 0.0997  4   0.301 0.9892
##
## P value adjustment: tukey method for comparing a family of 4 estimates

multcomp::cld(Lsmeans.GAPL.cycles.des.ph, by = NULL, Letters = "abcdefg",
alpha = .05) # Tukey

## cycle.number emmean      SE df Lower.CL upper.CL .group
## 2             11.4 0.0705  4     11.2     11.6   a
## 4             11.4 0.0705  4     11.2     11.6   a
## 3             11.4 0.0705  4     11.2     11.6   a
## 1             11.5 0.0705  4     11.3     11.7   a
##
## Confidence Level used: 0.95
## P value adjustment: tukey method for comparing a family of 4 estimates

```

tes

```
## significance level used: alpha = 0.05
```

Algal Amino Acid Absorbent Plots and Analysis

Algal Amino Acid Absorbent Amino Acid Concentration throughout Absorption Cycles

```
# Organize Data for Plotting
```

```
cycle.0.conc <- LCMS.algae.cycles.data %>%  
  filter(Cycle == 0 & Type == "Original") %>%  
  select(Name, AA.Conc.M)
```

```
cycle.1.conc <- LCMS.algae.cycles.data %>%  
  filter(Cycle == 1 & Type == "Absorption") %>%  
  select(Name, AA.Conc.M)
```

```
cycle.2.conc <- LCMS.algae.cycles.data %>%  
  filter(Cycle == 2 & Type == "Absorption") %>%  
  select(Name, AA.Conc.M)
```

```
cycle.3.conc <- LCMS.algae.cycles.data %>%  
  filter(Cycle == 3 & Type == "Absorption") %>%  
  select(Name, AA.Conc.M)
```

```
cycle.4.conc <- LCMS.algae.cycles.data %>%  
  filter(Cycle == 4 & Type == "Absorption") %>%  
  select(Name, AA.Conc.M)
```

```
cycle.5.conc <- LCMS.algae.cycles.data %>%  
  filter(Cycle == 5 & Type == "Absorption") %>%  
  select(Name, AA.Conc.M)
```

```
cycle.6.conc <- LCMS.algae.cycles.data %>%  
  filter(Cycle == 6 & Type == "Absorption") %>%  
  select(Name, AA.Conc.M)
```

```
cycle.7.conc <- LCMS.algae.cycles.data %>%  
  filter(Cycle == 7 & Type == "Absorption") %>%  
  select(Name, AA.Conc.M)
```

```
cycle.8.conc <- LCMS.algae.cycles.data %>%  
  filter(Cycle == 8 & Type == "Absorption") %>%  
  select(Name, AA.Conc.M)
```

```
value.plot.2 <- c(cycle.0.conc$AA.Conc.M, cycle.1.conc$AA.Conc.M, cycl  
e.2.conc$AA.Conc.M, cycle.3.conc$AA.Conc.M, cycle.4.conc$AA.Conc.M, cy  
cle.5.conc$AA.Conc.M, cycle.6.conc$AA.Conc.M, cycle.7.conc$AA.Conc.M,
```

```

cycle.8.conc$AA.Conc.M)
cycle.plot.2 <- c(rep("0", 20), rep("1", 20), rep("2", 20), rep("3", 2
0), rep("4", 20), rep("5", 20), rep("6", 20), rep("7", 20), rep("8", 2
0))
name.plot.2 <- LCMS.algae.cycles.data %>%
  filter(Cycle == 1 & Type == "Absorption") %>%
  select(Name)
plot.2.data <- data.frame(cycle.plot.2, name.plot.2, value.plot.2)
plot.2.data$Cycle <- as.factor(plot.2.data$cycle.plot.2)

# Plot Algal Amino Acid Absorbent Amino Acid Concentrations throughout
Absorption Cycles
ggplot(plot.2.data, aes(x = Name, y = value.plot.2, fill = cycle.plot.
2)) +
  geom_bar(position = position_dodge(), stat = "identity") +
  theme_classic() +
  theme(axis.text.x = element_text(angle = 90), legend.position="botto
m")+
  labs(x = "Amino Acid", y = "Concentration (M)") +
  scale_fill_discrete(name = "Absorption Number")

```

Algal Amino Acid Absorption Cycles Plots

```

# Organize Data for Calculation
algae.cycles.amine <- LCMS.algae.cycles.data %>%
  mutate(aa.conc.amine = AA.Conc.M*N)

abs.aa.conc.amine.1 <- algae.cycles.amine %>%
  filter(Type == "Original" & Cycle == "0")
abs.aa.conc.amine.2 <- algae.cycles.amine %>%
  filter(Type == "Desorption Diluted" & Cycle == "1")
abs.aa.conc.amine.3 <- algae.cycles.amine %>%
  filter(Type == "Desorption Diluted" & Cycle == "2")
abs.aa.conc.amine.4 <- algae.cycles.amine %>%
  filter(Type == "Desorption Diluted" & Cycle == "3")
abs.aa.conc.amine.5 <- algae.cycles.amine %>%
  filter(Type == "Desorption Diluted" & Cycle == "4")
abs.aa.conc.amine.6 <- algae.cycles.amine %>%
  filter(Type == "Desorption Diluted" & Cycle == "5")
abs.aa.conc.amine.7 <- algae.cycles.amine %>%
  filter(Type == "Desorption Diluted" & Cycle == "6")
abs.aa.conc.amine.8 <- algae.cycles.amine %>%
  filter(Type == "Desorption Diluted" & Cycle == "7")

aa.conc.amine.1 <- algae.cycles.amine %>%

```

```

  filter(Type == "Absorption" & Cycle == "1")
aa.conc.amine.2 <- algae.cycles.amine %>%
  filter(Type == "Absorption" & Cycle == "2")
aa.conc.amine.3 <- algae.cycles.amine %>%
  filter(Type == "Absorption" & Cycle == "3")
aa.conc.amine.4 <- algae.cycles.amine %>%
  filter(Type == "Absorption" & Cycle == "4")
aa.conc.amine.5 <- algae.cycles.amine %>%
  filter(Type == "Absorption" & Cycle == "5")
aa.conc.amine.6 <- algae.cycles.amine %>%
  filter(Type == "Absorption" & Cycle == "6")
aa.conc.amine.7 <- algae.cycles.amine %>%
  filter(Type == "Absorption" & Cycle == "7")
aa.conc.amine.8 <- algae.cycles.amine %>%
  filter(Type == "Absorption" & Cycle == "8")

# Calculate the Amino Acid Concentration after each Absorption/Desorption
amine.vec <- c(sum(abs.aa.conc.amine.1$aa.conc.amine), sum(abs.aa.conc.amine.2$aa.conc.amine), sum(abs.aa.conc.amine.3$aa.conc.amine), NA, sum(abs.aa.conc.amine.5$aa.conc.amine), NA, sum(abs.aa.conc.amine.7$aa.conc.amine), sum(abs.aa.conc.amine.8$aa.conc.amine))
des.amine.vec <- c(sum(aa.conc.amine.1$aa.conc.amine), sum(aa.conc.amine.2$aa.conc.amine), sum(aa.conc.amine.3$aa.conc.amine), NA, sum(aa.conc.amine.5$aa.conc.amine), NA, sum(aa.conc.amine.7$aa.conc.amine), sum(aa.conc.amine.8$aa.conc.amine))

# Calculation to adjust for water dilution
volume.adj.vec.abs <- c(0.3, 0.24, 0.223024421, NA, 0.199450877, NA, 0.18205885, 0.17740077)
volume.adj.vec.des <- c(0.205, 0.229875, 0.213459057, NA, 0.193800216, NA, 0.180512888, 0.175345759)

algae.cycles.data <- algae.cycles.data %>%
  mutate(CO2.abs.amine = CO2.abs/amine.vec/volume.abs*volume.adj.vec.abs) %>%
  mutate(CO2.des.amine = CO2.des/des.amine.vec/volume.des*volume.adj.vec.des)

# Organize Data for Plotting
cycle.number.plot.3 <- c(algae.cycles.data$cycle.number, algae.cycles.data$cycle.number)
value.plot.3 <- c(algae.cycles.data$CO2.abs.amine, algae.cycles.data$CO2.des.amine)
name.plot.3 <- c(rep("Absorption", 8), rep("Desorption", 8))

```

```

plot.3.data <- data.frame(cycle.number.plot.3, name.plot.3, value.plot
.3)
plot.3.data$name.plot.3 <- as.factor(plot.3.data$name.plot.3)

# Plot Algal Amino Acid Absorbent Absorption Cycle Data in mol/mol Ami
ne
ggplot(plot.3.data, aes(x = cycle.number.plot.3, y = value.plot.3, fil
l = name.plot.3)) +
  geom_bar(position = position_dodge(), stat = "identity") +
  labs(x = "Cycle Number") +
  theme_classic() +
  theme(legend.position="bottom", text = element_text(size = 16)) +
  guides(fill=guide_legend(title="")) +
  scale_x_continuous(breaks = seq(1, 8, by = 1)) +
  ylab(expression(atop("Carbon Dioxide Absorbed/", paste("Released (mo
L/mol Amine)"))))

## Warning: Removed 4 rows containing missing values (geom_bar).

```

```

# Output Mean and Standard Deviation for mol/mol Amine Absorption and
Desorption Results excluding Absorption 1
mean(algae.cycles.data$CO2.abs.amine[-1], na.rm = T)

## [1] 1.271044

sd(algae.cycles.data$CO2.abs.amine[-1], na.rm = T)

## [1] 0.06145801

mean(algae.cycles.data$CO2.des.amine[-1], na.rm = T)

## [1] 1.177415

sd(algae.cycles.data$CO2.des.amine[-1], na.rm = T)

## [1] 0.09356362

# Organize Data for Plotting
cycle.number.plot.4 <- c(algae.cycles.data$cycle.number, algae.cycles.
data$cycle.number)
value.plot.4 <- c(algae.cycles.data$CO2.abs, algae.cycles.data$CO2.des
)
name.plot.4 <- c(rep("Absorption", 8), rep("Desorption", 8))
plot.4.data <- data.frame(cycle.number.plot.4, name.plot.4, value.plot
.4)
plot.4.data$name.plot.4 <- as.factor(plot.4.data$name.plot.4)

```

```

# Plot Algal Amino Acid Absorbent Absorption Cycle Data in mol/L
ggplot(plot.4.data, aes(x = cycle.number.plot.4, y = value.plot.4, fill = name.plot.4)) +
  geom_bar(position = position_dodge(), stat = "identity") +
  labs(x = "Cycle Number") +
  theme_classic() +
  theme(legend.position="bottom", text = element_text(size = 16)) +
  guides(fill=guide_legend(title="")) +
  scale_x_continuous(breaks = seq(1, 8, by = 1)) +
  ylab(expression(atop("Carbon Dioxide Absorbed/", paste("Released (mol/L)")))))

## Warning: Removed 4 rows containing missing values (geom_bar).

```

```

# Output Mean and Standard Deviation for mol/L Absorption Results excluding Absorption 1
mean(algae.cycles.data$CO2.abs[-1], na.rm = T)

## [1] 0.8252807

sd(algae.cycles.data$CO2.abs[-1], na.rm = T)

## [1] 0.06463184

```

Synthetic and Algal Amino Acid Absorbent Absorption Capacity Analysis

```

# Data Organization
GAPL.comparison.L <- c(0.391181771, 0.376117742)
GAPL.comparison.Amine <- c(0.387555799, 0.372631403)
algal.comparison.L <- plot.4.data$value.plot.4[c(2,3,5,7,8)]
algal.comparison.Amine <- plot.3.data$value.plot.3[c(2,3,5,7,8)]
comparison.L <- c(GAPL.comparison.L, algal.comparison.L)
comparison.Amine <- c(GAPL.comparison.Amine, algal.comparison.Amine)
comparisons.factor <- as.factor(c("synthetic", "synthetic", rep("algal", 5)))
comparison.L.data <- data.frame(comparisons.factor, comparison.L)
comparison.Amine.data <- data.frame(comparisons.factor, comparison.Amine)

# ANOVA and Pairwise Comparisons for Absorption Capacity in mol/L
comparison.L.lm <- lm(comparison.L ~ comparisons.factor, comparison.L.data)
joint_tests(comparison.L.lm) #Type 3 ANOVA Table

## model term          df1 df2 F.ratio p.value
## comparisons.factor    1   5  82.813 0.0003

```

```
lsmeans.comparison.L = emmeans(comparison.L.lm, "comparisons.factor")
summary(lsmeans.comparison.L)
```

```
## comparisons.factor emmean      SE df Lower.CL upper.CL
## algal                0.825 0.0259  5    0.759    0.892
## synthetic            0.384 0.0410  5    0.278    0.489
##
## Confidence Level used: 0.95
```

```
plot(lsmeans.comparison.L, comparisons=TRUE)
```

```
pairs(lsmeans.comparison.L)
```

```
## contrast          estimate      SE df t.ratio p.value
## algal - synthetic  0.442 0.0485  5  9.100  0.0003
```

```
multcomp::cld(lsmeans.comparison.L, by = NULL, Letters = "abcdefg", alpha = .05) # Tukey
```

```
## comparisons.factor emmean      SE df Lower.CL upper.CL .group
## synthetic          0.384 0.0410  5    0.278    0.489  a
## algal              0.825 0.0259  5    0.759    0.892  b
##
## Confidence Level used: 0.95
## significance level used: alpha = 0.05
```

```
# ANOVA and Pairwise Comparisons for Absorption Capacity in mol/mol Amine
```

```
comparison.Amine.lm <- lm(comparison.Amine ~ comparisons.factor, comparison.Amine.data)
```

```
joint_tests(comparison.Amine.lm) #Type 3 ANOVA Table
```

```
## model term          df1 df2 F.ratio p.value
## comparisons.factor  1    5 372.539 <.0001
```

```
lsmeans.comparison.Amine = emmeans(comparison.Amine.lm, "comparisons.factor")
```

```
summary(lsmeans.comparison.Amine)
```

```
## comparisons.factor emmean      SE df Lower.CL upper.CL
## algal                1.27 0.0247  5    1.21    1.33
## synthetic            0.38 0.0390  5    0.28    0.48
##
## Confidence Level used: 0.95
```

```
plot(lsmeans.comparison.Amine, comparisons=TRUE)
```

```

pairs(Lsmeans.comparison.Amine)
## contrast          estimate      SE df t.ratio p.value
## algal - synthetic    0.891 0.0462  5 19.301 <.0001

multcomp::cld(Lsmeans.comparison.Amine, by = NULL, Letters = "abcdefg"
, alpha = .05) # Tukey

## comparisons.factor emmean      SE df Lower.CL upper.CL .group
## synthetic          0.38 0.0390  5    0.28    0.48  a
## algal              1.27 0.0247  5    1.21    1.33  b
##
## Confidence Level used: 0.95
## significance level used: alpha = 0.05

```

APPENDIX E: ALGAL BIOMASS INFORMATION

Table 19: *C. sorokiniana* Biomass Composition

| Components | As Fed | Dry Matter |
|-------------------------|--------|------------|
| Moisture (%) | 6.9 | |
| Dry Matter (%) | 93.1 | |
| Crude Protein (%) | 54.9 | 59.0 |
| Soluble Protein (% CP) | | 25 |
| NDICP (%) | 1.3 | 1.4 |
| ADF (%) | 5.6 | 6.0 |
| Lignin (%) | 3.8 | 4.1 |
| Starch (%) | 2.3 | 2.5 |
| ESC “Simple Sugars” (%) | 3.0 | 3.2 |
| Total Fatty Acids (%) | 8.27 | 8.89 |
| RUFAL (%) | 3.82 | 4.10 |
| Ash (%) | 8.91 | 9.57 |
| Calcium (%) | 0.52 | 0.56 |
| Phosphorus (%) | 1.70 | 1.83 |
| Magnesium (%) | 0.27 | 0.29 |
| Potassium (%) | 0.92 | 0.98 |
| Sodium (%) | 0.014 | 0.015 |
| Iron (ppm) | 12,500 | 13,400 |
| Zinc (ppm) | 266 | 285 |
| Copper (ppm) | 218 | 234 |
| Manganese (ppm) | 34 | 36 |
| Molybdenum (ppm) | <0.1 | <0.1 |
| Sulfur (%) | 0.73 | 0.78 |
| Chloride Ion (%) | 0.06 | 0.06 |
| DCAD (mEq/100g) | | -25 |

*: Results from DairyOne, Inc.

Table 20: *C. sorokiniana* Fatty Acid Composition

| Fatty Acid | Percent of Total Fatty Acids | Percent of Dry Matter |
|-------------------------------------|-------------------------------------|------------------------------|
| C12:0 Lauric | 0.05 | 0.01 |
| C14:0 Myristic | 0.37 | 0.03 |
| C16:0 Palmitic | 18.42 | 1.67 |
| C16:1 Palmitoleic | 1.10 | 0.10 |
| C18:0 Stearic | 1.06 | 0.09 |
| C18:1 Oleic | 11.15 | 0.98 |
| C18:2 Linoleic | 22.92 | 2.02 |
| C18:3 Linolenic | 12.57 | 1.10 |
| C20:0 Arachidic | 0.11 | 0.01 |
| C20:1 Gadoleic | 0.09 | 0.01 |
| C20:5 Eicosapentaenoic (EPA) | 0.00 | 0.00 |
| C22:0 Behenic | 0.09 | 0.01 |
| C22:6 Docosahexanoic (DHA) | 0.00 | 0.00 |
| C24:0 Lignoceric | 0.00 | 0.00 |
| Other | 32.06 | 2.85 |
| Total Fatty Acids | 100.00 | 8.89 |
| Saturated | 20.11 | |
| MUFA | 12.34 | |
| PUFA | 35.49 | |
| RUFAL | | 4.10 |

*: Results from DairyOne, Inc.

APPENDIX F: DAIRY ONE FORAGE LABORATORY PROCEDURES

Ash, Total

AOAC Method 942.05 – Ash of Animal Feed.

Carbohydrates, Soluble

Ethanol Soluble Carbohydrates (ESC)

Hall, M.B., W.H. Hoover, J.P. Jennings and T.K. Miller Webster. 1999. A method for partitioning neutral detergent soluble carbohydrates. *J. Sci. Food Agric.* 79: p.2079-2086.

Samples shaken for 4 hours at 180 epm with 80% ethanol to extract ethanol soluble carbohydrates comprised of simple sugars. ESC determined using a Thermo Scientific Genesys 10S Vis Spectrophotometer after a colorimetric phenol-sulfuric acid reaction.

Water Soluble Carbohydrates (WSC)

West Virginia University Procedure by W.H. Hoover and T.K. Miller Webster. Determination of Nonstructural Carbohydrates.

Hall, M.B., W.H. Hoover, J.P. Jennings and T.K. Miller Webster. 1999. A method for partitioning neutral detergent soluble carbohydrates. *J. Sci. Food Agric.* 79: p.2081.

Samples incubated with water in a 40°C bath for 1 hour extracting water soluble carbohydrates comprised of simple sugars and fructan. WSC determined using a Thermo Scientific Genesys 10S Vis Spectrophotometer after acid hydrolysis with sulfuric acid and colorimetric reaction with potassium ferricyanide.

Dry Matter (DM)

Oven – 60°C for 4 hours (forced air)

Goering, H.K. and P.J. Van Soest. 1970. Forage Fiber Analyses (apparatus, reagents, procedures, and some applications).

ARS/USDA Handbook No. 379, Superintendent of Documents, US Government Printing Office, Washington, D.C. 20402. P15.

NFTA Method 2.2.1.1 – Partial Dry Matter using Forced-air Drying Ovens.

Oven – 135°C for 2 hours

AOAC 930.15 – Loss on Drying (Moisture) for Feeds.

Oven – 105°C for 3 hours

NFTA Method 2.2.2.5 – Dry Matter by Oven Drying for 3hr at 105C.

Fat

Crude, Acid Hydrolysis

AOAC 954.02 – Crude Fat in Pet Food.

Crude, Ether Extraction

AOAC 2003.05 – Crude Fat in Feeds, Cereal Grains, and Forages.

Dairy One Forage Lab, Equi-Analytical, Zooquarius Analytical Procedures Page 3 of 10

Extraction by Soxtec HT6 System using anhydrous diethyl ether. Crude fat residue determined gravimetrically after drying.

Foss North America, 8091 Wallace Road, Eden Prairie, MN 55344. www.foss.us

Crude, Roese-Gottlieb Method (Base Hydrolysis)

AOAC 932.06 A (b) and 932.06 B – Fat in Dried Milk.

Used for milk (liquid and powder), whey, and milk based byproducts.

Fatty Acids

Total Fatty Acids (TFA)

Direct FAME synthesis

O'Fallon, J.V., J.R. Busboom, M.L. Nelson and C.T. Gaskins. 2007. A direct method for fatty acid methyl ester synthesis: Application to wet meat tissues, oils, and feedstuffs. *J. Anim. Sci.* 85: p.1511-1521. Fatty acid methyl esters (FAME) determined directly from fresh tissue, oils, or feedstuffs, without the need for prior organic solvent extraction. FAME synthesis is conducted in the presence of up to 33% water. Wet tissues or other samples are permeabilized and hydrolyzed for 1.5 hr. at 55C in 1N KOH in MeOH containing C13:0 as an internal standard. The KOH is neutralized, and the FFA are methylated by H2SO4 catalysis for 1.5 hr. at 55C. Hexane is added to the reaction tube, vortex-mixed and centrifuged. The hexane layer pipetted into gas chromatography (GC) vials and then analyzed using a Thermo Trace 1310 Gas Chromatograph fitted with a Supelco SP-2560, 100m x 0.25mm x 0.20um capillary column and a Flame Ionization Detector (FID).

Thermo Fisher Scientific Inc., 81 Wyman Street, Waltham, MA 02454.
www.thermoscientific.com

Fiber

Acid Detergent Fiber (ADF)

ANKOM Technology Method 12 – Acid Detergent Fiber in Feeds – Filter Bag Technique (for A2000 and A20001), 05/19/2017.

Solutions as in AOAC 973.18 – Fiber (Acid Detergent) and Lignin (H₂SO₄) in Animal Feed. Samples individually weighed at 0.5g into filter bags and digested for 75 minutes as a group of 24 in 2L of ADF solution in ANKOM A2000 Digestion Unit.

Samples are rinsed three times with boiling water for 5 minutes in filter bags followed by a 3 minute acetone soak and drying at 105°C for 2 hours.

ANKOM Technology, 2052 O’Neil Road, Macedon, NY 14502. www.ankom.com

Lignin

ANKOM Technology Method 9 – Method for Determining Acid Detergent Lignin in the DaisyII Incubator – 01/24/2017.

Solution as in AOAC 973.18 – Fiber (Acid Detergent) and Lignin (H₂SO₄) in Animal Feed. ADF performed as above and

residue digested as a group of 24 in 72% w/w sulfuric acid for 3 hours in ANKOM DaisyII Incubator at ambient temperature.

Minerals

Ca, P, Mg, K, Na, Fe, Zn, Cu, Mn, Mo, Co, S, Al, B, Cr, Sr

Samples digested using CEM Microwave Accelerated Reaction System (MARS6) with MarsXpress Temperature Control using 50ml calibrated Xpress Teflon PFA vessels with Kevlar/fiberglass insulating sleeves then analyzed by ICP using a Thermo iCAP 6300 Inductively Coupled Plasma Radial Spectrometer.

Sample weights – 0.5g for forages, ingredients, byproducts (1.0g for Co or Cr); 0.5g for grain mixes; 0.2g for mineral mixes;

Manure - 0.5g dried, ground or 2-10g wet sample.

Samples first pre-digested at ambient temperature 10 minutes with 8ml nitric acid (HNO₃) and 2ml hydrochloric acid (HCl) and then an additional 10 minutes with 1ml 30% hydrogen peroxide (H₂O₂). After pre-digestion complete, samples digested in two stages: Stage one - 10-minute ramp to 135°C and held for 3 minutes at 1500W. Stage two - 12-minute ramp to 200°C and held for 15 minutes at 1600W. Vessels brought to 50-ml volume, aliquot used for analysis.

Method utilized based upon CEM Application Notes for Acid Digestion on the following matrices - Feed Grain, Alfalfa, Corn Flour, Milk Powder, Soybean Meal, Flour, Hair, Potato Chips, Wheat Crackers, Peanut Butter, Urine, Dog Feces, Wine. Water – 35ul concentrated nitric acid added to 14ml of water, mixed, then aspirated on ICP for analysis.

Manure Reference: Wolf, Ann, M. Watson, and N. Wolf. 2003. Digestion and dissolution methods for P, K, Ca, Mg and trace elements. Recommended methods of manure analysis. ed J. Peters, pp30-39. University of Wisconsin Extension Publication. A3769

CEM, 3100 Smith Farm Road, Matthews, NC 28106. www.cem.com

Thermo Fisher Scientific Inc., 81 Wyman Street, Waltham, MA 02454.
www.thermoscientific.com

Chloride Ion (Cl⁻)

Potentiometric Titration – 0.2-0.5g dried, ground sample or 1-5g wet sample extracted for 15 minutes in 50ml 0.1N HNO₃, followed by potentiometric titration with AgNO₃ (0.01N or 0.10N) using a Metrohm 905 Titrando Titration Unit equipped with an Ag-ring electrode controlled by Metrohm Tiamo software. For water samples, 25ml of 0.2N HNO₃ added to 25ml of sample.

Metrohm Application Bulletin No. 130 by Metrohm Ltd., C-H-9101 Herisau, Switzerland
Metrohm USA, 6555 Pelican Creek Circle, Riverview FL, 33578. www.metrohmusa.com

The method by Metrohm is similar to the concepts found in: Cantliffe, D.J., MacDonald, G.E. and Peck, N.H. 1970. The potentiometric determination of nitrate and chloride in plant tissue. New York's Food and Life Sciences Bulletin. No.3, September 1970. Plant Sciences. Vegetable Crops Geneva. No. 1: 5-7.

Selenium (Se)

Subcontracted to Michigan State University Veterinary Diagnostic Laboratory 4125 Beaumont Road, Lansing MI 48910-8104

Wahlen R, EvansL, Turner J, Hearn R: The use of collision/reaction cell ICP-MS for the determination of elements in blood and serum samples. Spectroscopy 20 (12): 84-89, 2005. 0.5g aliquots of dried, ground feed samples are digested overnight at 95°C in 5mL of nitric acid. The digested samples are diluted with water to 100x the initial feed mass. 200uL of each diluted digest is pipetted and diluted with a solution containing 0.5% EDTA and Triton X-100, 1% ammonium hydroxide, 2% propanol and 20ppb of scandium, rhodium, indium and bismuth as internal standards. An Agilent Inductively Coupled Plasma – Mass Spectrometer (ICP/MS)¹ is used for the analysis. The ICP/MS is tuned to yield a minimum of 7500 cps sensitivity for 1ppb yttrium (mass 89), less than 1.0% oxide level as determined by the 156/140 mass ratio and less than 2.0% double charged ions as determined by the 70/140 mass ratio.

Selenium concentration is calibrated using a 6-point linear curve of the analyte-internal standard response ratio. Standards were from Inorganic Ventures². A NIST³ Typical Diet standard was used as a control

1 Agilent Technologies Inc, Santa Clara CA 95051

2 Inorganic Ventures, Christiansburg, VA 24073

3 National Institute of Standards and Technology, Gaithersburg MD 20899

Nitrates (%NO₃ or ppm NO₃-N)

RQflex® Reflectometer Method

1g of dried, ground sample or 10g of wet sample is extracted in 50ml deionized water for 20 minutes by shaking at 280 oscillations/minute. Samples are filtered through Whatman 934-AH (1.5um) filter paper, then analyzed by RQflex® Reflectometer using Reflectoquant® Nitrate test strips.

When the Nitrate test strip is immersed in the aqueous sample, a reducing agent reduces nitrate ions to nitrite ions. In the presence of an acidic buffer, the nitrite ions react with an aromatic amine to form a diazonium salt. The salt reacts with N-(1-naphthyl)-ethylene-diamine to form a red-violet azo dye that is measured reflectometrically. Nitrate concentration is proportional to the color reaction.

Each strip contains two reaction zones generating dual replicate analyses per sample. The RQflex® Reflectometer's double optic system measures the analyte concentration based on the light reflected from the dual reaction zones. Barcode controlled software calculates the mean of those two measurements.

EMD Chemicals Inc., One International Plaza, Suite 300, Philadelphia, PA, 19113.
www.emdmillipore.com

Protein

Acid Detergent Insoluble Crude Protein (ADICP)

ADF residue analyzed using a Leco TruMac N Macro Determinator to determine the protein fraction bound to the acid detergent fiber.

Crude Protein (CP) and Total Nitrogen (N)

Dry, 1mm ground samples analyzed by combustion using a CN628 Carbon/Nitrogen Determinator. Liquid samples analyzed using a TruMac N Macro Determinator.

AOAC 990.03 – Protein (Crude) in Animal Feed

AOAC 992.15 – Crude Protein in Meat and Meat Products including Pet Foods

AOAC 992.23 – Crude Protein in Cereal Grain and Oilseeds

Leco Application Note – “Nitrogen/Protein in Feeds, Grains, and Pet Food” Form 20X-821-485, 03/15 – Rev0.

Leco Application Note – “Nitrogen in Soil and Plant Tissue” Form 203-821-443, 11/14 – Rev2.

Manure – Watson, M., A. Wolf, and N. Wolf. 2003. Total nitrogen. Recommended methods of manure analysis. ed J. Peters, pp18, 23-24. University of Wisconsin Extension Publication. A3769.

Leco Corporation, 300 Lakeview Avenue, St. Joseph, MI 49085. www.leco.com

Degradable Protein (Rumen Degradable Protein - RDP)

Cornell Streptomyces griseus (SGP) enzymatic digestion. Enzyme concentration held constant. Residues containing undegradable protein analyzed using Leco TruMac N Macro Determinator.

Concentrates incubated for 18 hrs. Cornell Nutrition Conference Proceedings, 1990. pp. 81-88.

Forage samples incubated for 2 hrs. at higher SGP concentration. J. Dairy Sci. 1999. 82: 343-354.

Leco Application Note – “Nitrogen/Protein in Feeds, Grains, and Oil Seeds” Form No. 203-821-392, 01/16 – Rev2

Dairy One Forage Lab, Equi-Analytical, Zooquarius Analytical Procedures Page 8 of 10

Neutral Detergent Insoluble Crude Protein (NDICP)

aNDF performed without sodium sulfite then residue analyzed using a Leco TruMac N Macro Determinator to determine the protein fraction bound to the neutral detergent fiber.

Soluble Protein (SP)

Cornell Sodium Borate-Sodium Phosphate Buffer Procedure. Soy products incubated at 39°C. All other samples incubated at ambient temperature. Residue containing insoluble protein analyzed using Leco TruMac N Macro Determinator.

Cornell Nutrition Conference Proceedings, 1990, pp. 85-86.

Leco Application Note – “Nitrogen/Protein in Feeds, Grains, and Oil Seeds” Form No. 203-821-392, 01/16 – Rev2

Starch, Total

YSI 2950D-1 or 2700 SELECT Biochemistry Analyzers

YSI Incorporated Life Sciences, 1725 Brannum Lane, Yellow Springs, Ohio 45387 Application Note Number 319.

www.ysilifescience.com

Dairy One Forage Lab, Equi-Analytical, Zooquarius Analytical Procedures Page 9 of 10

Samples are pre-extracted for sugar by incubation in 40°C water bath and filtration on Whatman 41 filter paper. Residues are thermally solubilized using an autoclave, then incubated with glucoamylase enzyme to hydrolyze starch to produce dextrose (glucose).

Prepared samples injected into sample chamber of YSI Analyzer where dextrose diffuses into a membrane containing glucose oxidase. The dextrose is immediately oxidized to hydrogen peroxide and D-glucono-4-lactone. The hydrogen peroxide is detected amperometrically at the platinum electrode surface. The current flow at the electrode is directly proportional to the hydrogen peroxide concentration, and hence to the dextrose concentration. Starch is determined by multiplying dextrose by 0.9.

Volatile Fatty Acids (VFA) and Lactic Acid

Extraction – 50g samples blended at 20000 rpm for 2 min. in 750ml deionized water (Manure 50g and 450ml water), filtered through cheesecloth, then filtered through disposable syringe filter. Adapted from Personal Communication, L.E. Chase,

Ph.D., Cornell University.

Gas Chromatography – Acetic, Propionic, Butyric, Iso-butyric acids

Aliquot of extract mixed 1:1 ratio with 0.06M oxalic acid containing 100ppm trimethylacetic acid (internal standard). Samples injected into a Perkin Elmer Clarus 680 Gas Chromatograph containing a Supelco packed column with the following specifications: 2m x 2mm Tightspec ID, 4% Carbowax 20M phase on 80/120 Carbopack B-DA.

Procedure based upon:

- “GC Separation of VFA C2-C5” Supelco GC Bulletin 749F, 1975.
- “Analyzing Fatty Acids by Packed Column Gas Chromatography” Supelco GC Bulletin 856A, 1990.
- “Volatile Fatty Acid SOP” W.H. Miner Institute, Chazy, NY.

Sigma Aldrich (Supelco), 3050 Spruce Street, St. Louis, MO 63103. www.sigmaaldrich.com

Perkin Elmer, 940 Winter Street, Waltham, MA 02451. www.perkinelmer.com

Biochemistry Analyzer – Lactic acid

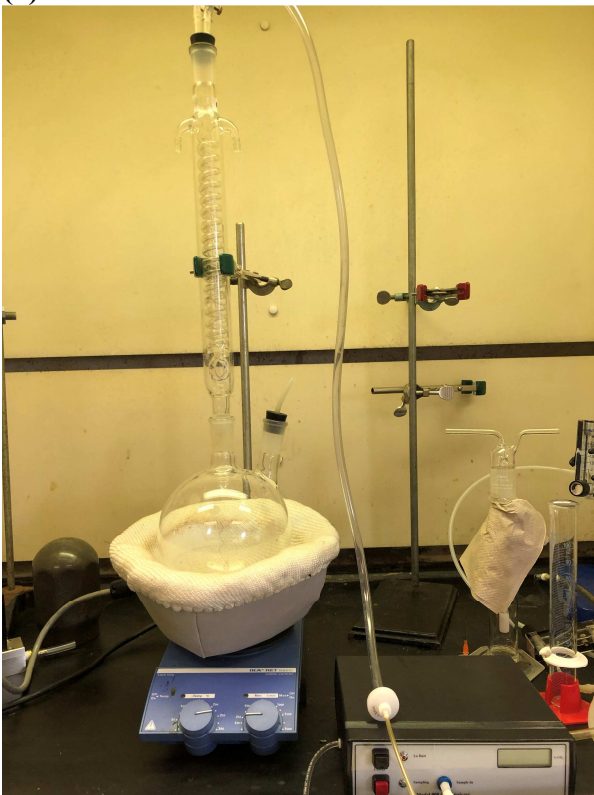
Aliquot of extract analyzed for L-Lactate using YSI 2950D-1 or 2700 SELECT Biochemistry Analyzer equipped with an LLactate membrane. YSI User’s Manual, page 4-7.

Samples injected into sample chamber of YSI Analyzer where L-Lactate diffuses into a membrane containing L-Lactate oxidase. The L-Lactate is immediately oxidized to hydrogen peroxide and pyruvate. The hydrogen peroxide is detected amperometrically at the platinum electrode surface. The current flow at the electrode is directly proportional to the hydrogen peroxide concentration, and hence to the L-Lactate concentration. Total lactic acid is determined by multiplying L-Lactate by 2.0.

YSI Incorporated Life Sciences, 1725 Brannum Lane, Yellow Springs, Ohio 45387.
www.ysilifescience.com

APPENDIX G: LAB IMAGES

(a)



(b)



Figure 83: Desorption Experimental Setup Photo a) not in use b) in use

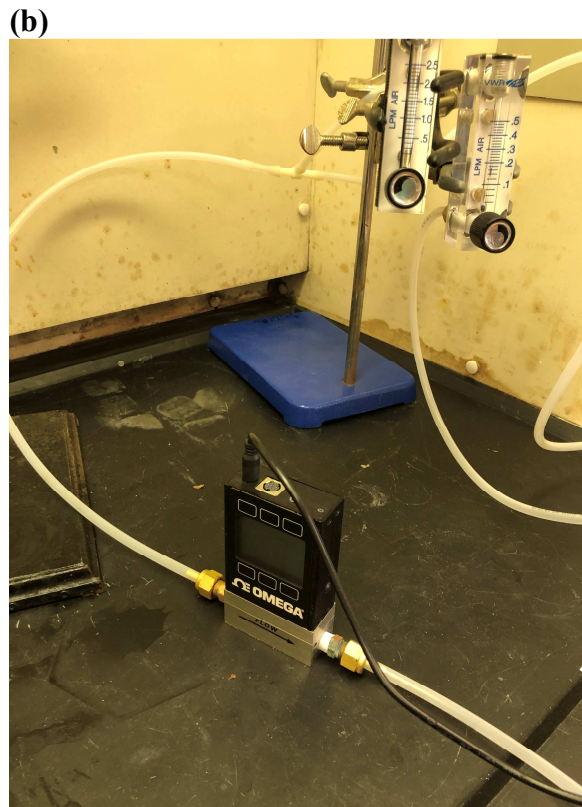


Figure 84: Absorption Experimental Setup Photo **a)** not in use **b)** gas flow control setup **c)** column in use **d)** setup in use

(a)



(b)



Figure 85: Algal Amino Acid Absorbent Photo **a)** before absorption **b)** after absorption

(a)



(b)

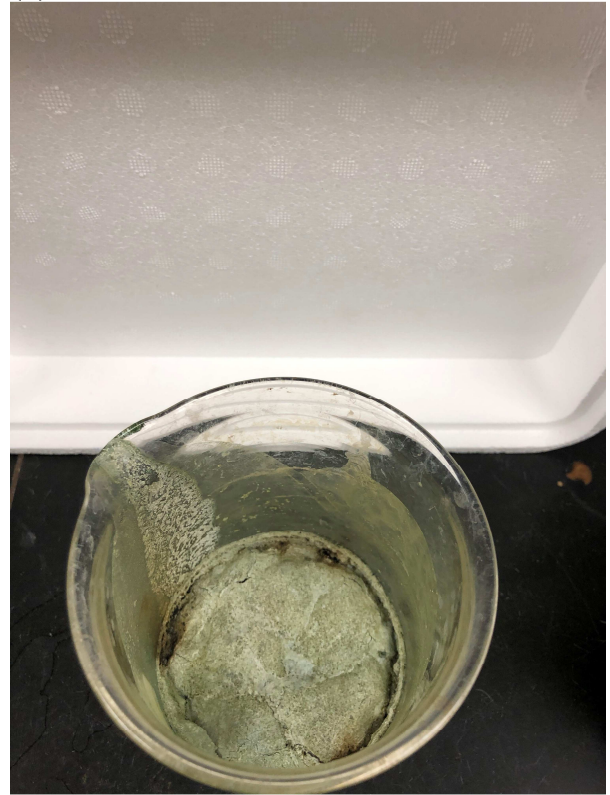


Figure 86: Precipitated Solids after Acidification Photos a) solids and liquids b) dried solids

REFERENCES

REFERENCES

- (1) Jackson, R. The Effects of Climate Change <https://climate.nasa.gov/effects> (accessed Oct 10, 2020).
- (2) US EPA, O. Global Greenhouse Gas Emissions Data <https://www.epa.gov/ghgemissions/global-greenhouse-gas-emissions-data> (accessed Oct 10, 2020).
- (3) Mazinani, S.; Ramazani, R.; Samsami, A.; Jahanmiri, A.; Van der Bruggen, B.; Darvishmanesh, S. Equilibrium Solubility, Density, Viscosity and Corrosion Rate of Carbon Dioxide in Potassium Lysinate Solution. *Fluid Phase Equilibria* **2015**, *396*, 28–34. <https://doi.org/10.1016/j.fluid.2015.03.031>.
- (4) Electricity in the U.S. - U.S. Energy Information Administration (EIA) <https://www.eia.gov/energyexplained/electricity/electricity-in-the-us.php> (accessed Nov 16, 2020).
- (5) Greenhouse Gas Inventory Data Explorer | US EPA <https://cfpub.epa.gov/ghgdata/inventoryexplorer/#electricitygeneration/entiresector/allgas/category/all> (accessed Apr 19, 2021).
- (6) US EPA, O. Sources of Greenhouse Gas Emissions <https://www.epa.gov/ghgemissions/sources-greenhouse-gas-emissions> (accessed Oct 10, 2020).
- (7) Frequently Asked Questions (FAQs) - U.S. Energy Information Administration (EIA) <https://www.eia.gov/tools/faqs/faq.php> (accessed Oct 10, 2020).
- (8) Akorede, M. F.; Hizam, H.; Ab Kadir, M. Z. A.; Aris, I.; Buba, S. D. Mitigating the Anthropogenic Global Warming in the Electric Power Industry. *Renewable and Sustainable Energy Reviews* **2012**, *16* (5), 2747–2761. <https://doi.org/10.1016/j.rser.2012.02.037>.
- (9) Leung, D. Y. C.; Caramanna, G.; Maroto-Valer, M. M. An Overview of Current Status of Carbon Dioxide Capture and Storage Technologies. *Renewable and Sustainable Energy Reviews* **2014**, *39*, 426–443. <https://doi.org/10.1016/j.rser.2014.07.093>.
- (10) Kanniche, M.; Gros-Bonnivard, R.; Jaud, P.; Valle-Marcos, J.; Amann, J.-M.; Bouallou, C. Pre-Combustion, Post-Combustion and Oxy-Combustion in Thermal Power Plant for CO₂ Capture. *Applied Thermal Engineering* **2010**, *30* (1), 53–62. <https://doi.org/10.1016/j.applthermaleng.2009.05.005>.

- (11) Herzog, H. J. Scaling up Carbon Dioxide Capture and Storage: From Megatons to Gigatons. *Energy Economics* **2011**, *33* (4), 597–604. <https://doi.org/10.1016/j.eneco.2010.11.004>.
- (12) Wang, M.; Lawal, A.; Stephenson, P.; Sidders, J.; Ramshaw, C. Post-Combustion CO₂ Capture with Chemical Absorption: A State-of-the-Art Review. *Chemical Engineering Research and Design* **2011**, *89* (9), 1609–1624. <https://doi.org/10.1016/j.cherd.2010.11.005>.
- (13) Bhowan, A. S.; Freeman, B. C. Analysis and Status of Post-Combustion Carbon Dioxide Capture Technologies. *Environ. Sci. Technol.* **2011**, *45* (20), 8624–8632. <https://doi.org/10.1021/es104291d>.
- (14) Resnik, K. P.; Yeh, J. T.; Pennline, H. W. Aqua Ammonia Process for Simultaneous Removal of CO₂, SO₂ and NO_x. *IJETM* **2004**, *4* (1/2), 89. <https://doi.org/10.1504/IJETM.2004.004634>.
- (15) Rinker, E. B.; Ashour, S. S.; Sandall, O. C. Absorption of Carbon Dioxide into Aqueous Blends of Diethanolamine and Methyldiethanolamine. *Ind. Eng. Chem. Res.* **2000**, *39* (11), 4346–4356. <https://doi.org/10.1021/ie990850r>.
- (16) Nwaoha, C.; Saiwan, C.; Tontiwachwuthikul, P.; Supap, T.; Rongwong, W.; Idem, R.; AL-Marri, M. J.; Benamor, A. Carbon Dioxide (CO₂) Capture: Absorption-Desorption Capabilities of 2-Amino-2-Methyl-1-Propanol (AMP), Piperazine (PZ) and Monoethanolamine (MEA) Tri-Solvent Blends. *Journal of Natural Gas Science and Engineering* **2016**, *33*, 742–750. <https://doi.org/10.1016/j.jngse.2016.06.002>.
- (17) Petrescu, L.; Bonalumi, D.; Valenti, G.; Cormos, A.-M.; Cormos, C.-C. Life Cycle Assessment for Supercritical Pulverized Coal Power Plants with Post-Combustion Carbon Capture and Storage. *Journal of Cleaner Production* **2017**, *157*, 10–21. <https://doi.org/10.1016/j.jclepro.2017.03.225>.
- (18) Singh, B.; Strømman, A. H.; Hertwich, E. Life Cycle Assessment of Natural Gas Combined Cycle Power Plant with Post-Combustion Carbon Capture, Transport and Storage. *International Journal of Greenhouse Gas Control* **2011**, *5* (3), 457–466. <https://doi.org/10.1016/j.ijggc.2010.03.006>.
- (19) Vaidya, P. D.; Kenig, E. Y. CO₂-Alkanolamine Reaction Kinetics: A Review of Recent Studies. *Chemical Engineering & Technology* **2007**, *30* (11), 1467–1474. <https://doi.org/10.1002/ceat.200700268>.
- (20) Goff, G. S.; Rochelle, G. T. Monoethanolamine Degradation: O₂ Mass Transfer Effects under CO₂ Capture Conditions. *Ind. Eng. Chem. Res.* **2004**, *43* (20), 6400–6408. <https://doi.org/10.1021/ie0400245>.

- (21) Kang, D.; Park, S.; Jo, H.; Min, J.; Park, J. Solubility of CO₂ in Amino-Acid-Based Solutions of (Potassium Sarcosinate), (Potassium Alaninate + Piperazine), and (Potassium Serinate + Piperazine). *J. Chem. Eng. Data* **2013**, *58* (6), 1787–1791. <https://doi.org/10.1021/je4001813>.
- (22) Wang, T.; Hovland, J.; Jens, K. J. Amine Reclaiming Technologies in Post-Combustion Carbon Dioxide Capture. *Journal of Environmental Sciences* **2015**, *27*, 276–289. <https://doi.org/10.1016/j.jes.2014.06.037>.
- (23) Hamborg, E. S.; Niederer, J. P. M.; Versteeg, G. F. Dissociation Constants and Thermodynamic Properties of Amino Acids Used in CO₂ Absorption from (293 to 353) K. *J. Chem. Eng. Data* **2007**, *52* (6), 2491–2502. <https://doi.org/10.1021/je700275v>.
- (24) Aronu, U. E.; Svendsen, H. F.; Hoff, K. A. Investigation of Amine Amino Acid Salts for Carbon Dioxide Absorption. *International Journal of Greenhouse Gas Control* **2010**, *4* (5), 771–775. <https://doi.org/10.1016/j.ijggc.2010.04.003>.
- (25) Hook, R. J. An Investigation of Some Sterically Hindered Amines as Potential Carbon Dioxide Scrubbing Compounds. *Ind. Eng. Chem. Res.* **1997**, *36* (5), 1779–1790. <https://doi.org/10.1021/ie9605589>.
- (26) Hu, G.; Smith, K. H.; Wu, Y.; Mumford, K. A.; Kentish, S. E.; Stevens, G. W. Carbon Dioxide Capture by Solvent Absorption Using Amino Acids: A Review. *Chinese Journal of Chemical Engineering* **2018**, *26* (11), 2229–2237. <https://doi.org/10.1016/j.cjche.2018.08.003>.
- (27) Song, H.-J.; Park, S.; Kim, H.; Gaur, A.; Park, J.-W.; Lee, S.-J. Carbon Dioxide Absorption Characteristics of Aqueous Amino Acid Salt Solutions. *International Journal of Greenhouse Gas Control* **2012**, *11*, 64–72. <https://doi.org/10.1016/j.ijggc.2012.07.019>.
- (28) Hussain, J.; Wang, X.; Sousa, L.; Ali, R.; Rittmann, B. E.; Liao, W. Using Non-Metric Multi-Dimensional Scaling Analysis and Multi-Objective Optimization to Evaluate Green Algae for Production of Proteins, Carbohydrates, Lipids, and Simultaneously Fix Carbon Dioxide. *Biomass and Bioenergy* **2020**, *141*, 105711. <https://doi.org/10.1016/j.biombioe.2020.105711>.
- (29) Costanzo, W.; Jena, U.; Hilten, R.; Das, K. C.; Kastner, J. R. Low Temperature Hydrothermal Pretreatment of Algae to Reduce Nitrogen Heteroatoms and Generate Nutrient Recycle Streams. *Algal Research* **2015**, *12*, 377–387. <https://doi.org/10.1016/j.algal.2015.09.019>.
- (30) Thomas, D. M.; Mechery, J.; Paulose, S. V. Carbon Dioxide Capture Strategies from Flue Gas Using Microalgae: A Review. *Environ Sci Pollut Res* **2016**, *23* (17), 16926–16940. <https://doi.org/10.1007/s11356-016-7158-3>.

- (31) Ruangsomboon, S.; Prachom, N.; Sornchai, P. Enhanced Growth and Hydrocarbon Production of *Botryococcus Braunii* KMITL 2 by Optimum Carbon Dioxide Concentration and Concentration-Dependent Effects on Its Biochemical Composition and Biodiesel Properties. *Bioresource Technology* **2017**, *244*, 1358–1366. <https://doi.org/10.1016/j.biortech.2017.06.042>.
- (32) Yen, H.-W.; Ho, S.-H.; Chen, C.-Y.; Chang, J.-S. CO₂, NO_x and SO_x Removal from Flue Gas via Microalgae Cultivation: A Critical Review. *Biotechnology Journal* **2015**, *10* (6), 829–839. <https://doi.org/10.1002/biot.201400707>.
- (33) Lam, M. K.; Lee, K. T.; Mohamed, A. R. Current Status and Challenges on Microalgae-Based Carbon Capture. *International Journal of Greenhouse Gas Control* **2012**, *10*, 456–469. <https://doi.org/10.1016/j.ijggc.2012.07.010>.
- (34) Song, C.; Qiu, Y.; Xie, M.; Liu, J.; Liu, Q.; Li, S.; Sun, L.; Wang, K.; Kansha, Y. Novel Regeneration and Utilization Concept Using Rich Chemical Absorption Solvent As a Carbon Source for Microalgae Biomass Production. *Ind. Eng. Chem. Res.* **2019**, *58* (27), 11720–11727. <https://doi.org/10.1021/acs.iecr.9b02134>.
- (35) Hsueh, H. T.; Chu, H.; Yu, S. T. A Batch Study on the Bio-Fixation of Carbon Dioxide in the Absorbed Solution from a Chemical Wet Scrubber by Hot Spring and Marine Algae. *Chemosphere* **2007**, *66* (5), 878–886. <https://doi.org/10.1016/j.chemosphere.2006.06.022>.
- (36) Vega, F.; Baena-Moreno, F. M.; Gallego Fernández, L. M.; Portillo, E.; Navarrete, B.; Zhang, Z. Current Status of CO₂ Chemical Absorption Research Applied to CCS: Towards Full Deployment at Industrial Scale. *Applied Energy* **2020**, *260*, 114313. <https://doi.org/10.1016/j.apenergy.2019.114313>.
- (37) Hitachi's Carbon Dioxide Scrubbing Technology with New Absorbent for Coal Fired Power Plants. *Energy Procedia* **2011**, *4*, 245–252. <https://doi.org/10.1016/j.egypro.2011.01.048>.
- (38) Yeh, J. T.; Pennline, H. W.; Resnik, K. P. Study of CO₂ Absorption and Desorption in a Packed Column. *Energy Fuels* **2001**, *15* (2), 274–278. <https://doi.org/10.1021/ef0002389>.
- (39) Notz, R.; Aspiron, N.; Clausen, I.; Hasse, H. Selection and Pilot Plant Tests of New Absorbents for Post-Combustion Carbon Dioxide Capture. *Chemical Engineering Research and Design* **2007**, *85* (4), 510–515. <https://doi.org/10.1205/cherd06085>.
- (40) Final Report Summary - CASTOR (CO₂, from Capture to Storage) | Report Summary | CASTOR | FP6 | CORDIS | European Commission <https://cordis.europa.eu/project/id/502586/reporting> (accessed Nov 2, 2020).

- (41) Wang, M.; Joel, A. S.; Ramshaw, C.; Eimer, D.; Musa, N. M. Process Intensification for Post-Combustion CO₂ Capture with Chemical Absorption: A Critical Review. *Applied Energy* **2015**, *158*, 275–291. <https://doi.org/10.1016/j.apenergy.2015.08.083>.
- (42) Baena-Moreno, F. M.; Rodríguez-Galán, M.; Vega, F.; Reina, T. R.; Vilches, L. F.; Navarrete, B. Synergizing Carbon Capture Storage and Utilization in a Biogas Upgrading Lab-Scale Plant Based on Calcium Chloride: Influence of Precipitation Parameters. *Science of The Total Environment* **2019**, *670*, 59–66. <https://doi.org/10.1016/j.scitotenv.2019.03.204>.
- (43) Aroonwilas, A.; Veawab, A. Characterization and Comparison of the CO₂ Absorption Performance into Single and Blended Alkanolamines in a Packed Column. *Ind. Eng. Chem. Res.* **2004**, *43* (9), 2228–2237. <https://doi.org/10.1021/ie0306067>.
- (44) Daiek, C.; Link to external site, this link will open in a new window. Effects of Water Recirculation on Pilot-Scale Microalgae Cultivation Using Flue Gas CO₂. M.S., Michigan State University, United States -- Michigan, 2020.
- (45) JONES, D. B. Factors for Converting Percentages of Nitrogen in Foods and Feeds into Percentages of Protein. *USDA Circ.* **1931**, *183*, 1–21.
- (46) Cutshaw, A.; Daiek, C.; Zheng, Y.; Frost, H.; Marks, A.; Clements, D.; Uludag-Demirer, S.; Verhanovitz, N.; Pavlik, D.; Clary, W.; Liu, Y.; Liao, W. A Long-Term Pilot-Scale Algal Cultivation on Power Plant Flue Gas – Cultivation Stability and Biomass Accumulation. *Algal Research* **2020**, *52*, 102115. <https://doi.org/10.1016/j.algal.2020.102115>.
- (47) The Amino-Acid and Sugar Composition of 16 Species of Microalgae Used in Mariculture. *Journal of Experimental Marine Biology and Ecology* **1991**, *145* (1), 79–99. [https://doi.org/10.1016/0022-0981\(91\)90007-J](https://doi.org/10.1016/0022-0981(91)90007-J).
- (48) Growth and Ω 3 Fatty Acid and Amino Acid Composition of Microalgae under Different Temperature Regimes. *Aquaculture* **1989**, *77* (4), 337–351. [https://doi.org/10.1016/0044-8486\(89\)90218-4](https://doi.org/10.1016/0044-8486(89)90218-4).
- (49) Brown, M. R.; Jeffrey, S. W.; Volkman, J. K.; Dunstan, G. A. Nutritional Properties of Microalgae for Mariculture. *Aquaculture* **1997**, *151* (1–4), 315–331. [https://doi.org/10.1016/S0044-8486\(96\)01501-3](https://doi.org/10.1016/S0044-8486(96)01501-3).
- (50) Tran, H.; Vakkilainen, E. THE KRAFT CHEMICAL RECOVERY PROCESS. **2016**.
- (51) Jackson, P.; Robinson, K.; Puxty, G.; Attalla, M. In Situ Fourier Transform-Infrared (FT-IR) Analysis of Carbon Dioxide Absorption and Desorption in Amine Solutions. *Energy Procedia* **2009**, *1* (1), 985–994. <https://doi.org/10.1016/j.egypro.2009.01.131>.

- (52) Robinson, K.; McCluskey, A.; Attalla, M. I. An FTIR Spectroscopic Study on the Effect of Molecular Structural Variations on the CO₂ Absorption Characteristics of Heterocyclic Amines. *ChemPhysChem* **2011**, *12* (6), 1088–1099. <https://doi.org/10.1002/cphc.201001056>.
- (53) Diab, F.; Provost, E.; Laloué, N.; Alix, P.; Souchon, V.; Delpoux, O.; Fürst, W. Quantitative Analysis of the Liquid Phase by FT-IR Spectroscopy in the System CO₂/Diethanolamine (DEA)/H₂O. *Fluid Phase Equilibria* **2012**, *325*, 90–99. <https://doi.org/10.1016/j.fluid.2012.04.016>.
- (54) Qaroush, A. K.; Alshamaly, H. S.; Alazzeah, S. S.; Abeskhron, R. H.; Assaf, K. I.; Eftaiha, A. F. Inedible Saccharides: A Platform for CO₂ Capturing. *Chem Sci* **2018**, *9* (5), 1088–1100. <https://doi.org/10.1039/c7sc04706a>.
- (55) Seifried, B.; Temelli, F. Density of Marine Lipids in Equilibrium with Carbon Dioxide. *The Journal of Supercritical Fluids* **2009**, *50* (2), 97–104. <https://doi.org/10.1016/j.supflu.2009.05.011>.
- (56) Aronu, U. E.; Hoff, K. A.; Svendsen, H. F. CO₂ Capture Solvent Selection by Combined Absorption–Desorption Analysis. *Chemical Engineering Research and Design* **2011**, *89* (8), 1197–1203. <https://doi.org/10.1016/j.cherd.2011.01.007>.
- (57) Portugal, A. F.; Sousa, J. M.; Magalhães, F. D.; Mendes, A. Solubility of Carbon Dioxide in Aqueous Solutions of Amino Acid Salts. *Chemical Engineering Science* **2009**, *64* (9), 1993–2002. <https://doi.org/10.1016/j.ces.2009.01.036>.